Automated Simulation Model for Crane Motion Planning in Heavy Industrial Projects

by

Zhen Lei

A thesis submitted in partial fulfillment of the requirements for the degree of

Doctor of Philosophy

in
Construction Engineering and Management

Department of Civil and Environmental Engineering
University of Alberta

Abstract

In North America, industrial projects are constructed using a modularization/offsite construction method. Modules, such as pipe racks and vessels, are prefabricated offsite in factories, assembled in module yards, and shipped to the site for installation. This process has been adopted by the industry to achieve high efficiency and reduce waste by eliminating as much on-site work as possible. During the on-site installation, expensive mobile cranes are used for lifting activities, and appropriate use of these cranes can reduce costs and shorten the construction process. On the contrary, improper management of crane operations can lead to budget overruns, schedule delays, and safety issues. To ensure a smooth lifting process, engineering design for crane motions becomes necessary as a reference for onsite lifting. However, the current design process is manual-based, and consequently day-to-day changes of the site information make the process tedious and error-prone. Thus, a solution must be sought which provides rapid and accurate design of crane motions. In this context, crane motions can be categorized into "pick-and-swing" and "crane walking": in the first case, the crane lifts the module from a fixed location, while in the second scenario the crane picks the module and walks a certain distance with the load before delivering it to its final location. This research proposes a generic methodology for crane motion planning which captures the characteristics and typical constraints of crane motion planning. This approach is implemented as a series of computer systems for automating the planning process. Actual industrial projects are used to test the proposed computer system and validate the approach.

Acknowledgements

First of all, I would like to express my gratitude to my co-supervisors, Dr. Mohamed Al Hussein and Dr. Ahmed Bouferguene, for their continuous encouragement and inspiration. Without their support, I would have never finished this degree. I have learned valuable lessons about how to be professional and how to conduct myself as a qualified researcher. The projects I participated in ignited my passion for engineering design, innovation and development.

Mr. Ulrich Hermann and Dr. Hosein Taghaddos from PCL Industrial Management Inc., and all other PCL colleagues (Matt, Travis, Sherry, Randy, Lev….) are very much appreciated for their support and sharing of their many years of knowledge and experience. This unique experience not only laid a solid foundation for me as an engineer, but also nurtured me as a thinker and innovator.

At the University of Alberta, I have also been surrounded by many exceptional colleagues: Sang, Sadiq, Hamid, Harry, Sherry, Rita, Leo, Monjur, Beda, Samer, Hongxian, Dawid, Mana, Mona, Gurjeet, Ahmad, Jacek, Nadim, Tanzia, Jonathan, Hamida, Shiv, Rokib, Jeremy…. I had opportunities to work with some of them, and produced interesting and high-quality research outputs.

At last, my deepest gratitude is given to my family who has been a great support behind me over the years, without which I would have never achieved this degree. My girlfriend, Lisa, is also very much appreciated for her kind and continuous company through this phase of my life.

TABLE OF CONTENTS

List of Figures

Chapter 1 Introduction

1.1 Background and Overview

With the continuing growth of the international oil and gas market, the province of Alberta in Canada, due to its rich oil sands reserves, has become a major oil supplier to the global market. Alberta's current proven oil reserve is approximately 170 billion barrels—13% of total global oil reserves, out of which 168 billion barrels is in the form of oil sands (Alberta Government 2014). These lucrative oil reserves continue to generate considerable revenue for Albertans: in the fiscal year 2012-2013, the oil sands industry generated $3.56 billion in royalty revenues and $4.51 billion in the fiscal year 2011-2012 (Alberta Government 2013). This revenue has also corresponded to the creation of numerous employment opportunities in Alberta. According to Statistics Canada and the Alberta Treasury Board and Finance, in 2011, there were approximately 116,000 people employed in Alberta's upstream energy sector, which alone accounted for 27.6% of Alberta's gross domestic product (Alberta Government 2014).

Over the years, substantial capital has been invested in Alberta to increase oil sands extraction, (see Figure 1-1 for the trend of oil sands industry investment over the past thirteen years), which has led to the expansion of industrial facilities built for oil extraction and upgrade. This expansion has garnered attention from the construction engineering and management perspective, where construction planners seek to achieve an accelerated project delivery process. One of the key elements in this regard is how to efficiently manage onsite equipment (e.g., mobile cranes for lifting), given the high cost of its utilization.

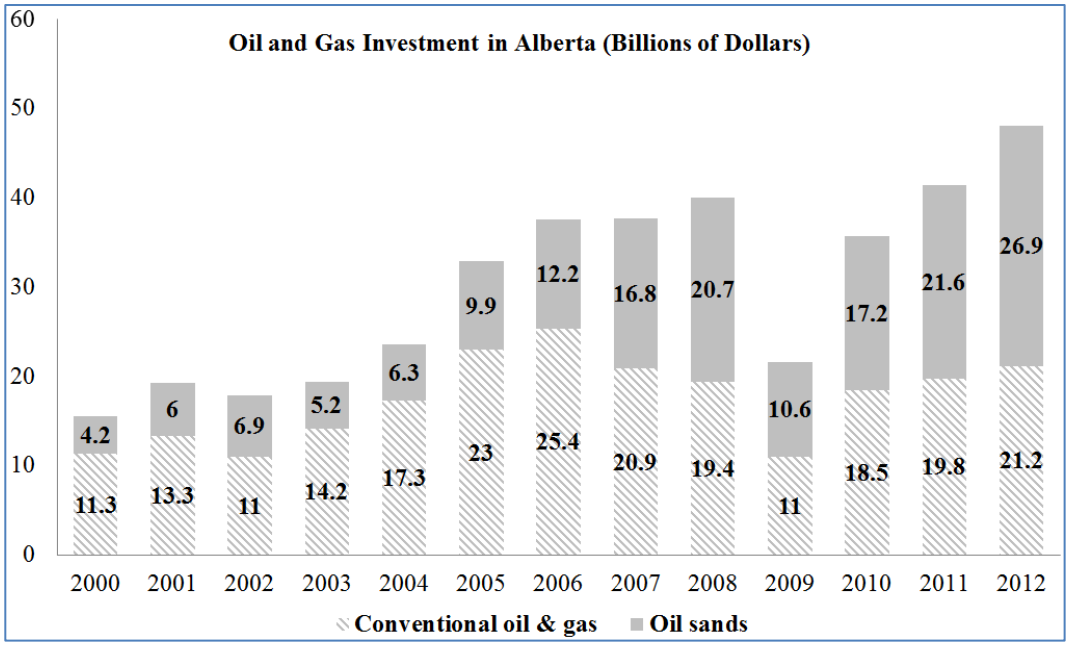

Figure 1-1 Oil and gas investment trend in Alberta (Statistics Canada 2014)

1.2 Challenges and Problem Statement

Today, as the construction industry is shifting from stick-built to offsite construction/modularization, prefabrication and onsite installation have become preferred methods of constructing industrial projects (Shapira et al. 2007). The move towards offsite construction in Northern Alberta's oil sands is rooted partly in severe weather conditions and also lack of ready access to a sufficient labor pool due to the remoteness of the sites, which are known to affect productivity and hinder efforts to recruit qualified workers (the average temperature in Fort McMurray between December/2012 and February/2013 was −20°C, and the lowest temperature reached was −40°C) (Canada Weather Stats, 2014). Using the modular approach, oil sands extraction facilities are divided into "pieces", called modules (see Figure 1-2 for an example of pipe rack module); these modules are prefabricated offsite and then shipped to the site for installation. During the

assembly process, large mobile cranes are used as the main lifting equipment. Figure 1-3 shows a typical industrial site where mobile cranes are used to lift the complete modules. These mobile cranes are expensive in terms of rental cost and crew fees. For example, for industrial projects in Alberta, Canada, a dual-crane lift of a single vessel (Demag CC1800 and Manitowoc 4100) costs CAD 320,000, including the rental cost, mobilization/demobilization, and ground preparation (Hermann et al. 2011).

Figure 1-2 Example of prefabricated module

Therefore, efficient utilization of mobile cranes is critical to the success of industrial projects, and to avoiding budget overruns, schedule delays, and safety issues. To ensure high productivity of crane operations, proper and accurate crane motion planning and analysis must be carried out before the actual lifting process. In current practice, heavy lift study is used to check the feasibility of the lifting process. In the heavy lift study, the total lifting weight is used to find the lifting

radius for the crane from the lifting capacity chart provided by the crane manufacturer, and the lifting radius, in turn, is used to determine where to locate the crane. Once the crane location has been selected, the clearance between the crane's body and the surrounding environment must be checked. However, there are many challenges in the current crane motion planning process:

(i) industrial projects usually involve a large number of lifts (often over 100 modules per project), which results in a labourious planning process;

(ii) heavy industrial projects are dynamic in nature, and prompt updates of planning results are necessary;

(iii) industrial project sites usually involve more constraints than other types of projects due to their complexity (see Figure 1-3 for a typical industrial project site); and

(iv) the time-sensitive nature of these projects and the frequent changes in design necessitate and timely modifications of the lift plans.

Due to these challenges, the industry demands a more efficient way of planning mobile crane motions. In general, crane motions can be categorized into two types: (i) "pick-and-swing", where the mobile crane performs lifts from a single fixed location, and (ii) "crane walking", where the mobile crane must move (with the load) a certain distance to complete the lift. Current heavy lift study practice often overlooks the possibility of the crane body clashing with the existing environment during operation, only capturing two snapshots of the lifting process (at the pick and set positions). This research thus proposes an approach that can

automate the crane motion planning process, implemented as a computer system linked with the server database. The system can read the required information from the server database and perform automatic motion planning. Actual industrial projects are used to verify the designed system and validate the proposed method.

Figure 1-3 Typical industrial installation site

1.3 Research Objectives

Based on the challenges of crane motion planning mentioned above, this research is developed based on the following hypothesis: "automation of mobile crane motion planning can achieve high efficiency in onsite lifting planning process and potentially reduce project cost." To achieve this hypothesis, the following

research objectives are pursued: (*i*) develop a generic method for crane path checking ("pick-and-swing" analysis); (*ii*) develop an algorithm that can automate the "crane walking" planning process; (*iii*) develop a fast and accurate crane location selection method, based on which a boom clearance method can be implemented for lift study; and (*iv*) integrate all the designed algorithms and automate the entire crane motion planning process.

1.4 Organization of the Thesis

This thesis is organized into the following chapters: Chapter 1 (Introduction) presents the challenges in current industrial project planning and the research motivations; Chapter 2 (Literature Review) introduces the state-of-the-art in crane research, including crane selection and optimization, crane operation simulation and visualization, crane motion planning and analysis, safety analysis of crane operations, and information technology in crane operation analysis. Chapter 3 (Proposed Methodology) elaborates the path checking algorithms for pick-and-swing and crane walking scenarios. A boom clearance system based on the Clipping Algorithm is also introduced, and, based on the analysis results, an automatic 3D visualization engine developed in 3ds Max is developed. Chapter 4 (Implementation and Case Studies) presents the system developed based on the proposed methodology, the database used as storage of the project and crane information, and, eventually, two real industrial projects used to demonstrate the designed system and validate the proposed methodology. Chapter 5 (Conclusions) summarizes the research work and outlines the corresponding research contributions and limitations. Directions for future research are also suggested.

Chapter 2 Literature Review

2.1 Introduction

Mobile cranes are used widely in the North American construction industry (Shapira and Glascock 1996). In past decades, researchers have been making efforts to improve the crane planning and analysis process by developing algorithms and automating these algorithms with the assistance of computer technologies. Another trend is that crane operation management systems are becoming more integrated and interdisciplinary, capable of handling various engineering analysis in an integrated system. In order to articulate the contributions of this research, it is necessary to outline these previous theories and algorithms, as they provide the foundation of this research. Meanwhile, the emerging offsite construction/modularization paradigm in industrial construction not only provides nutritious soil for mobile crane utilization, but also presents challenges to construction planners seeking to design and plan efficient operations. Thus, the work that has been conducted so far related to offsite construction in industrial projects is described here to understand these challenges.

In general, this information provided in this chapter is divided into the following sections:

(i) Offsite construction in industrial projects: This section provides the basic definitions pertaining to offsite construction, and describes the associated challenges of this construction method.

(ii) Crane selection and optimization: This section deals with how to select suitable crane types for a project, which determines the feasible/optimal crane locations that increase productivity.

(iii) Crane operation simulation and visualization: This section focuses on how to model the crane lifting process, whereby, using simulation techniques, the designed simulation model can serve as a decision support tool. The outputs from the simulation models are also presented using visualization.

(iv) Crane motion planning and analysis: This section describes a process of determining feasible and collision-free lifting paths for the cranes.

(v) Information technology in crane operation analysis: This section reports on the state-of-the-art in information technology, such as building information modelling (BIM), which is implemented to analyze crane operations.

(vi) Finally, other crane-related studies that have contributed to the construction science field as valuable additions are presented.

2.2 Offsite Construction in Industrial Projects

Offsite construction/modularization is not new to the construction technology, and it has been prevalent in the fast few decades. Many previous studies have listed the benefits that offsite construction method has brought to the construction industry (O'Connor et al. 2014). The productivity growth in offsite construction is proportionally outpacing that in onsite construction sectors (Eastman and Sacks 2008). For instance, the productivity and competitiveness of the capital facilities

sector of the US construction industry has advanced significantly as a result of increasing adoption of offsite construction (NRC 2009). The following definitions support understanding of this construction method:

(i) Haas et al. (2000) describe offsite construction as *"The preconstruction of a complete system away from the job site that is then transported to the site. The modules are large in size and possibly may need to be broken down in to several smaller pieces for transport."*

(ii) Tatum et al. (1987) define a module as *"a major section of a plant resulting from a series of remote assembly operations [that] may include portions of many systems; usually the largest transportable unit or component of a facility."*

(iii) CII (2002) describes offsite fabrication as *"the practice of preassembly or fabrication of components both off the site and onsite at a location other than at the final installation location."*

Offsite construction/modularization has been widely used in the development of Alberta's oil sands to reduce costs and cycle times, particularly as a measure to overcome the challenges of Alberta's severe weather and labor shortage. An industrial module is, as defined by Taghaddos et al. (2014), "*A preconstructed unit that is built off the project site, transported to the site, and interconnected to make the larger structure (e.g., refineries and oil-processing plants, buildings)."* In practice, industrial modules have various categories, including structural, pipe racks, and miscellaneous modules. In most cases these modules are prefabricated in offsite module yards near Edmonton, Alberta, and shipped to remote sites in the

oil sands region for installation (Figure 2-1). Considering the many disciplines involved in this construction process, the efficiency and productivity become the keys to project success from the perspective of construction management. In this regard, researchers at the University of Alberta have collaborated with PCL Industrial Management Inc. to improve the efficiency of the offsite construction process. This collaboration has included the following studies: (*i*) simulation of offsite industrial construction processes (Taghaddos et al. 2014); (*ii*) heavy lift planning from a technical perspective (e.g., crane selection, location positioning, path planning, and analysis) (Hermann et al. 2010; Lei et al. 2013a, 2013b); and (*iii*) visualization of crane operations (AbouRizk et al. 2011).

Figure 2-1 A typical module yard layout

2.3 Crane Selection and Optimization

Two of the critical issues in crane operation planning and management are to select the proper crane type, and, based on the selected crane type, to choose the feasible crane locations. Crane type selection is mainly factor-based, meaning that practitioners have defined different factors that are critical in the selection. Rodriguez-Ramos and Francis (1983) have proposed a single-crane location optimization model which aims to minimize the total transportation cost between the crane and the construction supportive facilities. Hanna and Lotfallah (1999) have utilized a fuzzy logic approach for crane selection, based on various selection factors; their main categories of factors are: (*i*) site conditions; (*ii*) building design; (*iii*) economy; (*iv*) capability; and (*v*) safety. Following that, Sawhney and Mund (2002) have introduced a crane type selection tool called IntelliCranes, based on 9 different factors including site spaciousness, construction footprint, and construction height. An artificial intelligence technique, neural networks, is used to automate the selection process.

Through the crane selection process, a database is often used for data storage of crane configurations. For example, a "D-Crane" database has been developed for crane selection, and the crane's minimum boom length and/or minimum lifting radius are taken into consideration as the selection criteria (Al-Hussein et al. 2000; Al-Hussein et al. 2005). As selection factors/criteria are defined, researchers have begun to integrate crane selection with other techniques, such as 3D visualization and simulation. This integration can validate selection results and provide a more visual way of presenting the results. One example is an algorithm developed by

Wu et al. (2012) for selecting mobile cranes; similarly to previous work, many factors are considered in their study, such as the lifting capacity, the geometrical characteristics of the crane, and the dimensions of rigging. The selection is then incorporated into a 3D computer-aid system for simulation, design, and rigging calculation purposes.

Based on the crane type selection, crane location selection involves further calculations: the geometry of the crane needs to be taken into account, along with the site layout geometry; checking is usually performed to ensure the crane location is collision-free. Also, since there is more than one possible feasible crane location, optimization techniques are adopted to determine the optimal locations. Zhang et al. (1999) have proposed a computerized model to optimize the locations of a group of tower cranes. The lifting tasks are classified into groups, based on which the feasible locations for each crane are identified. Minimal conflicts of different cranes are achieved by adjusting the task groups; then, an optimization model is used to search for optimal solutions based on the hook travel time. A genetic algorithm has also been used to optimize the supply locations of tower cranes (Tam et al. 2001). The hook travel time developed by Zhang et al. (1999) has been studied, modified and used in the study by Tam et al.. The supply location optimization topic has also been studied by Huang et al. (2011). In their research, a mixed-integer linear programming method is used, also based on the model proposed by Zhang et al. (1999). More recently, mobile crane location selection has garnered increasing attention due to the emergence of offsite construction of industrial projects in North America. Mobile crane location

selection differs from tower crane location selection, where the constraints of the tower crane come from the crane body and its boom. With mobile cranes, the tail-swing or superlift structure can impose constraints on the area in which the crane can move and operate and must thus be considerd. An integrated system to select, position, and simulate the mobile crane operations for industrial projects has been developed accordingly (Hermann et al. 2010), and, in specific, a detailed algorithm used in this system for selecting the mobile crane's location based on its geometry and lifting capacity has been introduced by Safouhi et al. (2011).

2.4 Crane Operation Simulation and Visualization

Computer simulation techniques have proven to be very effective in providing the tools required to design and analyze construction processes, regardless of complexity or size, such as excavations and embankments, pipe installation, and tunnel and road construction (AbouRizk 2010). The CYCLONE system, developed by Halpin (1977), has opened the gate for modern construction simulation. Paulson et al. (1987) have developed a simulation tool called INSIGHT. In addition, AbouRizk and Hajjar (1998) have developed a simulation language, called Simphony, which is a general-purpose modelling template for construction users. Based on these, many special-purpose templates have been developed for different type of construction projects. More recently, previously introduced simulation tools have been integrated with 3D/4D tools for visualization purposes (Xu and AbouRizk 1999; Xu et al. 2003; Kamat and Martinez 2003; Zhang et al. 2012).

Regarding crane operations, simulation tools are applied to simulate the lifting process, investigate bottlenecks, and thus improve the productivity. A special-purpose simulation model for tower crane operations has been proposed by Al-Hussein et al. (2006), which also integrates with 3D visualization to verify and validate simulation results. In their research, 3ds Max is used as a visualization tool that is customized and added to the simulation engine. A discrete-event simulation (DES) model has been developed for the purpose of determining possible locations for mobile cranes (Tantisevi and Akinci 2008). Other than crane operation process simulation, recently some research has focused on physical simulation of the crane and analysis of crane motions. This macro-to-micro transit has taken crane simulation research to a more detailed analysis, focusing on individual lifts and simulating the corresponding lifting process. For example, Kang et al. (2009) have suggested a 3D physics-based simulation model that captures crane maneuvering. The model is used for analyzing motions for both tower cranes and crawler cranes. Based on this work, Chi and Kang (2010) have solved the dual-crane lifting mechanism by using a physics-based simulation technique. A similar work by Lin et al. (2012) has shown a statics-based simulation approach for dual-crane lifts. Their study utilizes the principle of minimum potential energy to develop an optimization problem with geometric and physical constraints. More recently, a framework and system architecture has been proposed by AlBahnassi and Hammad (2012) for near real-time motion planning and simulation of cranes in construction. A 3D visualization tool has been developed based on this framework. Li and Liu (2012) have developed a

data-driven remote monitoring and alarming system for tower cranes based on 3D simulation techniques.

2.5 Crane Motion Planning and Analysis

Crane motion planning is similar in nature to robotic motion planning, as cranes can be considered to correspond to robots in operation. Initially, research in robotics aimed to create autonomous robots capable of accepting high-level task descriptions and executing these tasks without human intervention (Latombe 1991). Many problems need to be solved in this process, and one of them is to design algorithms/methods that help robots to find collision-free paths. In this regard, a configuration space (C-Space) method has been developed which can be considered as a foundation for robotic motion planning (Lozano-Pérez 1983). The key idea of C-Space is to convert the moving robot into a representing point considering its own orientations, and instead of seeking paths for the moving robot, the path finding problem is simplified to finding paths for the representing point. Many methods have been developed since then to search for moving paths for robots, such as roadmap method (Asano et al. 1985; Aurenhammer 1991), cell decomposition method (Lingelbach 2004), and potential field method (Ge and Cui 2002). A number of applications have been built based on these pioneering theories, such as a multi-agent robot motion planning method (Ota 2006), a robotic motion performance platform (Kato et al. 2012), and a mobile robot motion planning method based on a heat conduction equation (Liang and Lian-Cheng 2011).

Due to the success of these theories in robotics, researchers in the field of construction management have begun to study the robotic theory and create construction robots, which here are referred to as construction machines. For instance, Warszawski and Navon (1991) have developed a single-purpose construction robot for interior-finishing jobs, such as painting and plastering; Bryson et al. (2005) have introduced a fully autonomous robot for paving operations in construction. A wireless sensor-driven navigation system has been proposed for mobile robot applications in construction (Williams et al. 2007). Some researchers have focused on how to apply motion planning methods to the construction field, and the developed algorithms are often integrated with state-of-the-art visualization tools. Soltani et al. (2002) have reviewed and evaluated the performance of various path planning algorithms in construction sites, such as Dijkstra and A* algorithms. In more recent research, Lin et al. (2013) have utilized Building Information Modeling (BIM) techniques to facilitate path planning for 3D indoor spaces. The research related to crane path planning can be dated back to the early-2000s, when Reddy and Varghese (2002) developed an automated path planning system for single-crane lifting in an AutoCAD environment. Algorithms have subsequently been developed for cooperative crane lifting/dual-crane lifting using a robotic motion planning method (Sivakumar et al. 2000 and 2003; Ali et al. 2005). Ali et al. (2002 and 2005) have also adopted the genetic algorithm (GA) to search for optimal paths. With the development of visualization techniques, Kang and Miranda (2006) have used visualization to build a virtual crane model that can be used to present erection processes based on

the found lifting paths. In a more recent work, a C-Space method has been used to create crane motions in which the mobile crane is treated as a robot with many degrees-of-freedom (DOF) (Lei et al. 2011; AlBahnassi and Hammad 2012). Another widely used method in robotics for planning the paths for robots, called the probabilistic road map (PRM) method, has been adopted and implemented in planning crane lifting paths (Chang et al. 2012). In their application, the PRM method has been tested in both single- and dual-crane erection processes. In addition, based on previous works, the author has successfully developed an automatic crane path checking mechanism (Lei et al. 2013a, 2013b, and 2013c).

2.6 Information Technology in Crane Operation Analysis

Information technology has been the key to enhanced efficiency and reduced error recently in the construction industry. Developed mathematical models and algorithms can be programmed to achieve automation and eliminate the human components involved in the planning/design process. Databases are used to store project information, and interfaces are built which allow users to access and analyze data in order to appropriately design or plan construction projects. Such decision support systems can be found in previous research. For instance, a database approach has been proposed to solve contractual issues in construction (Chong and Phuah 2013). Industry Foundation Classes (IFC) has been developed as a common schema for data transfer and has been implemented in major drafting tools in construction. Lee et al. (2012a) have developed a space database for establishing automated building design review systems in which IFC has been adopted. Meanwhile, computer-aided design (CAD) has become a major approach

in construction design, and many systems have been developed. As the most widely used system in the market, Autodesk provides users with channels by which to customize the system. Studies in a number of areas, such as BIM, virtual reality (VR), and augmented reality (AR), have been conducted to automate the designing process since then (Alwisy et al. 2012; Moghadam et al. 2012; Cho et al. 2010; Wang et al. 2012; Jung et al. 2014). Lin and Gerber (2014) have introduced a system, called Evolutionary Energy Performance Feedback for Design (EEPFD), which supports early stage design by providing energy performance; this system is developed based on Autodesk Revit. Akinci et al. (2002) have developed a 4D model that can automatically generate project-specific work spaces based on IFC.

Today, due to the development of information technologies, previously manual-based crane operation analyses are now automated. Among the earliest trials of using information technology to assist in crane operation analysis has been a crane database developed by Al-Hussein et al. (2000), which was later integrated with 3D modelling to demonstrate the results (Moselhi et al. 2004). This database contains required information for crane analysis, and interfaces are programmed that allow communications with the database. For example, Hasan et al. (2010) have developed a supporting design system for mobile cranes based on a database. By communicating with the database, the programmed system can perform fast and accurate supporting design for mobile cranes, where the main programming languages used to develop the systems are Microsoft Visual Studio languages (e.g., Visual Basic.Net and C#). Simulation technique has been incorporated with

the programming system and implemented in industrial construction projects (Taghaddos et al. 2009, 2010, 2012, 2014).

Hornaday et al. (1993) have utilized the computer-aided method to analyze and plan heavy crane lifts. In their work, a system database is used to store all the required data, such as the crane information and site information. A visualization interface is then built and integrated with an analyzing engine that checks and formulates the lift plan. A study by Mahalingam et al. (2000) has used similar system architecture to achieve automated lift planning for cranes, in which AutoCAD is used to present the outputs. 3ds Max as an animation tool has been used to present the crane lifting process, linked with an optimization model to determine optimal crane locations (Manrique et al. 2007);

2.7 Other Crane-Related Research

In crane planning research there have been many efforts to improve crane operation from a variety of perspectives. Some have focused on how to utilize sensor technology to develop crane control systems for more safe lifting in construction. For instance, level luffing control system has been developed for crawler cranes which consists of controller, sensors, and hydraulic actuators (Araya et al. 2004). Lee et al. (2012b) have proposed a tower crane navigation system using sensor technology and BIM, which provides live 3D information about the relevant position of the crane and the surroundings to the crane operators. A recurrent neural network (RNN) has been used to develop a control algorithm for 3D tower crane systems (Duong et al. 2012). A recent study by Kuo

and Kang (2014) has focused on efficiently controlling fast crane operations by reducing the sway angle and reaching high speed operations.

In order to ensure safety in crane operations, efforts have also been made to reduce the likelihood of crane accidents (Shapira and Lyachin 2009a and 2009b; Cheng and Hammad 2012; Ray and Teizer 2012). Visual monitoring and alarming systems have proven to be an effective way to avoid accidents in crane lifting (Li and Liu 2012). A visual training system can be helpful to workers in tower crane dismantlement jobs so that fewer injuries and fatalities occur (Li et al. 2012). Also, site information can be collected to model tower crane operator visibility in order to minimize crane accidents (Cheng and Teizer 2014). In addition, the effects of wind on cranes have been studied (Mara 2010). Hasan et al. (2012) have developed an algorithm that calculates the effects of strong winds on mobile cranes and tower cranes, and used BIM to present the analysis results.

Chapter 3 Proposed Methodology

3.1 Overview and System Architecture

The objective of this research is to establish a generic approach for mobile crane motion planning. Mobile crane motions are generally categorized into two types of operation: (*i*) pick-and-swing, where the mobile crane sits at one specific location and performs the lifts without moving (Figure 3-1); and (*ii*) crane walking, where the mobile crane must pick and set the module from different crane locations (Figure 3-2).

Figure 3-1 Pick-and-swing crane operation

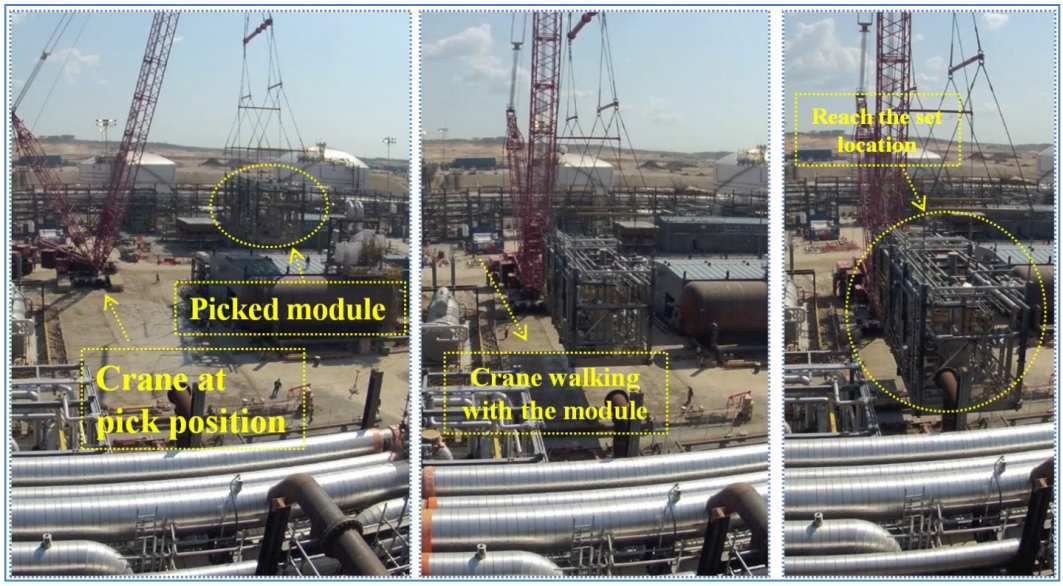

Figure 3-2 Crane walking on congested industrial site

In general, in order to ensure onsite lifting efficiency and safety, several questions need to be addressed at the planning stages: (*i*) What crane types are to be used, and where are the cranes to be positioned? (*ii*) When should the lifts be performed from a logistical perspective? and (*iii*) Is the lifting feasible (does the crane have a feasible lift path and/or walking path)? With respect to these three questions, efforts have been made to find a generic methodology and algorithms. The collaboration between PCL Industrial Management Inc. and the University of Alberta has produced an integrated system for mobile crane planning in industrial construction, as shown in Figure 3-3. The core of the crane management system is the company's central database, which stores the crane and project information, and the computed outcomes. Currently, the database stores 300 cranes, 26,000 crane configurations/combinations, and 394,000 capacity entries. The inputs for all the systems are extracted from AutoCAD drawings, and are then entered into the company's database. Some of the typical inputs of the system include: (*i*)

crane capacity charts; (*ii*) module information, such as weights and set points; (*iii*) crane configurations; and (*iv*) site layout and boundaries. The Advanced Crane Planning and Optimization (ACPO) system then reads the information from the database and performs the calculations in order to find all the potential crane locations for each module (Hermann et al. 2010). Meanwhile, the Advanced Simulation in Industrial Crane Operations (ASICO) system plans the lifting sequence according to the pre-defined lifting logics (Taghaddos et al. 2012). The sequence, together with the selected crane locations, is then utilized by the Crane Path Checking and Planning (CPCP) system, which is developed within the scope of this research, in order to analyze the crane motions. 4D animations that show the crane's movements are generated by 3ds Max based on the determined sequence and crane locations. All the systems communicate with one another, such that the results updated in one of the systems can automatically update other systems.

3.1.1 Crane Location Selection

In PCL's crane management system, ACPO mathematically calculates the crane locations considering various site constraints (Figure 3-3). Crane location selection involves analyses of several factors, such as the crane's geometry and site constraints. On industrial sites, an area where the crane can be settled to perform the lifts without any conflict with the surroundings is called the mobile crane position work area. In defining the crane position work area, two site constraints are considered: (*i*) the inside boundary limit; and (*ii*) the outside boundary limit. An inside boundary limit is a set of 2D points joined into

connected segments that define areas unavailable for crane positioning; the outside boundary limit defines the outer limits of the project site (see Figure 3-4a for a typical industrial project site represented by the inside and outside boundary limits).

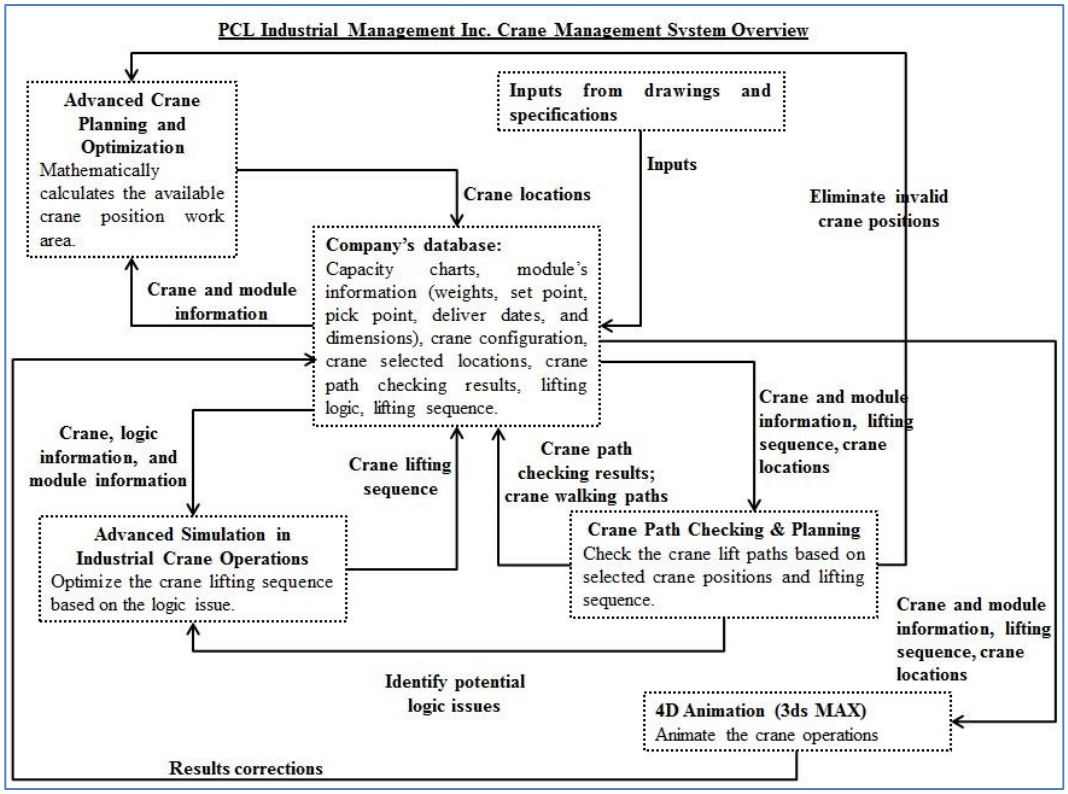

Figure 3-3 PCL Industrial Management Inc. crane management system

Based on the boundary limits, the crane's tail-swing geometry is used to create the crane position work area; (a detailed algorithm for cranes without tail-swing has been presented by Safouhi et al. (2011)). Meanwhile, the entire site is gridded (Figure 3-4b), and the grid points located in the crane position work area are obtained (Figure 3-4c). Based on these obtained grid points, the points where the crane has sufficient capacity and boom clearance to lift the modules are selected

as possible crane locations (Figure 3-4d). However, these locations may not be applicable for performing the lifts, and thus need to be passed to the CPCP program for further checking.

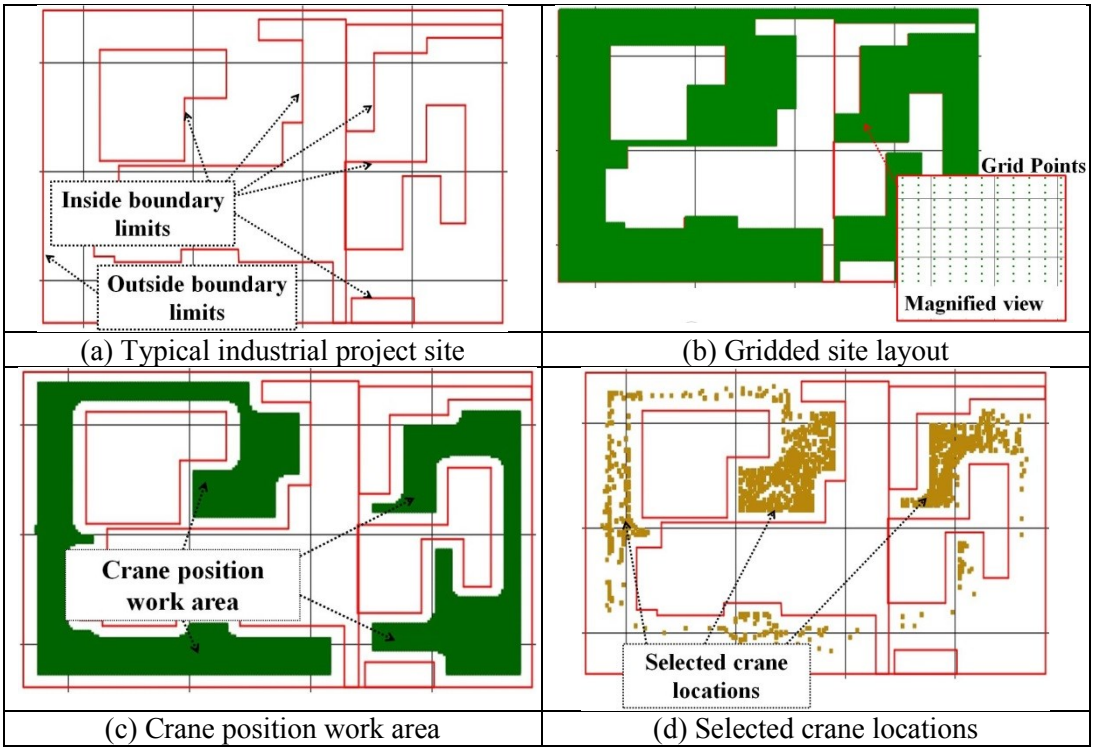

(a) Typical industrial project site | (b) Gridded site layout

(c) Crane position work area | (d) Selected crane locations

Figure 3-4 Crane location selection

3.1.2 Crane Lift Sequencing

In PCL's crane management system, ASICO plans the lifting sequence according to the pre-defined lifting logics (e.g., the modules at the lower elevations need to be installed before erecting the modules at the higher elevations). Field installation of the prefabricated modules is the last step in industrial project construction. The sequence of lifting these modules has a significant impact on project cost and schedule, and the process of planning the lift sequence is complex and must accommodate several logical considerations (Taghaddos et al. 2010),

outlined as follows: (*i*) it is efficient to erect the modules in sequence rather than randomly placing them on the site; (*ii*) it is technically challenging to place a module between two adjacent modules; (*iii*) the module at the bottom position should precede the above modules on the lift sequence; (*iv*) for some predefined areas, cranes are only available for a limited period of time; and (*v*) once a given module is installed on site, the occupied area is no longer available, such that the newly installed module becomes a site constraint. Based on these constraints, Taghaddos et al. (2010) have proposed a computer-aided system to be used in arranging the field construction lift sequence. A case of implementation of this system has been presented by Taghaddos et al. (2012). The outputs of the system include: (*i*) selection of suitable mobile cranes for all lifts during the project period; and (*ii*) a lifting schedule satisfying the availability and accessibility of the cranes, which considers crane mobilization and demobilization time, initial locations, configurations, and riggings. The generated outputs are visualized in a 4D animation module, and the produced lifting sequence is used for CPCP as one of the inputs. One limitation of the current system is that once CPCP identifies the crane locations that do not have lift paths, the results must be fed back into ASICO for re-planning of the sequence. Research efforts are ongoing to solve this problem, with two alternative strategies currently underway: (*i*) establish a loop mechanism between ASICO and CPCP to optimize the lifting sequence; and (*ii*) integrate the CPCP algorithms into the current ASICO system in order to identify the logical constraint once and thus generate a more reasonable sequence without any loop calculation.

3.2 General Assumptions for Crane Motion Planning

As for the crane motion planning, it is assumed that the project structure is constructed by modules simplified as box shapes; (see Figure 3-5 for a typical industrial module and its simplification as a rectangular box). In addition, since the project structure comprises stacked components that can be simplified as rectangular boxes, the 3D site layout can be described and represented in terms of site elevations, where the project structure is assumed to remain invariant between adjacent elevations (Figure 3-6). Ideally, all of the site elevations are taken into account. However, a trade-off is required: too many elevations can increase the computation workload, and thus result in inefficiency, while too few elevations can lead to oversimplification of the site layout. Therefore, an elevation tolerance is provided as a user-defined parameter which determines the minimum height difference between two adjacent elevations. Eq. (1) is proposed to be used to determine the elevations. In this research, it is also assumed that the ground bearing is sufficient for the mobile crane movements, and the proper ground preparation has already been conducted prior to the analysis.

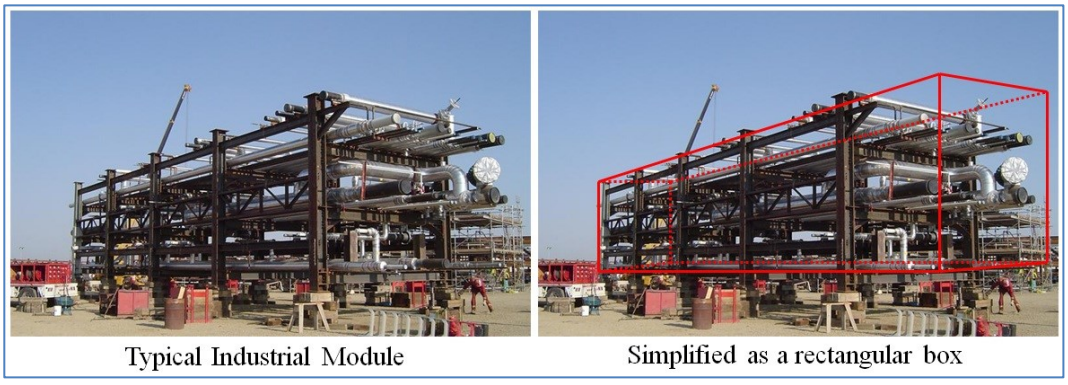

Figure 3-5 Shape simplification of industrial module

Figure 3-6 Site elevations

$$ET \le \left| E_i - E_{i+1} \right| \qquad (i = 0,1,2...,n-1) \tag{1}$$

Where:

ET = elevation tolerance;

E_i = elevation i; and

E_{i+1} = elevation i+1; there are a total of n elevations.

3.3 Path Checking (Pick-and-swing Analysis) in General

Based on the assumptions mentioned in section 3.2 above, the proposed methodology investigates the feasibility of lift paths at each specific elevation (i.e., path checking). The investigations begin from the highest elevation down to the module's set elevation, and each investigation is performed on one elevation at a time. In addition, if the module does not have a lift path after all the elevations have been checked individually, the methodology subsequently checks the feasibility of the lift path through the overlaid elevation combination. The main process of the proposed path checking approach follows the flowchart shown in Figure 3-7. In this process, there are three primary functions: (*i*) determination of elevations; (*ii*) path checking on individual elevations; and (*iii*)

path checking on the overlaid elevation combination. The function "path checking on individual elevations" consists of three sub-algorithms: (*i*) elevation determination algorithm; (*ii*) crane feasible operational range algorithm; and (*iii*) pick area algorithm. These algorithms will be explained in detail in the following section.

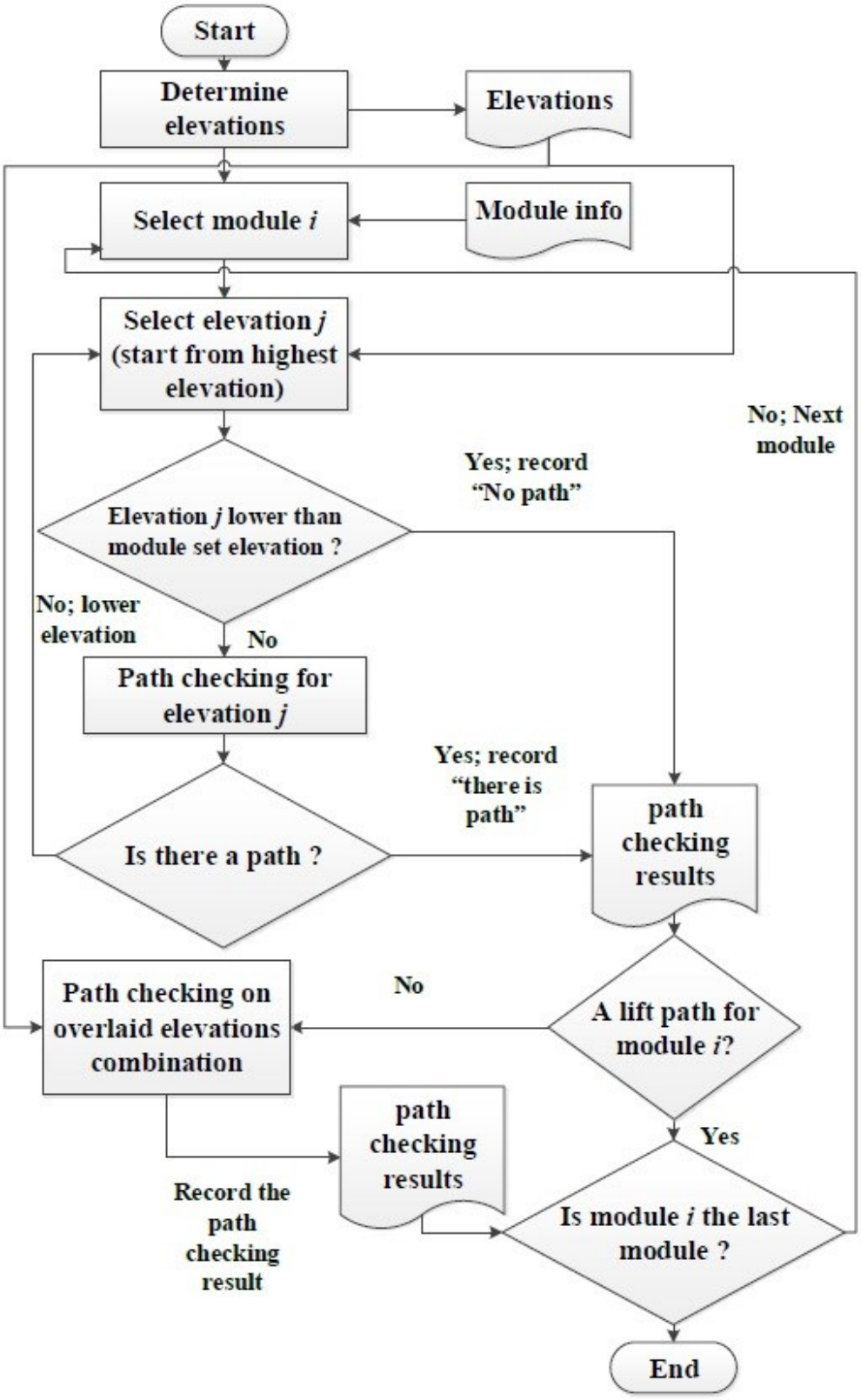

Figure 3-7 Flowchart for path checking

3.4 Path Checking on Individual Elevations

The flowchart for the path checking on individual elevations is illustrated in Figure 3-8. Inputs related to site layout, which includes the site boundary and onsite existing obstructions, are represented by the coordinates of object vertices obtained from the CAD models. The modules are installed based on a planned schedule; modules are usually delivered by trucks to predetermined pick locations, and then erected by mobile cranes. Modules' pick dates and locations are also entered as inputs. In addition, specific crane locations are selected for lifting modules and entered as inputs. All the inputs are stored in the company's central database, and the lift path check system reads the data and performs path checking. The path checking is subject to several criteria, such as site boundaries, crane categories, module delivery time, and site truck route. The lift path checking program consists of four steps:

(i) Calculate the minimum and maximum radii (referred to subsequently as R_{min} and R_{max}) for a specific crane based on the boom clearance and crane capacity.

(ii) Adjust the lifting range according to the site obstructions and the crane's tail-swing or superlift constraints.

(iii) Generate the configuration space obstacle (*C-Obstacle*) using the configuration space (C-Space) approach to simplify the layout.

(iv) Plot all calculated results on a 2D plan view and check feasibility of the lift path.

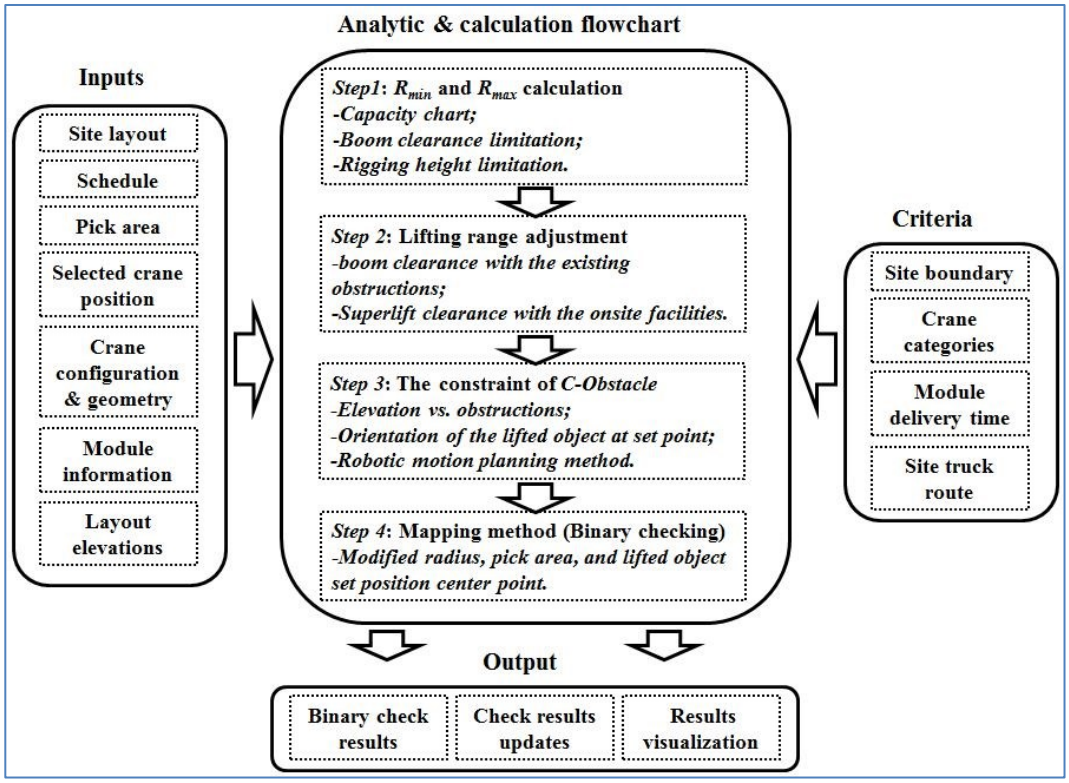

Figure 3-8 Methodology for path checking on individual elevations

The outputs are the binary (yes-or-no) check results, which indicate the feasibility of the lift path; (a visualization function is available to present the results). Results are written back to the database, and can be recalculated when project information is updated. Two elevations are selected for path checking for this case. The first is the lifted module set elevation on which the lifted module is placed at its set point, and the second is the pick/sit elevation on which the mobile crane sits and the lifted module is picked from its pick point (see Figure 3-9). It is assumed that the lifted module is hoisted up from the pick point to its set elevation directly and then swung to its set position, which is consistent with common mobile crane practice. Obstructions with a higher elevation than the set elevation are considered as barriers for the lift path. The calculation of the mobile crane's R_{min} and R_{max} is

based on the module's set elevation, which will be discussed in the following section.

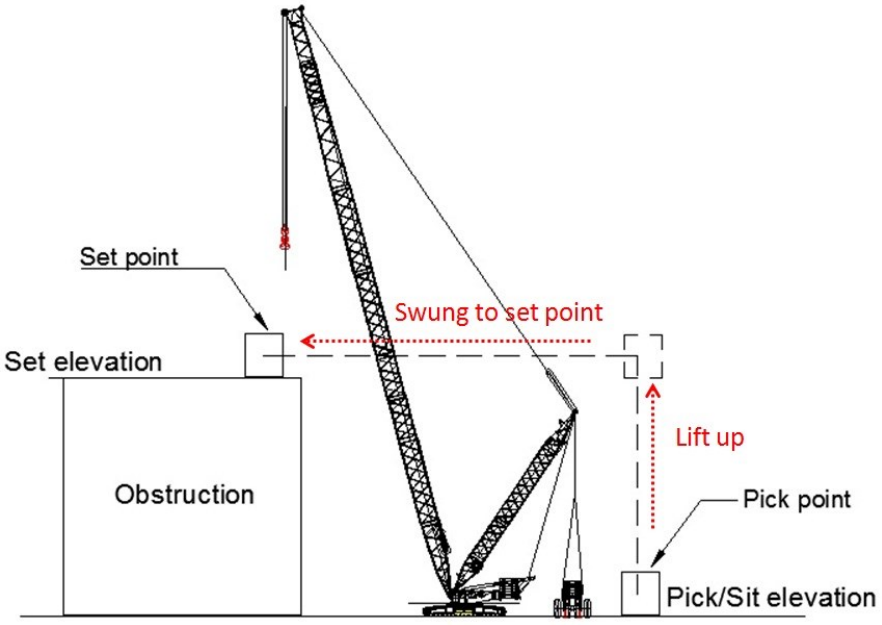

Figure 3-9 Set elevation and pick elevation

3.4.1 Step 1: R_{min} and R_{max} Calculation

The first step for the path check is to calculate the mobile crane's R_{min} and R_{max}, which represent the nearest and furthest lifting range for the mobile crane, respectively. The determination of R_{min} and R_{max} depends on two factors: (*i*) Total weight of the lifted module (W_t), which is calculated satisfying Eq. (2); and (*ii*) Boom clearance and rigging height requirements. The total weight of the lifted module (W_t) is used to identify the crane's feasible lift range based on the capacity chart provided by the crane manufacturer. Practitioners often apply a user-defined safety percentage (P_s) (e.g., 85%) to ensure the lift's safety.

$$W_t = \frac{(W_m + W_l + W_w + W_a + W_s + W_r)}{P_s} \quad (2)$$

Where:

W_t = total weight of lifted module;

W_m = module weight;

W_l = load block weight;

W_w = wire rope weight;

W_a = auxiliary head weight;

W_s = sheave block weight;

W_r = rigging weight; and

P_s = safety percentage.

R_{min} and R_{max} also depend on boom clearance and rigging height requirements. The boom clearance ensures sufficient free space between the lifted module and the crane's boom. A minimum boom clearance buffer (B_{mbc}) (see Figure 3-10(a)) is required for safe operations. The corresponding boom angle (Θ_{mbc}) to this buffer (B_{mbc}) with the horizontal line (see Figure 3-10(a)) defines the corresponding distance (D_{mbc}) to the crane's center, which is calculated satisfying Eq. (3). D_{mbc} is compared to the lifting range from the capacity chart to determine the value of R_{min}. The rigging design for the lifted module determines the crane's maximum reach (D_r) (see Figure 3-10(b)), which is calculated satisfying Eq. (4), accounting for the rigging equipment height (H_r) and the module location height (H_{se}). The calculated D_r must also satisfy Eq. (5), which gives the range of R_{max}. Figure 3-11 illustrates an example of the calculated R_{min} and R_{max} shown on the plan view. The grey area in Figure 3-11 presents the mobile crane's feasible lift range, and R_{min} and R_{max} define the crane's minimum and maximum lifting range, respectively.

$$D_{mbc} = L_b \times \cos(\theta_{mbc}) \tag{3}$$

$$D_r = \sqrt{(L_b)^2 - (H_r + H_m + H_{se})^2} \tag{4}$$

$$D_r \leq R_{\max} \tag{5}$$

Where:

D_{mbc} = crane's minimum reach;

L_b = crane boom length;

Θ_{mbc} = boom angle satisfying the minimum boom clearance buffer in Figure 3-10(a) (B_{mbc});

D_r = crane's maximum reach;

H_r = minimum rigging height;

H_m = module height; and

H_{se} = module's set elevation height.

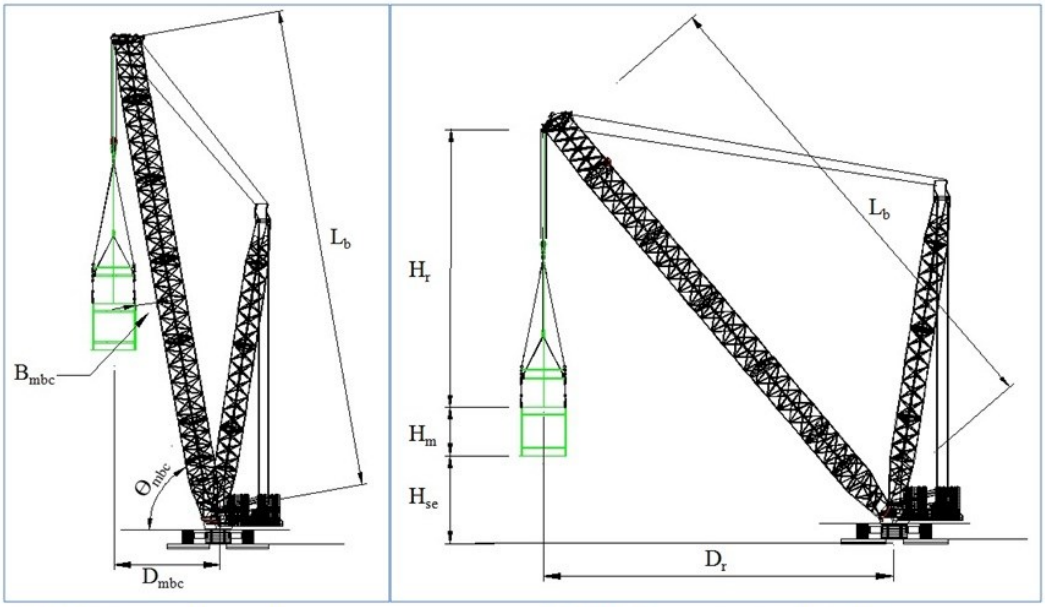

(a) Minimum boom clearance (b) Minimum rigging height

Figure 3-10 Boom clearance and rigging height limitations

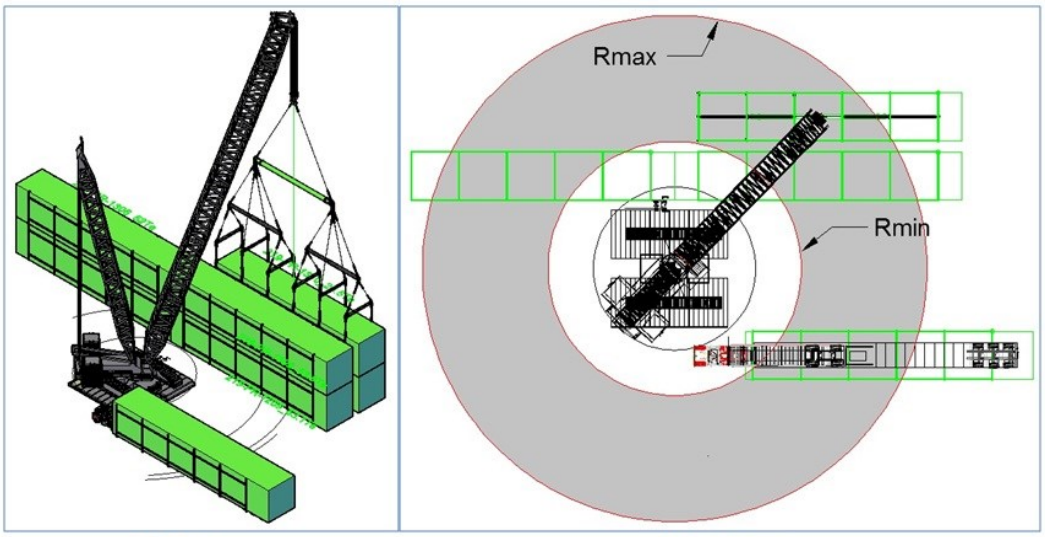

Figure 3-11 R_{min} and R_{max} on plan view

3.4.2 Step 2: Lifting Range Adjustment

Industrial project sites often are congested with existing obstructions. As a result, crane lifts become increasingly challenging, and the lifting range determined in step 1 may not represent the actual feasible lifting range for the mobile crane. Two more constraints must be accounted for: (*i*) the height of the existing obstruction; and (*ii*) the crane's tail-swing or the superlift, an attachment to the mobile crane used to increase crane lift capacity. The effect of these two constraints on R_{min} and R_{max} will be discussed in the following sections.

Effect of Site Obstruction Height on the Lifting Range

The height of the existing obstruction may cause conflicts with the crane's boom at R_{max} (see Figure 3-12(a)). As a result, R_{max} should be adjusted to provide sufficient boom clearance by determining a minimum boom clearance for the obstruction (BC_m in Figure 3-12(b)). The crane's boom has to boom back a certain

distance ($D_{adjusted}$ in Figure 3-12(b)) and, consequently, R_{max} is reduced to a new lifting range ($R_{adjusted}$), shown as Figure 3-12(b), that allows the crane to perform lifting without any conflict. In order to calculate $R_{adjusted}$ and enhance the readability of this work, Figure 3-12(b) is simplified as Figure 3-13. According to Figure 3-13, the $R_{adjusted}$ is calculated using Eq. (6), Eq. (7), Eq. (8), Eq. (9), and Eq. (10), which are subject to the values of L_b, H_o, and D_{to}. D_{to} is the shortest distance from the crane's centre to the obstruction (see Figure 3-12(c)). In Figure 3-12(c), the R_{min} and R_{max} are shown, and an adjusted range (the grey section) is defined by $\Theta_{adjusted}$, within which the R_{max} must be reduced to $R_{adjusted}$. We assume that within $\Theta_{adjusted}$, R_{max} is adjusted by the same amount for every angle. Points A and B in Figure 3-12(c) represent the starting and ending angles of $\Theta_{adjusted}$ considering half the width of the boom ($1/2W_b$), which can be calculated satisfying Eq. (11). Θ_B and Θ_A in Figure 16c can be calculated using Eq. (12) and Eq. (13), respectively. Figure 16d presents the crane's feasible lifting area in the plan view.

$$D_1 = \sqrt{H_o^2 + D_{to}^2} \tag{6}$$

$$\theta_1 = \tan^{-1}\left(\frac{H_o}{D_{to}}\right) \tag{7}$$

$$\theta_2 = \cos^{-1}\left(\frac{BC_m}{D_1}\right) \tag{8}$$

$$\Delta h = \frac{BC_m}{\cos(\theta_1 + \theta_2)} \tag{9}$$

$$R_{adjusted} = \frac{D_{to} L_b}{\sqrt{D_{to}^2 + (H_o + \Delta h)^2}} \tag{10}$$

$$\theta_{adjusted} = \theta_B - \theta_A \tag{11}$$

$$\theta_B = (\tan^{-1} \frac{|y_b - y_c|}{|x_b - x_c|}) + \pi \tag{12}$$

$$\theta_A = (\tan^{-1} \frac{|y_a - y_c|}{|x_a - x_c|}) + \frac{\pi}{2} \tag{13}$$

Where:

$R_{adjusted}$ = crane's adjusted radius, considering the boom clearance in Figure 3-12(b);

L_b = boom length in Figure 3-12(b);

D_{to} = shortest distance between crane's sit position and obstruction in Figure 3-12(b);

H_o = obstruction height;

$\Theta_{adjusted}$ = angle within which R_{max} needs to be reduced to $R_{adjusted}$ in Figure 3-12(c);

Θ_B = angle formed by three points (Point *B*, crane centre point, and Point *D* in Figure 3-12(c));

Θ_A = angle formed by three points (Point *A*, crane centre point, and Point *D* in Figure 3-12(c)).

(x_b, y_b) = coordinates of Point *B* in Figure 3-12(c);

(x_a, y_a) = coordinates of Point *A* in Figure 3-12(c); and

(x_c, y_c) = coordinates of the crane centre in Figure 3-12(c).

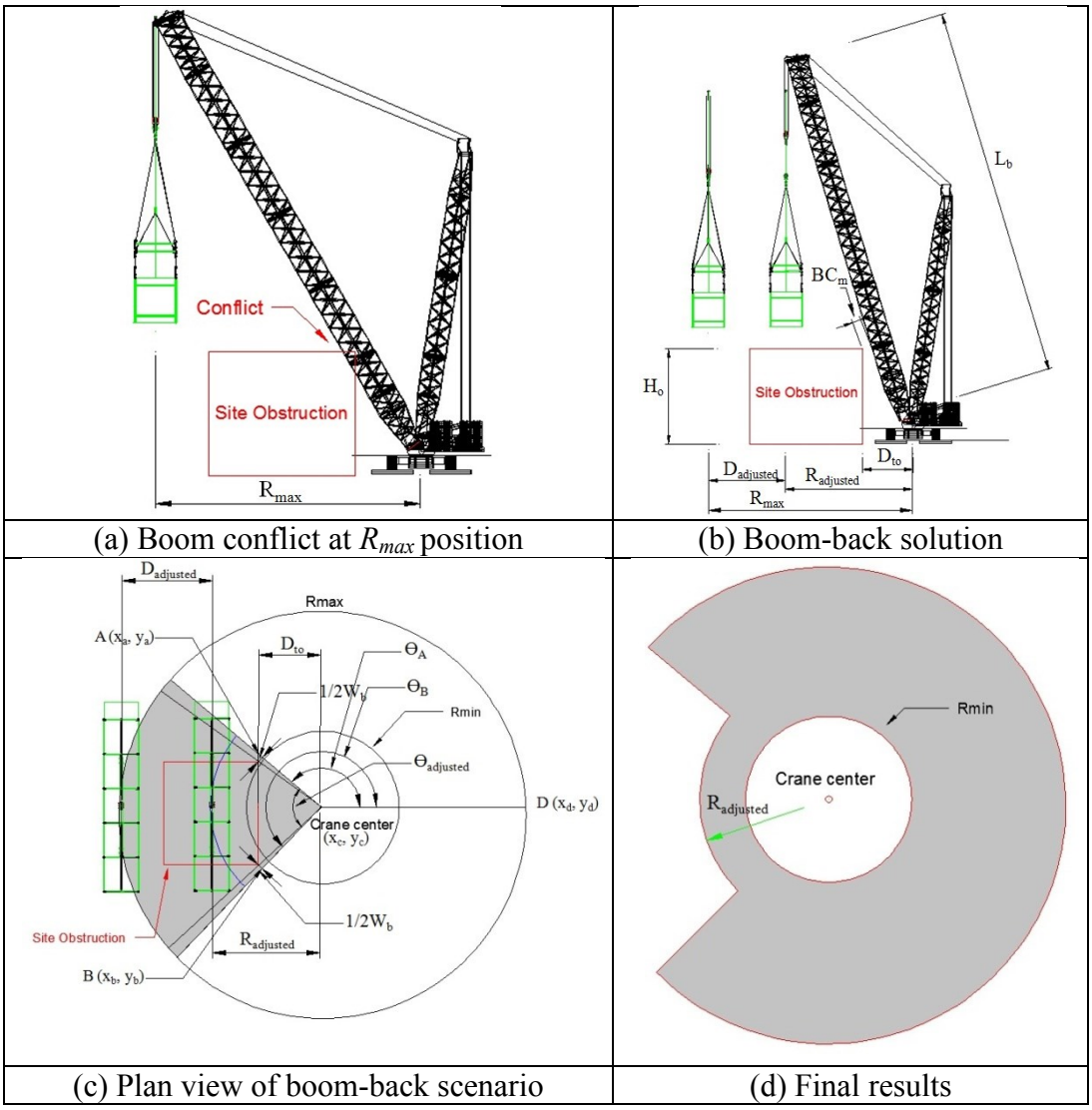

(a) Boom conflict at R_{max} position | (b) Boom-back solution

(c) Plan view of boom-back scenario | (d) Final results

Figure 3-12 Impact of boom clearance on R_{max}

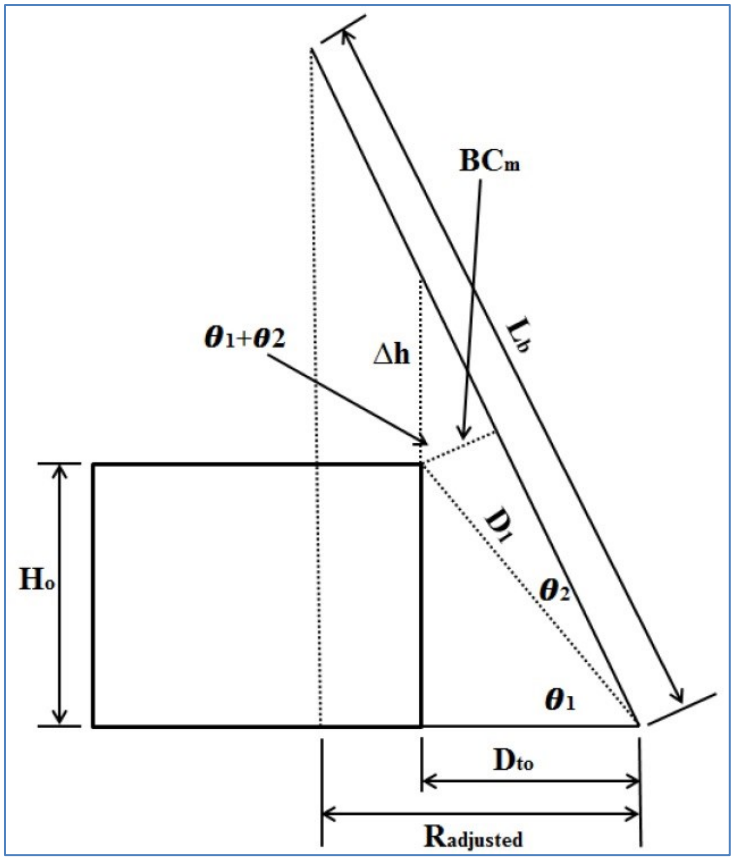

Figure 3-13 Simplification of Figure 3-12b

Effect of Crane Tail-swing and Superlift Structure on Lifting Range

The crane's tail-swing, including counterweight or superlift equipment, may affect the crane's feasible lifting range (see Figure 3-14 for examples of tail-swing and superlift structure). During the crane lift, the superlift's movement (tail-swing movement can be handled using the same method) at ground elevation may conflict with existing site obstructions surrounding the crane. Figure 3-15(a) provides a plan view example where the superlift collides with the site obstruction in the range that is bounded by Θ_{sl}. Since the superlift cannot move into the range, Θ_{sl}, the mobile crane's boom cannot move into the corresponding area (A_{sl} in Figure 3-15(a)) of the opposite side angle (Θ_{osl}) of Θ_{sl}. Θ_{sl} is determined by points

A_{sl} and B_{sl}, considering a superlift buffer (B_{sl}), while Θ_{osl} is calculated satisfying Eq. (14). Based on the range of Θ_{osl}, a new feasible lifting area is formed (Figure 3-15(b)).

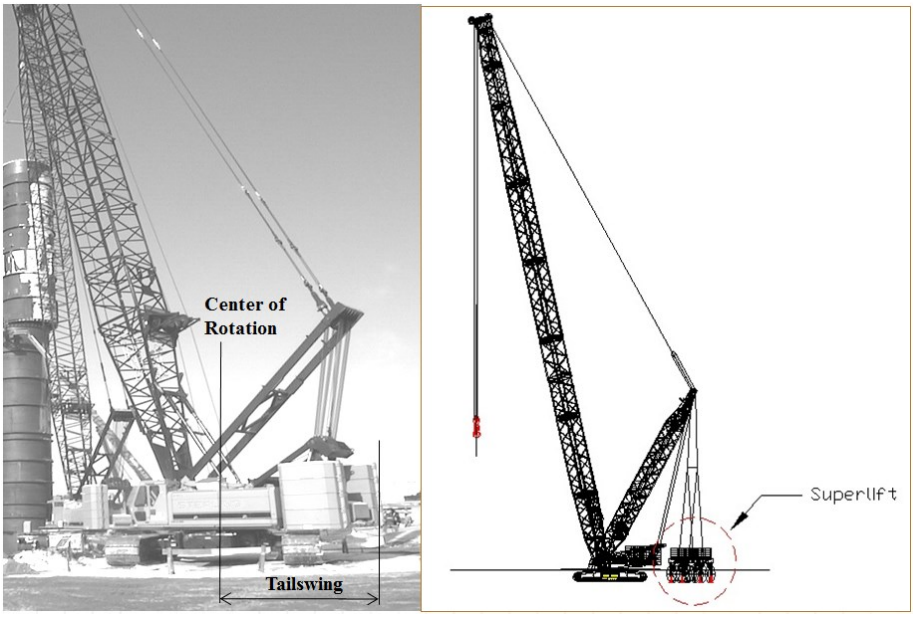

Figure 3-14 Crawler Crane with tail-swing/superlift structure

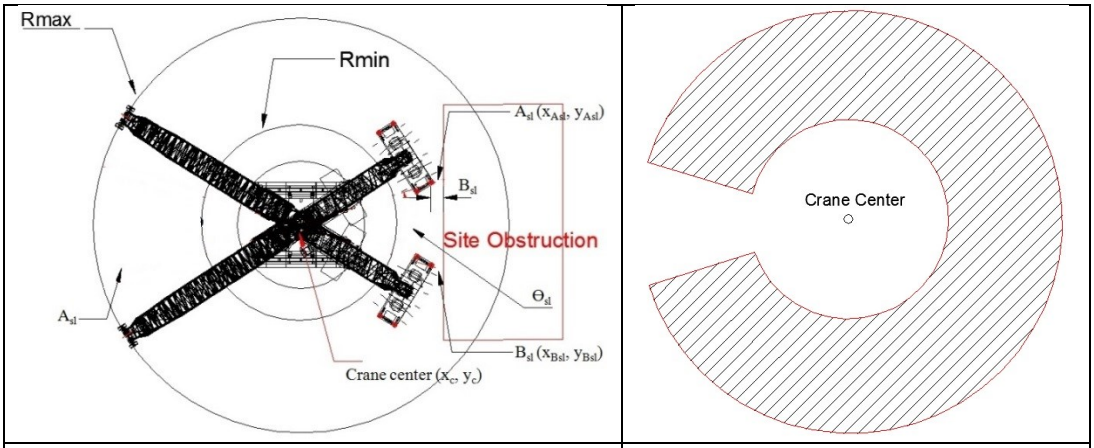

(a) Superlift conflict with site obstruction plan view

(b) Feasible lifting area after erasing A_{sl}

Figure 3-15 Superlift constraint and impact

$$\theta = \cos^{-1}\left(\frac{(x_{Asl} - x_c)(x_{Bsl} - x_c) + (y_{Asl} - y_c)(y_{Bsl} - y_c)}{\sqrt{(x_{Asl} - x_c)^2 + (y_{Asl} - y_c)^2}\sqrt{(x_{Bsl} - x_c)^2 + (y_{Bsl} - y_c)^2}} \right) \quad (14)$$

Where:

Θ = the angle within which the superlift collides with the site obstruction in Figure 3-15(a);

Θ_{osl} = the opposite angle of Θ_{sl} in Figure 3-15(a);

(x_c, y_c) = the coordinates of the crane centre in Figure 3-15(a);

(x_{Asl}, y_{Asl}) = the coordinates of Point A_{sl} in Figure 3-15(a); and

(x_{Bsl}, y_{Bsl}) = the coordinates of Point B_{sl} in Figure 3-15(a).

3.4.3 Step 3: The Constraint of C-Obstacle

In this research, the site layout is simplified by applying the C-Space approach. The site obstructions are converted into C-Obstacles, and the lifted module is represented by its geometric center. The nature of robot movements and module crane lifts from a plan view is similar, and therefore the C-Space approach can be employed to solve the module lift problem. The methodology of the C-Space approach originated from Lozano-Pérez (1983), who proposed a method, called obstacle growth, which uses Minkowski point-set operations to solve a 2D robotic path planning problem. The core idea of this method is to simplify the shape of the moving robot into a single representing point, converting the existing obstacles into C-Obstacles. This simplification makes it possible to search the path for only the representing point rather than arranging the trajectory based on the entire shape of the robot (in this paper, the lifted module). Figure 3-16(a) shows a case of C-Obstacle creation for a square site obstruction and a square lifted module. The coordinates for the lifted module's four vertices are (x_{lmi}, y_{lmi}) (i=1, 2, 3, and 4), and the coordinates for the site obstruction's four vertices are

(x_{obi}, y_{obi}) (i=1, 2, 3, and 4). The geometric center of the lifted module is selected as the representing point (x_{rp}, y_{rp}) in Figure 3-16(a), and the coordinates (x_i, y_i) (i = 1, 2, 3, and 4) of the vectors, which point from the vertices of the lifted module to the representing point, are calculated satisfying Eq. (15) and Eq. (16).

$$x_i = x_{rp} - x_{lmi} (i = 1, 2, 3, and\, 4) \tag{15}$$

$$y_i = y_{rp} - y_{lmi} (i = 1, 2, 3, and\, 4) \tag{16}$$

Where:

(x_i, y_i) (i = 1, 2, 3, and 4) = the coordinates of the vector that points from the vertex, (x_{lmi}, y_{lmi}) (i = 1, 2, 3, and 4), to the representing point (x_{rp}, y_{rp}).

The calculated vertices $(\vec{x_i}, \vec{y_i})$ (i = 1, 2, 3, and 4) from Figure 3-16(a) are then added to each vertex of the site obstruction, and each vertex of the site obstruction is split into four nodes (Figure 3-16(b)). Therefore, sixteen nodes are generated from four vertices of the site obstruction, as shown in Figure 3-16(b), and their coordinates are calculated satisfying Eq. (17) and Eq. (18). A convex hull is created to encompass all the nodes, shown as the red dashed line in Figure 3-16(b) and Figure 3-16(c), which is also the generated C-Obstacle. In Figure 3-16(c), if the geometric center (which in this case is also the selected representing point) of the lifted module is located outside of the C-Obstacle (Position A), there is no conflict between the lifted module and the site obstruction. At position B in Figure 3-16(c), where the geometric center of the lifted module lies on one edge of the C-Obstacle, the lifted module and site obstruction just come into contact with one another. A conflict occurs at position C in Figure 3-16(c) since the

geometric center of the lifted module enters the C-Obstacle. Instead of tracking the lifted module's position by its entire shape and avoiding the collision, the position of the lifted module's geometric center (i.e., the representing point) can be used to detect collisions between the lifted module and site obstruction. In practice, when the lifted module is rotated while lifting, the C-Obstacle should be recalculated based on the corresponding rotation angle.

$$x_{obi}^{lmj} = x_{obi} + \vec{x}_j (i = 1, 2, 3 \; and \; 4; j = 1, 2, 3, and \; 4) \tag{17}$$

$$y_{obi}^{lmj} = y_{obi} + \vec{y}_j (i = 1, 2, 3 \; and \; 4; j = 1, 2, 3, and \; 4) \tag{18}$$

Where:

$(x_{obi}^{lmj}, y_{obi}^{lmj})$ = the node in Figure 3-16(b) with vector, $(\vec{x_i}, \vec{y_i})$ (j=1, 2, 3, and 4), added to vertex, (x_{obi}, y_{obi}) (i=1, 2, 3, and 4).

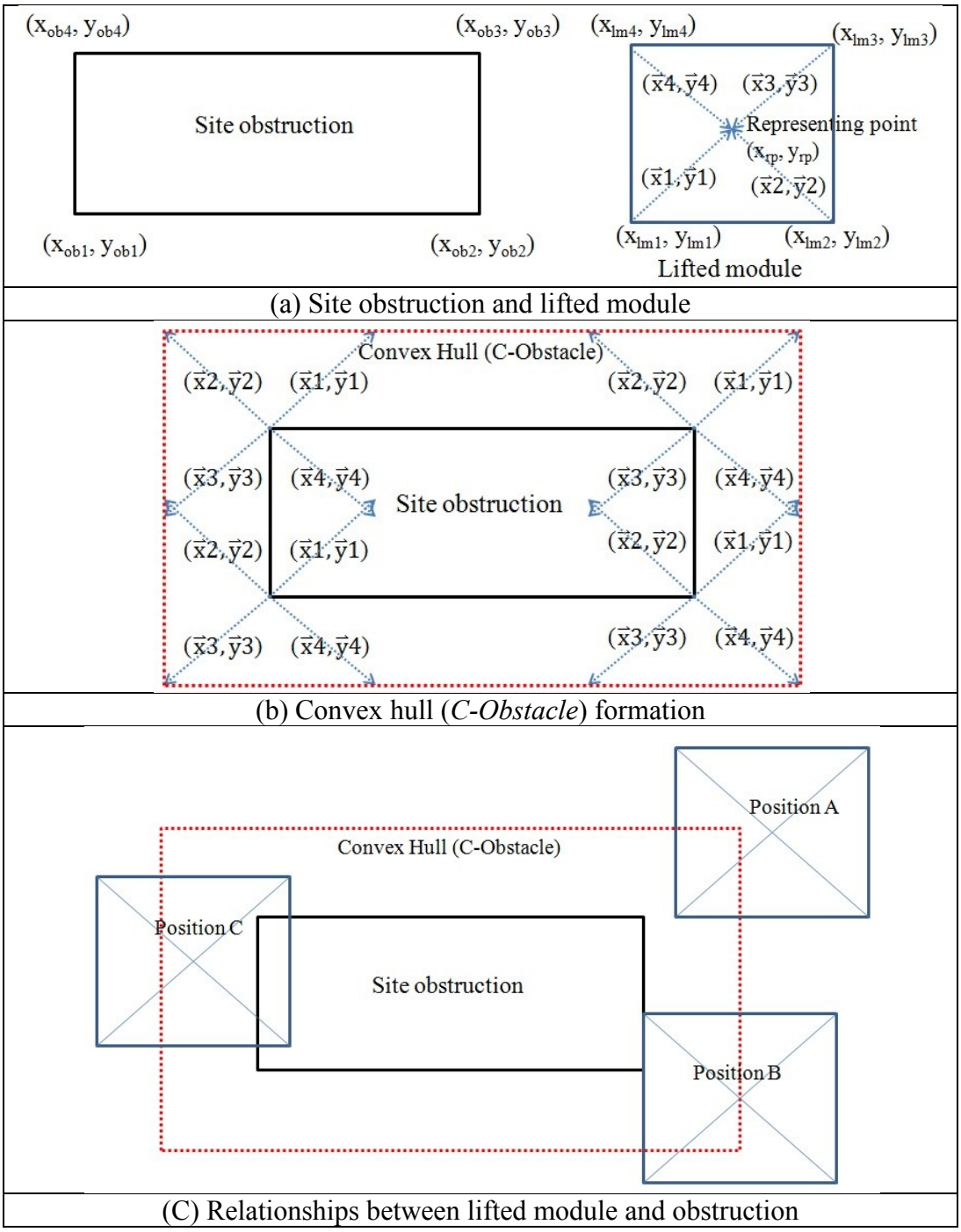

Figure 3-16 Case of C-Obstacle formation

3.4.4 Step 4: Mapping Method

The last step for the proposed method illustrated in Figure 3-8 is the mapping step, which integrates the previous three steps (R_{min} and R_{max} calculation, lifting

range adjustment, and constraint of C-Obstacle) to perform path checking. Figure 3-17 presents a series of figures illustrating the mapping process. Figure 3-17(a) and Figure 3-17(b) show the 3D view and front view of a case lift, respectively. This case has three obstructions, (OB1, OB2, and OB3), and the lifted module is picked from the pick area and moved to its set point. The mobile crane in this case has a superlift attachment (see Figure 3-17(a)). On the plan view (Figure 3-17(c)), the mobile crane's R_{min} and R_{max} are calculated and presented (refer to "step 1: R_{min} and R_{max} calculation"). Due to the height of OB2 and a superlift conflict with OB3 on the pick elevation, R_{min} and R_{max} are modified by erasing the shaded area in Figure 3-17(c) (refer to "step 2: lifting range adjustment"). Figure 3-17(d) illustrates the C-Obstacle generation for OB2, where OB2 is higher than the set elevation and its corresponding geometric configuration on the plan view needs to be considered as a barrier for the path checking. The *C-Obstacle* for OB2 is eliminated and the crane's feasible lifting area is shown as the grey area in Figure 3-17(e). The pick area overlaps with the crane's feasible operation range (yellow area in Figure 3-17(e)), and the module can be lifted from the pick area to the set elevation and swung to its set point. A possible path (PP) is drawn as a red curve in Figure 3-17(e).

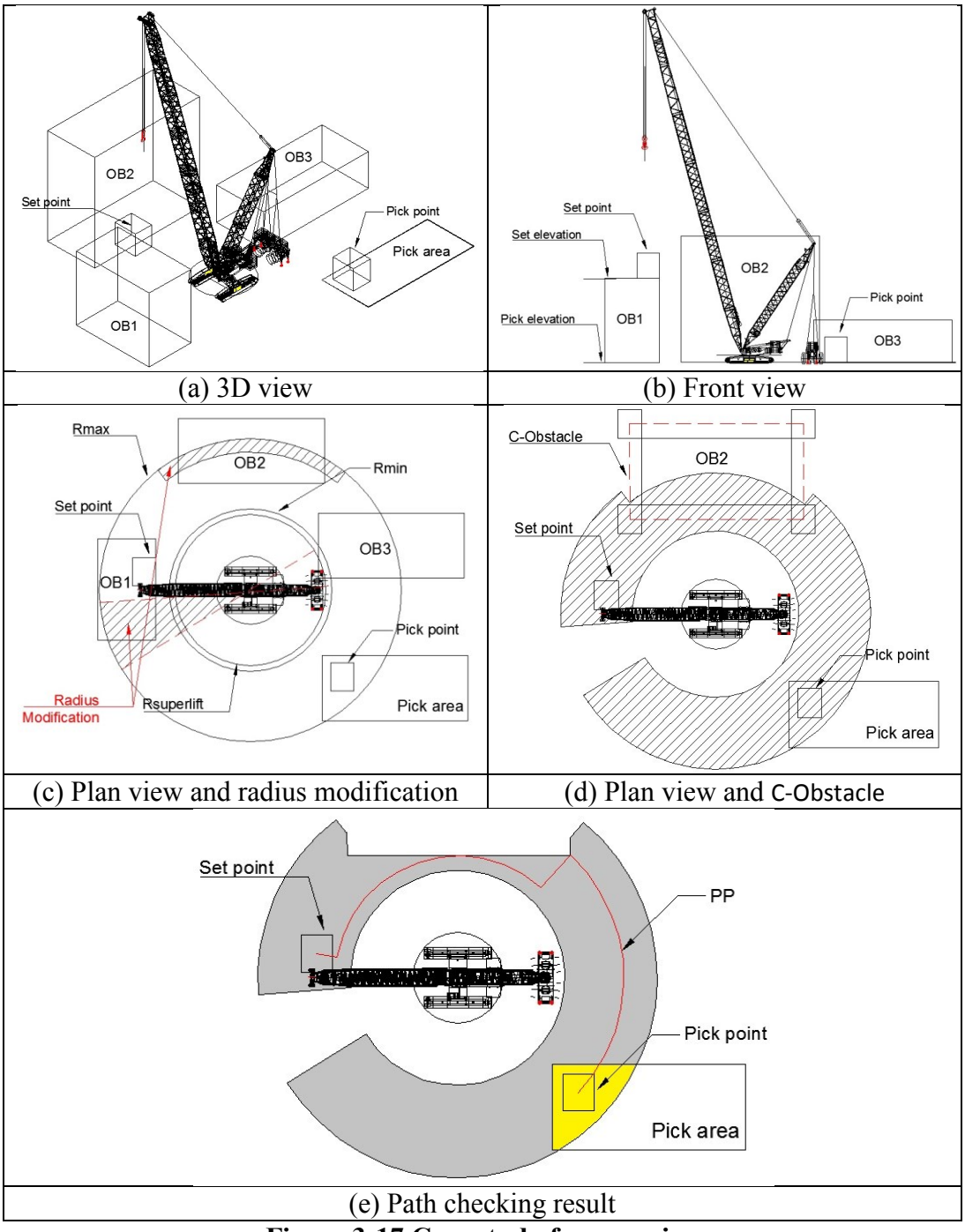

(a) 3D view | (b) Front view

(c) Plan view and radius modification | (d) Plan view and C-Obstacle

(e) Path checking result

Figure 3-17 Case study for mapping

The crane's feasible operation range is calculated for each individual elevation, and represents the area in which the crane can perform the lift without any collisions. The crane's feasible operation range is calculated following three steps:

(i) The mobile crane's minimum and maximum radii (referred as R_{min} and R_{max}) are used to define an area where the crane can lift the module without exceeding its lifting capacity. R_{min} and R_{max} are usually calculated according to the crane's capacity chart such that they satisfy the boom clearance and minimum required rigging height requirements.

(ii) The R_{min} and R_{max} are then modified, considering the crane's boom clearance together with the obstruction and tail-swing equipment constraints; the crane's feasible operation range is then modified accordingly.

(iii) The motion planning method (Lozano-Pérez 1983) is applied in order to simplify the layout on the selected elevation. The pick area for the lifted module is calculated satisfying Eq. (19), fulfilling three requirements: (a) the pick area should overlap with the crane's feasible operation range and the site boundary so that the crane can reach the module; (b) within the pick area, the lifted module should not have any conflicts with the surrounding structures at the ground elevation; and (c) the pick area should also overlap with potential pick areas, which are specific areas, such as roads for delivery trailers, which have been pre-defined for module pick up. Once the crane's feasible operation range and pick area have been calculated, the feasibility of the lift path is checked employing Eq. (20).

$$A'_{pick} = (A_{feasible} \cap A_{site} \cap A_{p-pick}) - A^{i}_{obstruction} \tag{19}$$

$$result = \begin{cases} 0 \text{ (there is path)} & A_{feasible} \cap A'_{pick} \neq \varnothing \text{ and } P_{\text{set}} \in A_{feasible} \\ 1 \text{ (no path)} & A_{feasible} \cap A'_{pick} = \varnothing \text{ or } P_{\text{set}} \notin A_{feasible} \end{cases} \tag{20}$$

Where:

A'_{pick} = pick area for the lifted module;

$A_{feasible}$ = crane's feasible operational range;

A_{site} = site boundary;

A_{p-pick} = potential pick area;

$A^{i}_{obstruction}$ = area of site obstruction i (i=1,2,…,m); there are total m site obstructions; and

P_{set} = module set point (x, y).

3.4.5 Illustrative Example of Pick-and-swing Analysis

In this section, a simple case is provided in order to demonstrate the path checking process. Figure 3-18 presents the case scenario: a mobile crane is employed to lift a module from its pick point to its set point. In this case, the lifted module's set point elevation is selected for analysis. From a plan view of the case scenario (Figure 3-19(a)), the R_{min} and R_{max} are calculated and modified, considering boom clearance and tail-swing equipment (superlift equipment) constraints. Based on these modifications, a robotic motion planning method is applied to simplify the site layout. In Figure 3-19(b), "Obstruction 3" is grown by the shape of the lifted module to form a C-Obstacle. For "Obstruction 1" and "Obstruction 2", since they are lower than the module's set point elevation, there is no need to include them for C-Obstacle formation. The crane feasible operation range is formed as shown in Figure 3-19(b).

The module's pick area is created based on the crane's feasible operational range (Figure 3-19(c) and Figure 3-19(d)). The site obstruction area is generated based on the ground elevation layout, and the obstructions are grown by half the module's diagonal length (dashed lines shown in Figure 3-19(c)). The obstruction areas are then subtracted from the crane's feasible operational range to form the pick area, shown as the green area in Figure 3-19(d). The module path is checked using Eq. (20), verifying that there is a possible lift path for the module.

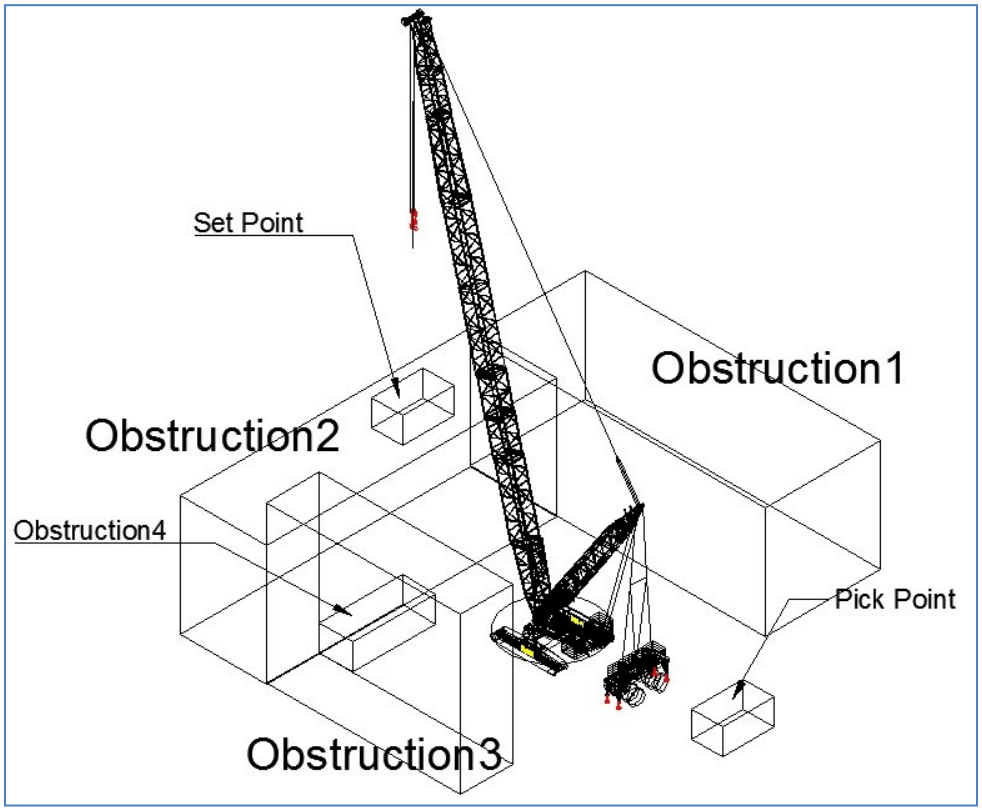

Figure 3-18 Case scenario for path checking on individual elevations

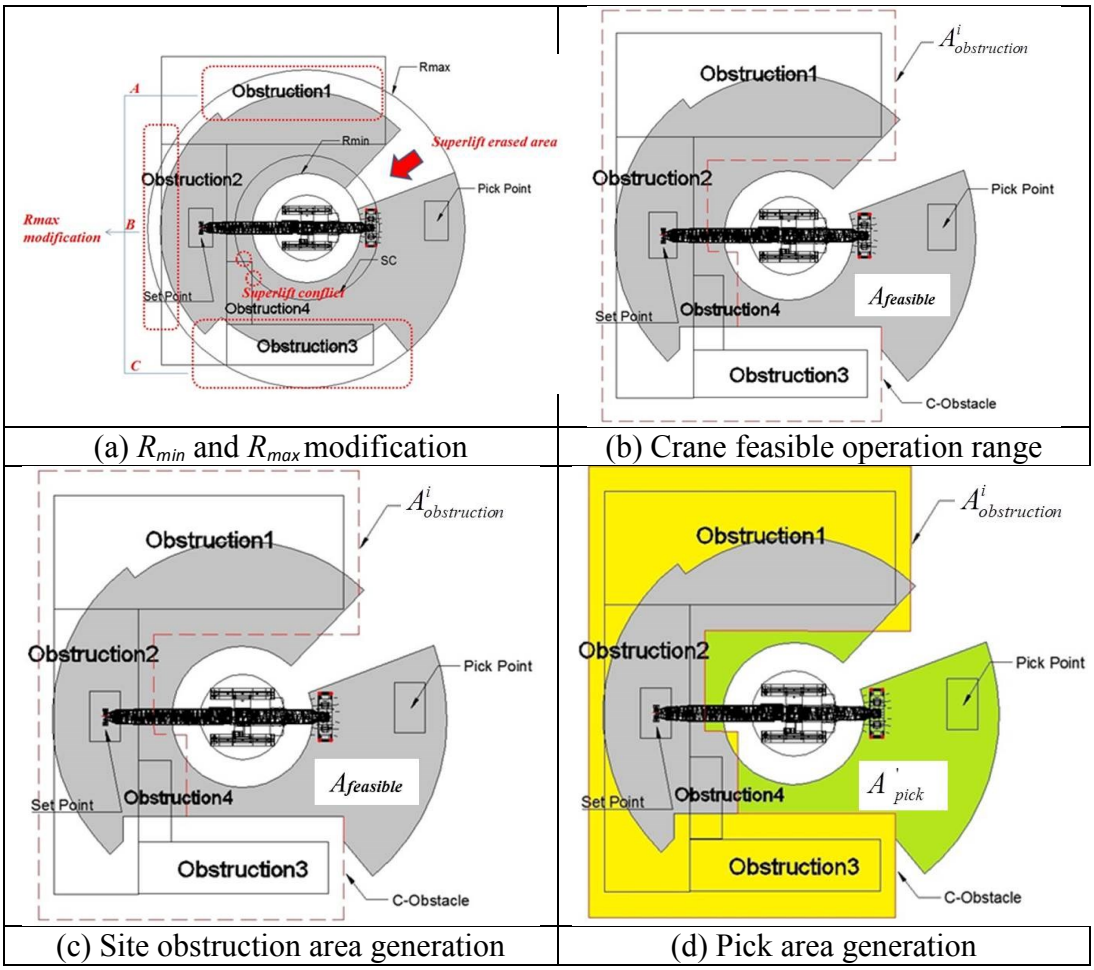

(a) R_{min} and R_{max} modification | (b) Crane feasible operation range

(c) Site obstruction area generation | (d) Pick area generation

Figure 3-19 Crane's feasible operational range and pick area

3.5 Path Checking on Multi-Elevations

If the path checking fails at each individual elevation, the algorithm further investigates the possibility of a lift path on the overlaid elevation combination. To obtain the overlaid elevation combination, (*i*) the crane's feasible operational ranges and pick areas are calculated for each determined elevation, and (*ii*) the calculated crane feasible operational ranges and pick areas are overlaid, and their unions are obtained using Eq. (21) and Eq. (22) beginning from the highest project elevation and descending to the module's set elevation. The obtained unions are the overlaid crane feasible operational range and overlaid pick area.

The overlaid crane feasible operational range allows for lift path shuttling among different elevations, while the overlaid pick area presents the module pick areas for different elevations. Similar to the path checking requirements for a single elevation (see Eq. (20)), the feasibility of the lift path for the overlaid elevation combination can be checked using Eq. (23).

$$A_{overlaid-feasible} = \bigcup_{i=0}^{n} A_{feasible}^{i} \tag{21}$$

$$A_{overlaid-pick} = \bigcup_{i=0}^{n} A_{pick}^{i} \tag{22}$$

$$result = \begin{cases} 0(\text{there is path}) & A_{overlaid-feasible} \cap A_{overlaid-pick} \neq \phi \text{ and } P_{\text{set}} \in A_{overlaid-feasible} \\ 1 \text{ (no path)} & A_{overlaid-feasible} \cap A_{overlaid-pick} = \phi \text{ or } P_{\text{set}} \notin A_{overlaid-feasible} \end{cases} \tag{23}$$

Where:

$A_{overlaid-pick}$ = overlaid pick area;

$A_{overlaid-feasible}$ = overlaid crane feasible operational range;

$A_{feasible}^{i}$ = crane feasible operation range on elevation, i (total n elevations);

A_{pick}^{i} = pick area on elevation i (total n elevations); and

P_{set} = module set point (x, y).

3.6 Crane Walking Analysis

The proposed methodology for crane walking path planning is illustrated in Figure 3-20. The inputs include: (*i*) the site layout, consisting of the site boundary limits, which are the inaccessible areas for the mobile cranes (e.g., existing obstructions or ongoing construction activities); (*ii*) the selected crane geometry and configuration; (*iii*) information about the lifted modules, including module size and set position coordinates; (*iv*) the lifting schedule from which snapshots of the site layout can be obtained as the modules are installed over time; and (*v*) the

selected crane locations from which the crane is able to deliver the modules to their set points (Hermann et al. 2010; Safouhi et al. 2011). In ideal situations there would be at least one selected crane location from where the crane can reach every pick area and set point, in which case the crane can assume a fixed location for the entire duration of the project. This case can be formalized as follows:

$$A_{cf} \cap A_{pick} \neq \phi \tag{24}$$

Where:

A_{cf} is the crane feasible operation area; and

A_{pick} is the module pick area.

Accordingly, the feasible crane operation area can be represented as a 2D plan-view which is constructed based on crane lifting capacity and site constraints (see Lei et al. (2013a) for detailed algorithms). However, when the crane operation area, which is defined as the region bounded by the crane's minimum and maximum radii (R_{min} and R_{max}), does not overlap with the pick area, the mobile crane is required to walk in order perform the lift (Figure 3-21). More specifically, the mobile crane needs to walk from the location where it is able to pick the payload to the point from where it can be delivered to its final resting point. For the purpose of this work, since several modules are identified as requiring crane relocation, a crawler crane is selected because it offers the possibility of using the crane walking solution introduced above. The inputs to the main process are used to calculate the pick area and crane collision-free operation area, based upon which the walking start points and corresponding walking paths are determined (see Figure 3-20). The outputs are (*i*) decisions for crane walking—whether or not the mobile crane can walk with the load; (*ii*) the walking start points, from which

the mobile crane can begin walking toward its selected crane location; and (*iii*) the walking paths—straight-line paths that connect the walking start points and the selected crane locations. The algorithms for calculating the pick area, crane collision-free operation area, and walking paths will be elaborated on in the following sections.

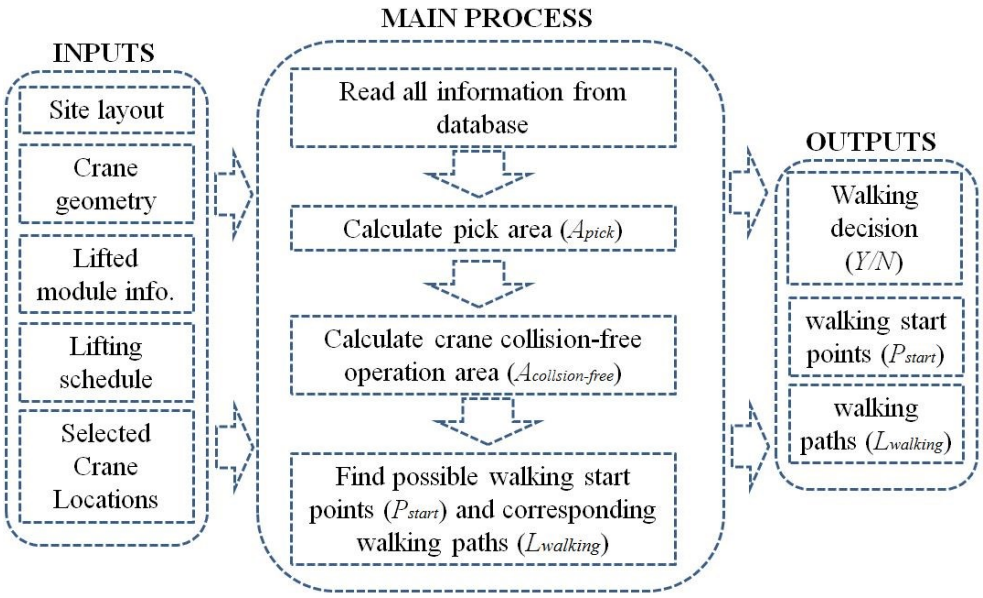

Figure 3-20 Proposed methodology for crane walking

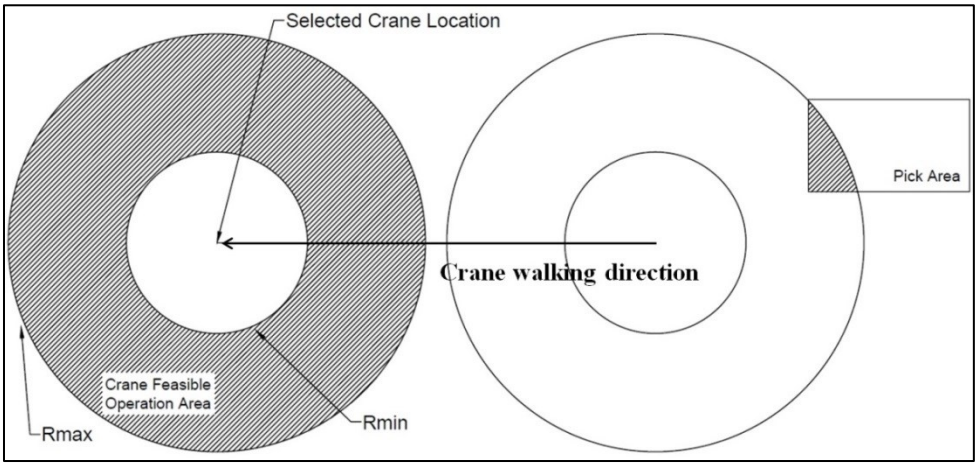

Figure 3-21 Crane walking scenario

3.6.1 Crane Pick Area Calculation

On industrial sites, modules are lifted either directly from transportation trailers or from the ground, and a module's pick areas define the areas from which it can be lifted without any conflict with its surroundings. Generally, there are two constraints for picking up the module: the inside boundary limits and the outside boundary limit; Figure 3-22(a) shows an example site layout with both constraints. The inside boundary limits (P_j^{ISB}) represent areas inaccessible for crane positioning and operation due to existing structures (e.g., pipe racks, equipment, and foundations), while the outside boundary limits (P_i^{OSB}) define the area available for construction work and encompass all the site structures. A module's pick area should not violate the inside boundary limits or the outside boundary limit. In order to calculate the pick area, the inside boundary limits and outside boundary limit are dilated and contracted by the geometry of the lifted module to form the expanded boundary limits and the reduced outside boundary limits, respectively. (The orientation of the module can also be adjusted.) Figure 3-22b) illustrates this task with the example of an inside boundary limit (P_3^{ISB}) being dilated to the expanded inside boundary area (A_3^{EBI} shown as the hatched area). Figure 3-22(c) shows how the outside boundary limit is contracted inward to form the reduced outside boundary area (A_1^{ROB} shown as the hatched area). The pick area is calculated satisfying Eq. (25), and the pick areas for the presented example site are shown in Figure 3-22(d).

$$A_{pick} = \cup_{i=1}^{m} A_i^{ROB} - \cup_{j=1}^{n} A_j^{EBI} \tag{25}$$

Where:

m is the total number of P_i^{OSB};

n is the total number of P_j^{ISB};

A_{pick} is the pick area for a lifted module;

A_i^{ROB} is the reduced outside boundary area of P_i^{OSB}; and

A_j^{EBI} is the expanded inside boundary area of P_j^{ISB}.

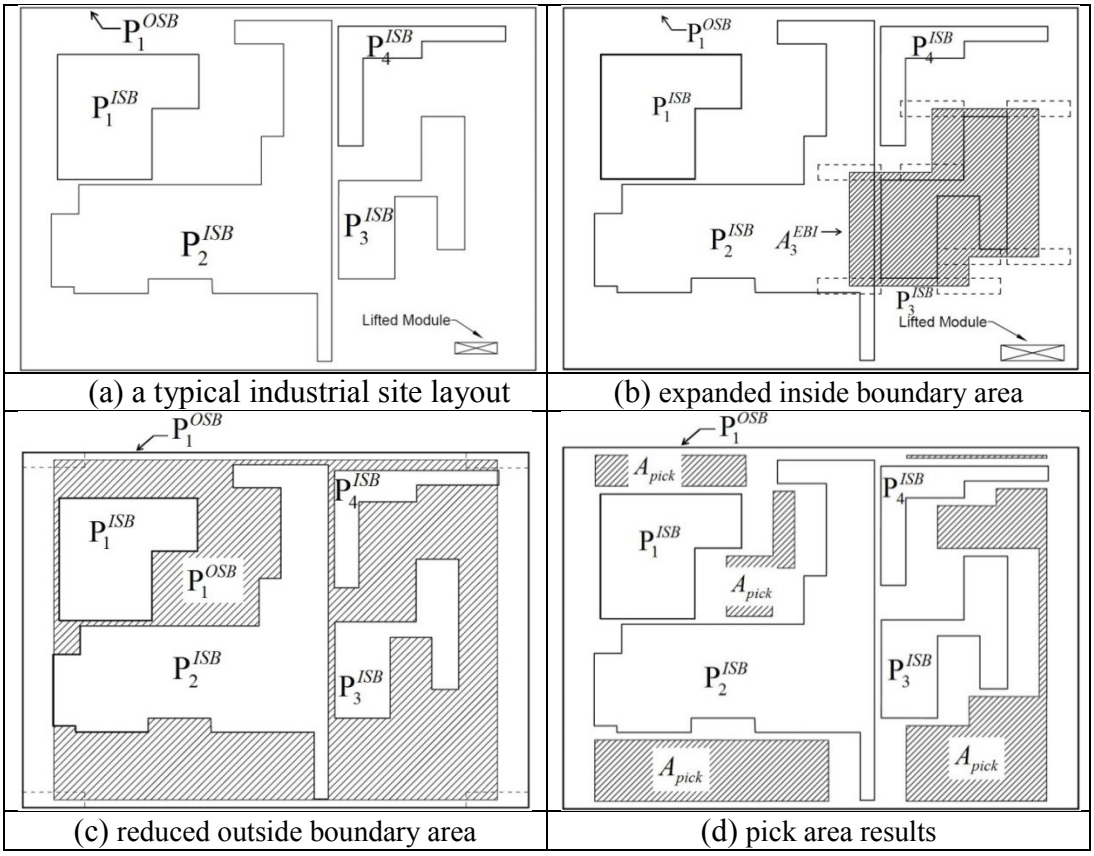

(a) a typical industrial site layout

(b) expanded inside boundary area

(c) reduced outside boundary area

(d) pick area results

Figure 3-22 Module pick area calculations

3.6.2 Crane Collision-free Operation Area Calculation

Mobile cranes are usually equipped with additional counterweights at a larger tail-swing radius to increase their lifting capacity. However, these counterweights may reduce the rotation range of the boom since the tail counterweights may

interfere with their surroundings. The crane collision-free operation area is calculated in order to guarantee that the mobile crane can rotate 360°, providing enough clearance for the crane to pick up the module. Similar to dealing with the calculation of the pick area, the inside boundary limits are dilated to the tail counterweight expanded inside boundary limits and the outside boundary limit is contracted to the tail counterweight reduced outside boundary limits based on the crane's tail-swing length (see Figure 3-23). Figure 3-23(a) presents the example of creating the tail-swing expanded inside boundary area (A_3^{TEB}) based on an inside boundary limit (P_3^{ISB}) and the tail-swing length (L), while Figure 3-23(b) shows how the tail-swing reduced boundary area (A_1^{TRB}) is obtained. The crane collision-free operation area ($A_{collision-free}$) is calculated satisfying Eq. (26), and the results for the example are shown in Figure 3-24.

$$A_{collision-free} = \cup_{i=1}^{m} A_i^{TRB} - \cup_{j=1}^{n} A_j^{TEB} \tag{26}$$

Where:

m is the total number of P_i^{OSB};

n is the total number of P_j^{ISB};

$A_{collision-free}$ is the crane collision-free operation area;

A_i^{TRB} is the tail-swing reduced outside boundary area of P_i^{OSB}; and

A_j^{TEB} is the tail-swing expanded inside boundary area of P_j^{ISB}.

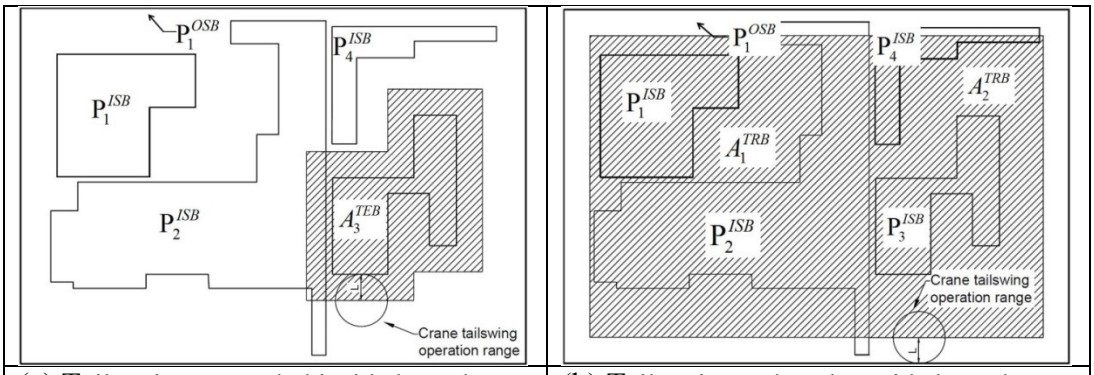

(a) Tail-swing expanded inside boundary area

(b) Tail-swing reduced outside boundary area

Figure 3-23 Tail-swing reduced area and tail-swing expanded boundary area calculations

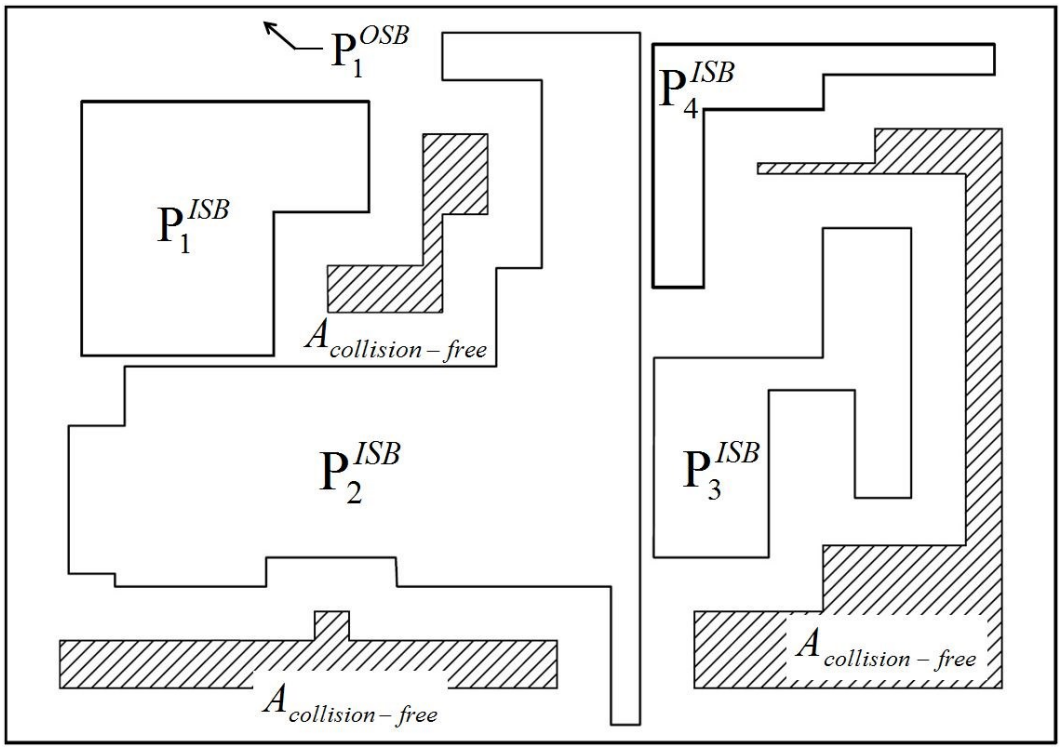

Figure 3-24 Crane collision-free operation area

3.6.3 Walking Start Points and Walking Path Calculation

Once the module's pick area and crane collision-free operation area are calculated, the crane's walking paths can be calculated satisfying three criteria: (*i*) The mobile crane should be located within the collision-free operation area when picking up the module, in order to have sufficient clearance to swing its tail counterweight. (*ii*) The mobile crane's maximum reach range should overlap with the pick area with sufficient crane capacity to lift the module. The crane's maximum reach range is usually described by its maximum lifting radius, which is calculated based on the crane's capacity table (provided by the manufacturer), module weight, minimum rigging height, and boom clearance requirement. (*iii*) For each walking path, the crane's movement should not collide with any existing structures. It is also assumed that the mobile crane only walks in a straight line.

The crane walking paths are calculated using a method referred to as "checking envelopes". The key idea of this method is to create a virtual envelope based on the crane base's width and length, and rotate the envelope counter-clockwise at the mobile crane's set location in order to determine the orientation (i.e., angle) of the walk. Figure 3-25 illustrates the use of the above described procedure to derive the crane's walking paths, in which point B is the crane location from where the module is delivered to its final resting position. Since point B does not belong to the collision-free operation area ($A_{collision\text{-}free}$), the crane cannot rotate freely to complete the lift. As a result, it is necessary to explore whether the crane can relocate to a more spacious area to pick the payload, rotate the module to a position which makes it possible to set it on its resting position, and finally walk

to a location from where the crane reach the set point. To achieve this, a horizontal (i.e., polar angle $\theta = 0$) rectangular envelope the width of which is defined as max(CBW, CBL) is built at point B. The envelope is then gradually rotated counter-clockwise at angle, Θ_1. The overlap between the checking envelope and the collision-free operation area has a shorter distance to point B than the distance of the overlap between the checking envelope and the inside boundary limits to Point B. This implies that, from this direction, the mobile crane can remain in the collision-free operation area to pick up the module, and that it walks following the envelope at that specific angle. There thus exists a walking path for the crane at this given angle, Θ_1 (Figure 3-25).

Furthermore, Θ_2 is the last angle at which the checking envelope passes by the crane collision-free operation area during its counter-clockwise rotation. Therefore, the range (Θ_3) defined by the angles, Θ_1 and Θ_2 ($\Theta_3 = \Theta_2 - \Theta_1$), determines the angles from which the mobile crane can walk. Figure 3-26 shows a random point, Point A, located within Θ_3. At Point A, the crane has a 360° rotation feasibility and the mobile crane's maximum lifting radius overlaps with the pick area, allowing the mobile crane to pick up the lifted module. A walking envelope is created based on the crane base width, which verifies that there are no collisions with the surrounding environment. The line that connects Points A and B is the planned crane walking path, and Point A is the proposed walking start point. Based on the procedures described above, Figure 3-27 provides the pseudo-code for the detailed algorithm used to calculate all the walking start points for a given selected crane location.

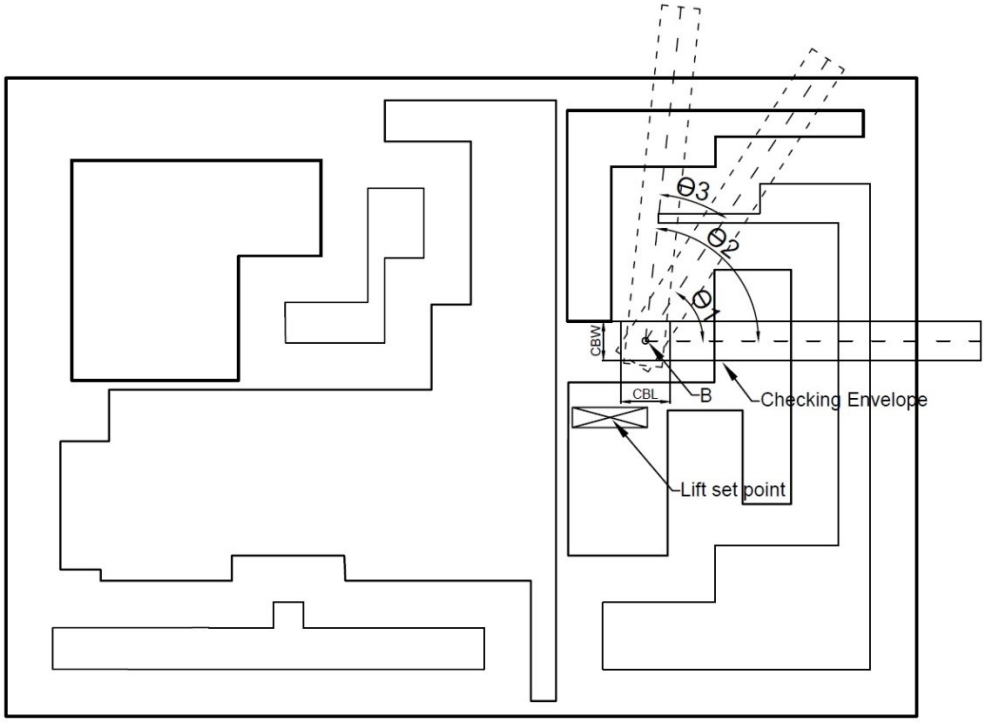

Figure 3-25 Checking envelope and walking path determination

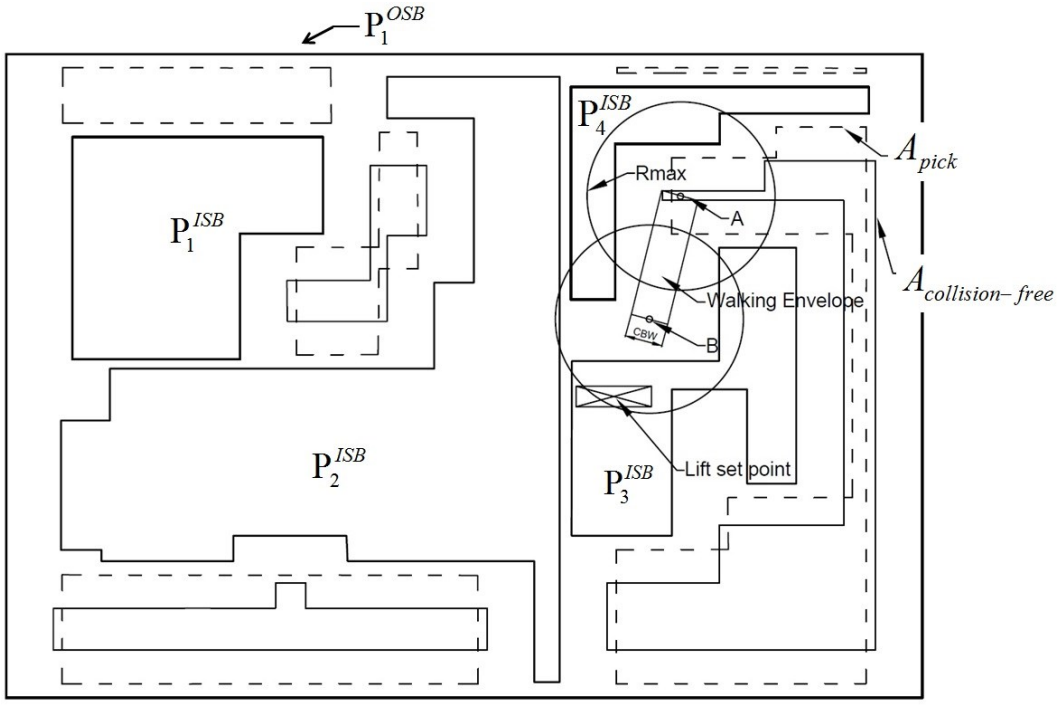

Figure 3-26 Walking path planning example

/* The crane walking planning is conducted in a X, Y plane*/

CBL: crane base length;
CBW: crane base width;
$A_{collision-free}$: crane collision-free operation area;
$\wp$ (*Θ*, *CBW*, *CBL*, P_{crane}): checking envelope based on the relevant degree *Θ*, *CBW*, *CBL* and the P_{crane};
P_j^{ISB} : a set of the inside boundary limits;
P_i^{OSB} : outside boundary limits;
A_{pick} : a set of the pick area (s);
P_{crane}: Selected crane location;
R_{max}: crane maximum lifting radius;
$L_{walking}$: walking path;
$D_{walking}$: a set of the distance of the walking paths;
P_{start} : a set of the walking start points;

Condition one: for a given $\wp$ (*Θ*, *CBW*, *CBL*, P_{crane}), the distance of the overlap between $\wp$ and nearest P_j^{ISB} to the P_{crane} is shorter than the distance of the overlap between $\wp$ and $A_{collision-free}$ to the P_{crane}; or no overlap between $\wp$ and $A_{collision-free}$.

For each degree *Θ* (0 degree to 360 degree) do:
    Create a checking envelope $\wp$ at P_{crane}, based on *Θ*, *CBW*, *CBL*, and P_{crane}
        If "Condition one" then
        Else
            Get the point with shortest distance to the P_{crane} from the overlap between $\wp$ and
                $A_{collision-free}$
            Create a R_{max} range with the center as newly found point
            If R_{max} overlaps with the A_{pick} then
                Record degree *Θ*, add the found point to the P_{start}
            End if
        End if
Next
Calculate the distance between each P_{start} and the P_{crane}, record the P_{start} with the shortest distance as the $L_{walking}$.

Figure 3-27 Pseudo-code for walking path and walking start point calculations

3.6.4 Illustrative Example of Crane Walking Path

In cases where pick-and-swing operation is impossible for the selected crane location, the crane must walk to complete the lifting job. Three criteria must be satisfied when planning the walking paths: (*i*) the crane should have sufficient space to pick up the module at the walking start point; (*ii*) at the walking start point the crane should have clearance for its crane body and tail-swing equipment; and (*iii*) the crane should have a collision-free walking path. To satisfy criterion (*i*), the module's envelope should not conflict with the site obstructions, while criterion (*ii*) necessitates conflict checking between the crane body and the site obstructions. The area in which the crane can pick up the modules and also remain collision-free is the crane feasible pick area. Thus, a crane walking envelope is created based on the crane track width and crane track length, and the length of the crane envelope is kept infinitely long, and rotated counter-clockwise, (Figure 3-28(a)). In Figure 3-28(a), the crane needs to perform the lifting at the crane location; there are three site obstructions on site and the crane has two crane feasible pick areas. When the crane envelope begins rotating, at some angles the crane walking envelope clashes with the site obstructions (e.g., an example is shown as Figure 3-28(b)). This means that, at this angle, the crane cannot reach the crane feasible pick area without overlapping with the site obstruction, and thus the walking path does not exist. However, Figure 3-28(c) shows a scenario in which the crane can reach the crane feasible pick area, and consequently can be considered as a potential walking path. All the areas that are possible for crane walking are then generated as the shaded areas in Figure 3-28(d).

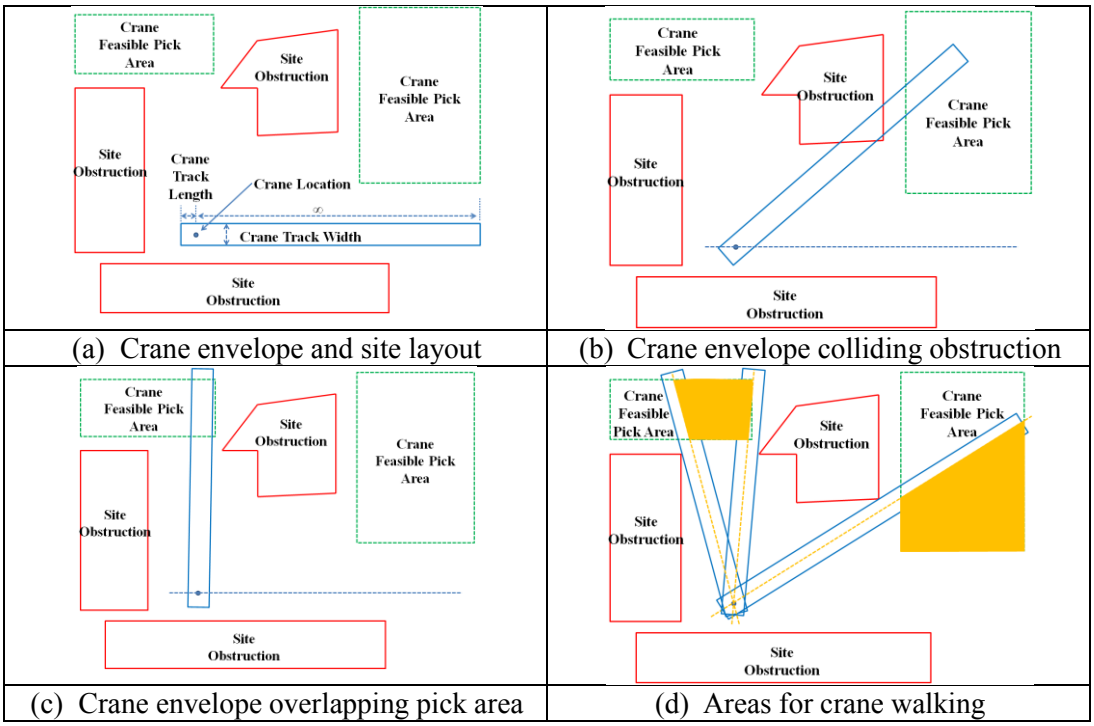

Figure 3-28 Crane walking envelope and walking planning

3.7 Clearance Checking at Selected Crane Locations

In most heavy lifting scenarios, a minimum of two crane locations need to be defined for mobile cranes, the pick location and the set location. At the pick location the mobile crane picks up the module, while at the set location the mobile crane sets the module at its final installation location. These two locations are coterminous in the pick-and-swing scenario, but vary in the crane walking scenario. In heavy lift study, both pick and set locations need to be checked for clearance, subject to the following criteria: (*i*) the crane body should not interfere with any onsite objects; and (*ii*) the crane boom should have sufficient clearance with respect to its surroundings. In order to understand and perform the clearance checking, the mobile crane's geometry needs to be studied. For the purpose of calculation, the mobile crane is represented by the numerical parameters shown in

Figure 3-29 and Figure 3-30. The values of these parameters are retrieved from the manufacturer-provided manuals and are stored in the central database. Other relevant information pertaining to the mobile cranes is also entered in the database, such as: (*i*) the lifting capacity chart, which defines the heaviest working load that could be safely lifted by the crane given a specific lifting radius; (*ii*) hook block information, including the safe workload of the hook block and the number of hoist lines; and (*iii*) the reeving capacity information that defines the safe working load for the different combinations of hoist lines. Rigging information is also taken into account, such as information regarding slings, shackles, spreader beams, and turnbuckles. In the database, each different mobile crane configuration is distinguished by a unique configuration ID used to track the crane's parameters through the entire system. Once the crane parameters are defined, the clipping algorithm is used to calculate the boom clearances. The clipping algorithm can be traced back to Vatti's polygon clipping method (Vatti 1992), which is a widely used concept in computer graphics to determine whether the portion of a given image is within, overlapping, or outside of another region. A General Polygon Clipper (GPC) library has been developed by the University of Manchester that supports four types of clipping operations: *intersection*, *exclusive*, *union*, and *difference* of subject and clip polygons (GPC online library 2014). The main process of using GPC to calculate the boom clearance of the mobile crane consists of two steps: (*i*) detecting the potential collision points for boom; and (*ii*) calculating the boom clearances based on the potential collision points.

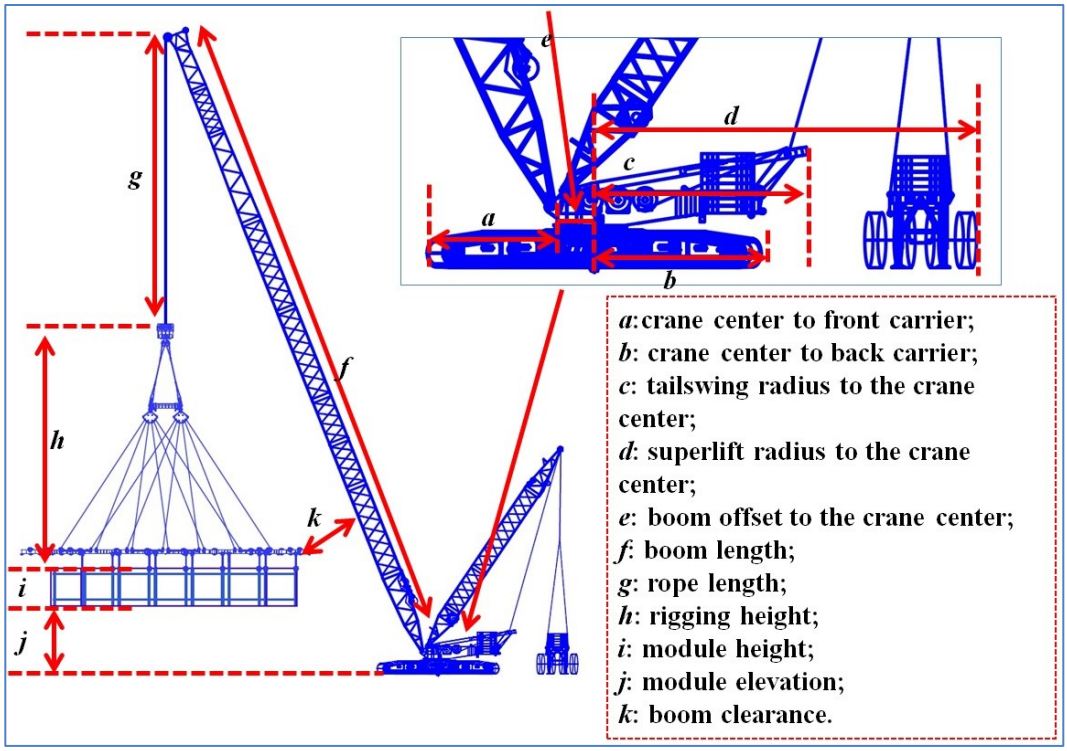

Figure 3-29 Crawler crane geometry and parameters—elevation view

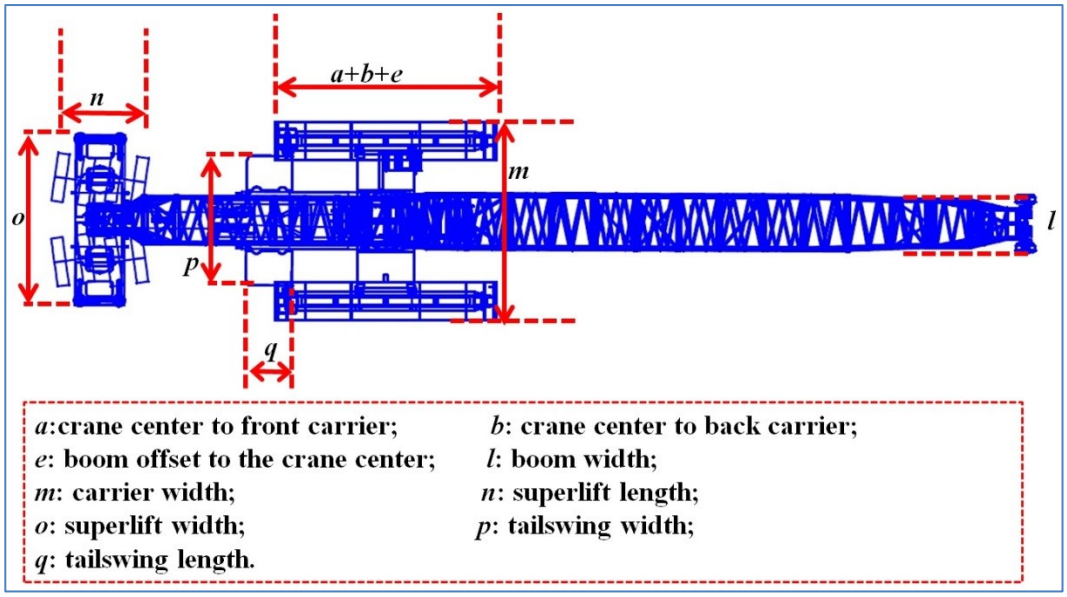

Figure 3-30 Crawler crane geometry and parameters—plan view

Given the general crane lifting case illustrated in Figure 3-31, the boom clearance checking process is as follows:

(i) Create a virtual downward boom envelope BE^3 (Figure 3-31).

(ii) Find the potential collision polygon ($P_{collision}$) using Eq. (27) (clipping algorithm). The $P_{collision}$ represent a point set(s) that may have potential collision with the boom (or jib, if there is one). The surrounding objects (Oi) are checked with the envelope BE^3 to find the intersections where the potential collision points belong.

$$P_{collision} = \{(x,y,z) \mid (x,y,z) \in BE^3 \cap O_i (i = 0, 1, 2, ..., n)\} \quad (27)$$

(iii) Calculate the perpendicular distance (D_i) from each potential collision point to the boom.

(iv) Compare all the distances with allowed boom clearance, and record all potential collision points that satisfy the boom clearance requirement in the safe point set formulized as Eq. (28). If it is the case that any potential collision point does not satisfy the requirement, then the crane lift has a collision.

$$P_{safe} = \{(x,y,z) \mid D_i \geq D_{buffer} \text{ and } (x,y,z) \in P_{collision}\} \quad (28)$$

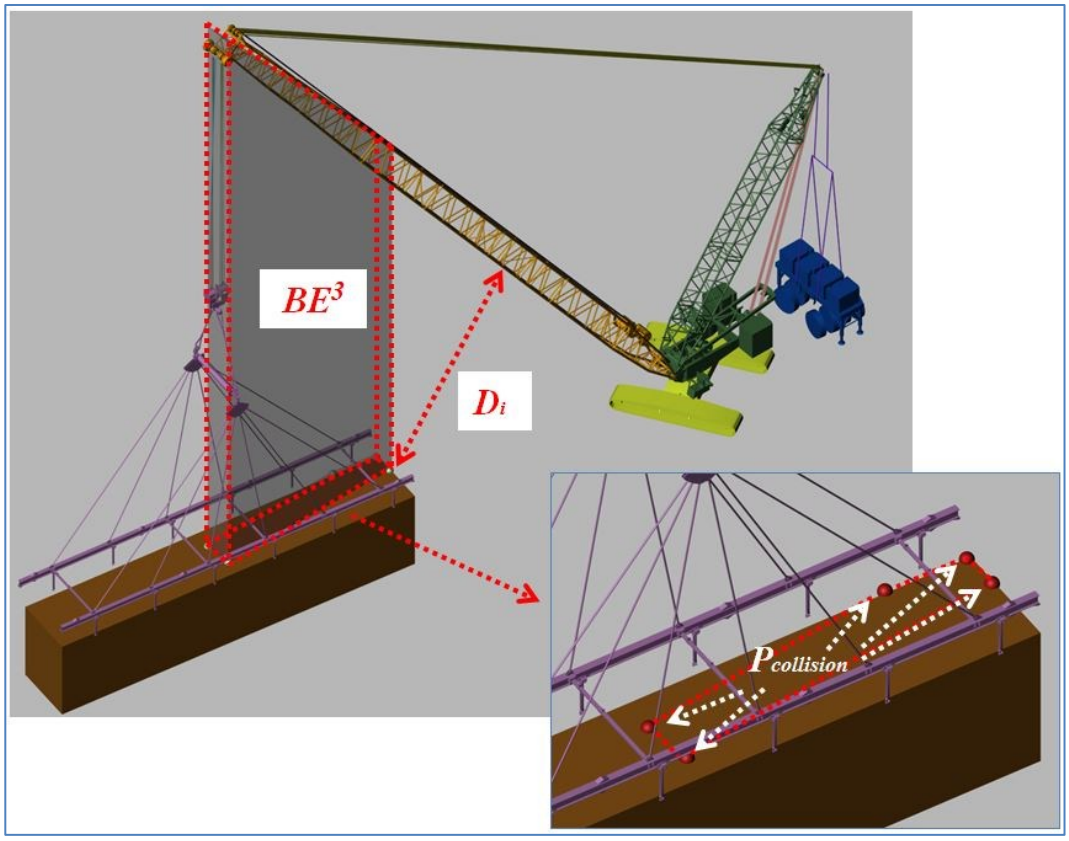

Figure 3-31 Boom envelope and potential collision points in 3D space

3.8 Crane Operation Visualization

The proposed methodology for crane operation visualization is illustrated in Figure 3-32. The inputs of the designed process consist of: (*i*) site information, including the coordinates of the site boundaries and module information (e.g., weight, set location, pick location, dimensions); (*ii*) AutoCAD crane and module models; (*iii*) selected crane locations for lifting the modules, which are determined based on the crane's lifting capacity, boom and tail-swing/superlift clearance; and (*iv*) the lifting sequence for the modules. In PCL Industrial Management Inc., a central server database is used to store the required information, and an AutoCAD library is created which contains both mobile crane

and module models. Some systems have been developed previously to deal with crane location selection, crane path checking, and lifting sequence planning. All these systems are linked to the central server database. In this research, the developed 3ds Max tool is also connected to the central database to read required information such as crane location and lifting sequence. In the main process of the proposed methodology, the heavy lift study is generated in an AutoCAD-based system by automatically retrieving information from the database and AutoCAD library. The generated lift study is then imported into 3ds Max system, and a customized add-on using MAXScript is developed in 3ds Max that automatically makes adjustments to the imported CAD models for animation generation. The outputs of the system consist of (*i*) time-dependent crane lift animation; (*ii*) critical lift analysis for congested areas; and (*iii*) potential collision detection of the heavy lifts.

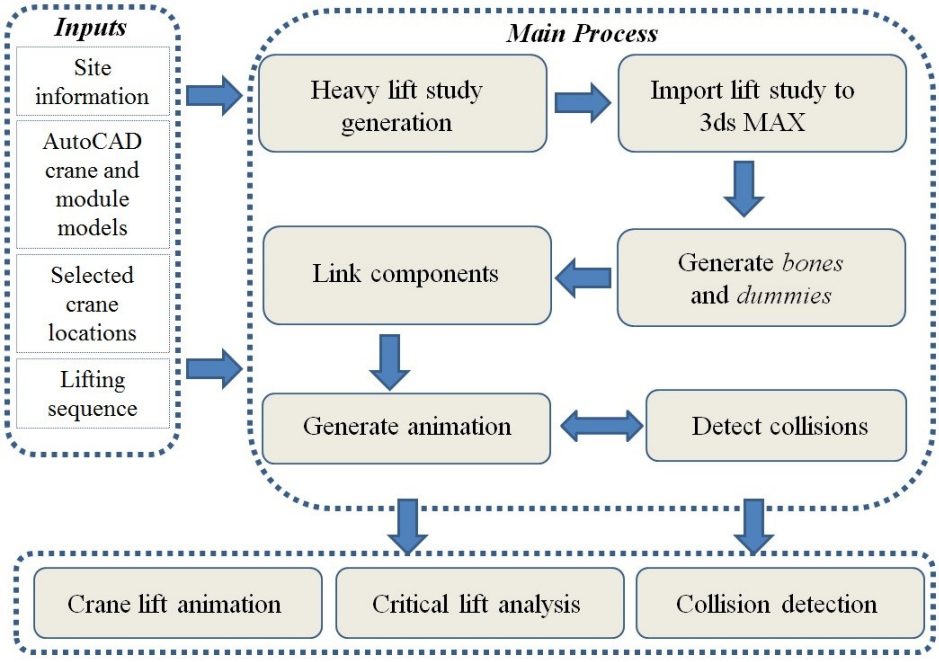

Figure 3-32 Proposed methodology for crane operation visualization

3.8.1 Mobile Crane Modelling and Kinematics

In order to animate the mobile crane lifting process, the kinematics must be studied to define different crane movements. In general, there are two types of mobile crane lifting processes: *pick-and-swing lifting* and *crane walking lifting*. In pick-and-swing lifting, the mobile crane performs the lift at one fixed location, and only a picking-swinging-dropping process is involved. Crane walking lifting operation, on the other hand, allows the mobile crane to walk a certain distance with the load in order to reach the module's set position, which is a common lifting approach for congested areas. In mechanical engineering, degrees-of-freedom (DOF) is a concept that is used to define the configuration of a machine or a robot. In this research, a mobile crane's DOF for both pick-and-swing lifting and crane walking lifting are categorized into types (see Figure 3-33 for an illustrative example of a crawler crane with its DOF): (*i*) *x*: straight-line walking following the crane track direction on the ground elevation; (*ii*) *y*: hoist up and down with the lifted module; (*iii*) α: clockwise and counter-clockwise rotation of the hook block (the lifted module rotates accordingly); (*iv*) β: rotation of the crane's upper portion, including the crane derricks (mast), tail-swing/superlift counterweight, main boom, hook block and hoist lines, riggings and module; and (*v*) μ: boom up and down with the fixed hoist line length. The configuration of a mobile crane can accordingly be formulized as Eq. (29).

$$C = [x, y, \alpha, \beta, \mu] \tag{29}$$

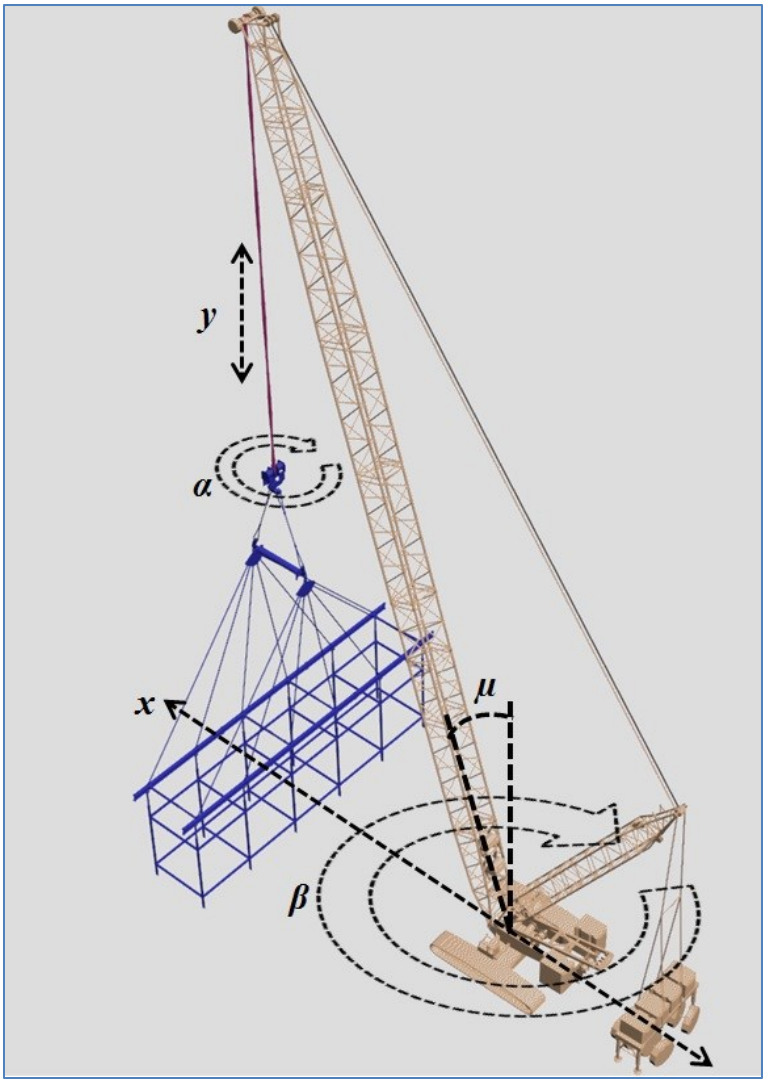

Figure 3-33 Degrees-of-freedom (DOF) of a crawler crane

3.8.2 Detailed Algorithms for Mobile Crane Movements

Although various lifting processes exist, the main lifting process can be summarized as shown in Figure 3-34. The mobile crane starts at its pick configuration and lifts the module from its pick elevation (E_{pick}) up to the module's set elevation (E_{set}), and in the interest of safety an elevation buffer ($B_{elevation}$) (e.g., usually 10 ft) is added to the set elevation which satisfies Eq. (30).

$$E_{lift-up} = E_{set} + B_{elevation} \tag{30}$$

Where: $E_{lift\text{-}up}$ is the lift-up elevation that the module should be lifted to at its pick position. Once the module has been lifted up to $E_{lift\text{-}up}$, it is then rotated by angle α (see Eq. 29) to be perpendicular to the boom's vertical projection.

Given that the modules to be lifted are often rectangular cuboids (in industrial projects, the most common modules are rectangular cuboid piperacks), as shown in the plan view in Figure 3-35, they need to be adjusted after reaching the lift-up elevation to be aligned perpendicular to the boom representation. It is common practice for each lifted module to be defined by its northeast corner ("*N-E corner*") coordinates and its geometric dimensions. According to these dimensions, the vectors, $\vec{v}_1$ and $\vec{v}_2$, can be obtained in order to calculate the required rotation angle θ_{rot}. The θ_{rot} can be determined by the cross and dot products of these two vectors, where the dot product determines the value of θ_{rot}, while the cross product can determine the direction of the angle based on the right-hand rule (Eq. (31) and Eq. (32)).

$$\theta_{rot} = a\cos\left(\frac{\vec{v}_1 \bullet \vec{v}_2}{|\vec{v}_1| \times |\vec{v}_2|}\right) \tag{31}$$

$$\text{Let } a = (x_1 - x_{cg}) \times (y_2 - y_{cg}) - (y_1 - y_{cg}) \times (x_2 - x_{cg})$$

$$\begin{cases} \text{if } a \geq 0, \text{then } \theta_{\text{rot}} \text{ is clockwise;} \\ \text{if } a < 0, \text{then } \theta_{\text{rot}} \text{ is counter - clockwise} \end{cases} \tag{32}$$

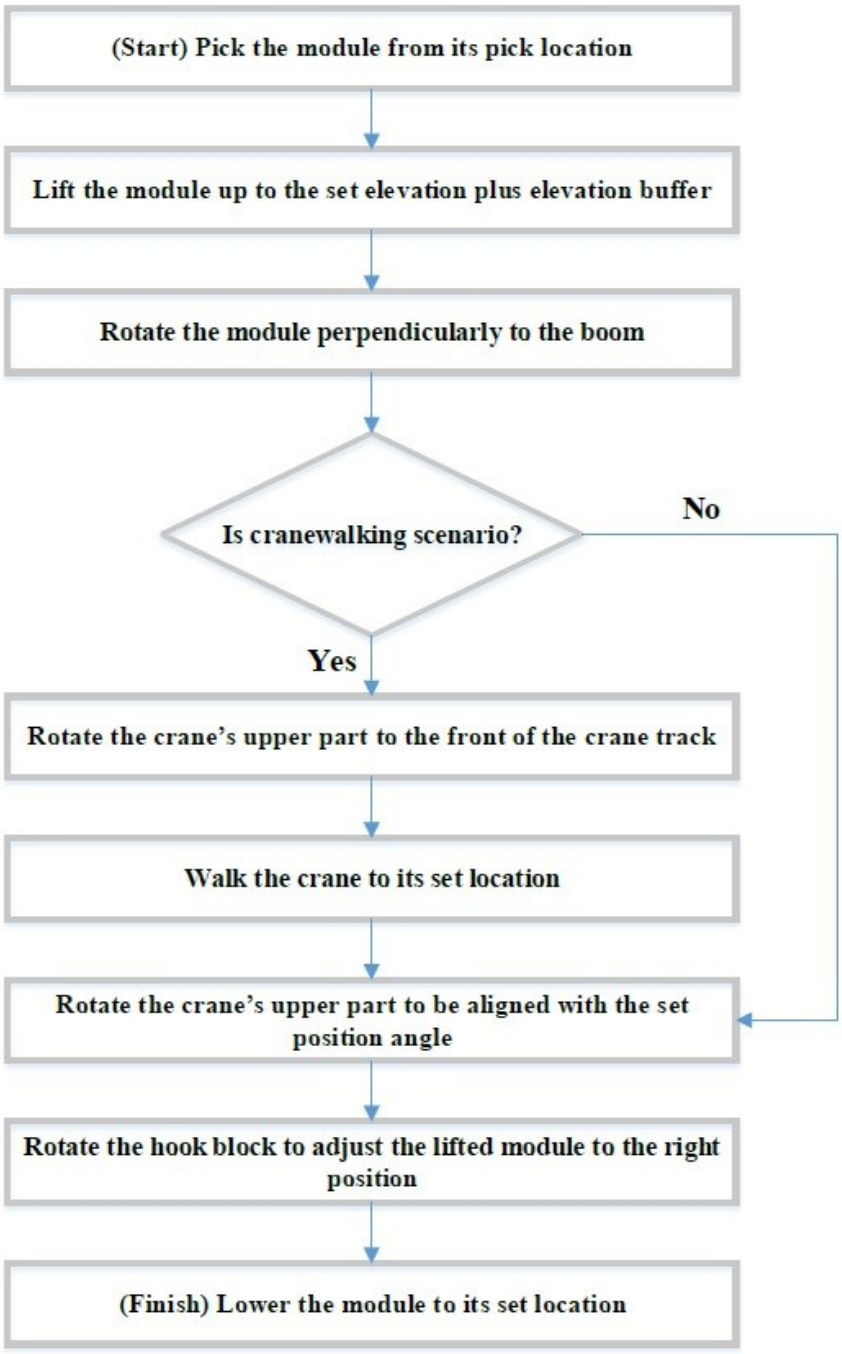

Figure 3-34 Flowchart of mobile crane lifting process

In the crane walking lifting case, the module is assumed to be placed in front of the crane body; however, in some rare cases (e.g., congested site locations that give limited boom clearance), the boom does not necessarily align with the

crane's moving direction. The mobile crane reaches its set position after walking, while in the case of pick-and-swing lifting, this process is removed. Here the mobile crane adjusts its boom angle and lowers the module to its final set location.

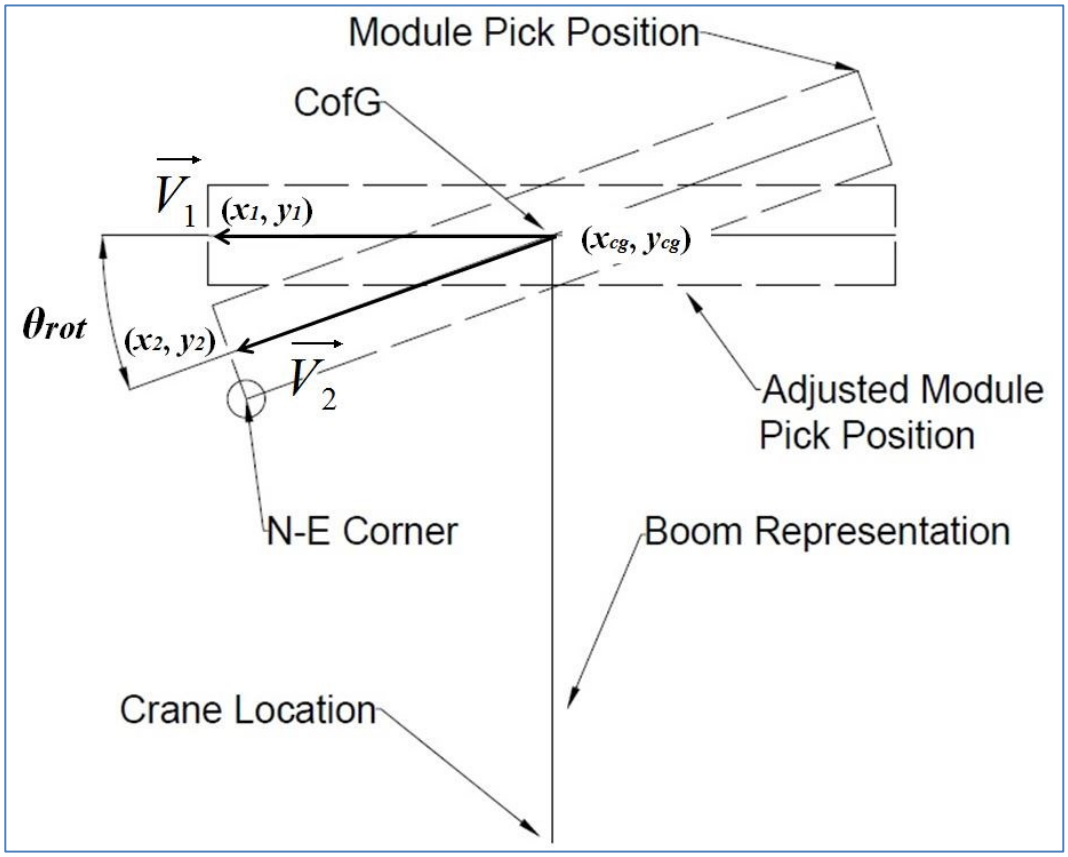

Figure 3-35 Pick position adjustment

For the pick-and-swing lifting case, the mobile crane performs the lifting without walking. The crane's movement involves swinging the lifted module from its pick position to its set position. The generic case for pick-and-swing lifting, (i.e., regardless of the *z*-coordinate), is illustrated in Figure 3-36 from a plan view. The boom swings from the angle of module pick location to the angle of the module set location. The swinging corresponds to β among the crane's DOF in Eq. (29).

In application, the rotating direction can vary in different programs (e.g., in 3ds Max the counter-clockwise rotation is considered by default to make a positive angle). Similarly to the algorithm used for pick position adjustment, the $\theta_{pick\text{-}set}$ is calculated based on two vectors, $\vec{v}_p$ and $\vec{v}_s$, satisfying Eq. (33) and Eq. (34). Again, the cross product of the vectors is used to control the direction of rotation. In animation, it is preferable to maintain as small a rotation as possible (<180°); however, adjustments may be needed in some cases where the mobile crane is not allowed to rotate to certain angles (e.g., a collision between the superlift equipment of the mobile crane and the surroundings). In the crane walking lifting case, the additional movement compared to pick-and-swing lifting is the walking. Figure 3-37 shows the symbolic model of the mobile crane walking from a plan view. It is assumed that the lifted module hangs in front of the crane body during the walking process (rotation θ_{pick}). The walking from the crane's pick location to the crane's set location is expressed by vector, $\vec{v}_{walking}$, and the boom's position needs to be re-adjusted at the crane's set location (rotation θ_{set}). For the calculation of θ_{pick} and θ_{set}, the algorithm used to calculate $\theta_{pick\text{-}set}$ in Figure 3-35 can be used.

$$\theta_{pick-set} = a\cos\left(\frac{\vec{v}_p \bullet \vec{v}_s}{\left|\vec{v}_p\right| \times \left|\vec{v}_s\right|}\right) \tag{33}$$

$$\text{Let } b = (x_3 - x_{cl}) \times (y_4 - y_{cl}) - (y_3 - y_{cl}) \times (x_4 - x_{cl})$$

$$\begin{cases} \text{if } b \geq 0, \text{then } \theta_{pick-set} \text{ is clockwise;} \\ \text{if } b < 0, \text{then } \theta_{pick-set} \text{ is counterclockwise} \end{cases} \tag{34}$$

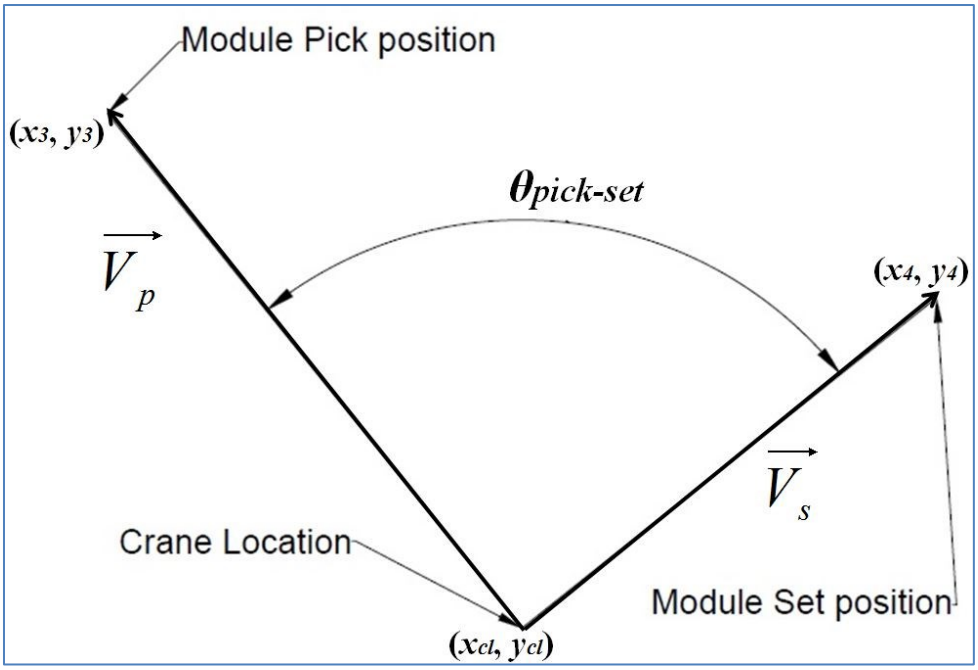

Figure 3-36 Pick-to-set rotation

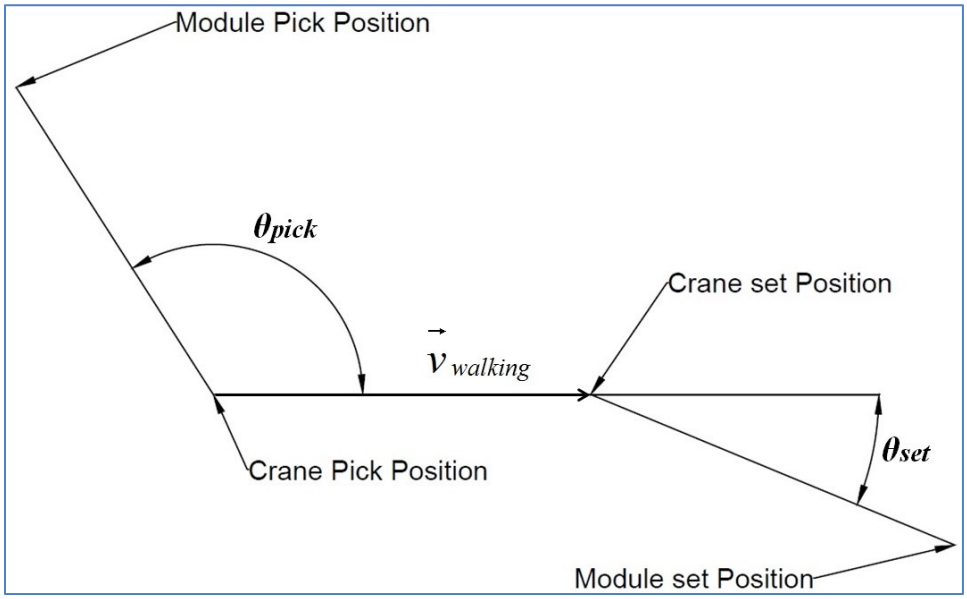

Figure 3-37 Crane walking model

3.8.3 Algorithm Implementation and Programming

The heavy lift study is drafted in an AutoCAD system which contains the 3D models of the mobile crane, rigging, and the module. These models can be created using *blocks* in AutoCAD, which can be recognized by 3ds Max (Figure 3-38 shows the example of different blocks of a mobile crane). The challenge of using these models in 3ds Max is the lack of a *bone* system that can be used to "operate" the mobile crane for animation purposes. (A bone system is a jointed, hierarchical linkage of bone objects that can be used to animate other objects or hierarchies.) Implementation of the above algorithms follows two steps: (*i*) automatically setting up the bones and links; and (*ii*) animating the mobile crane movement based on the algorithms. The first step is represented as function, *.CreateBones()*, and the second step as function, *.CreateAnimation()*. These two functions are programmed in MAXScript, a script language that allows the user to customize or write new 3ds Max functions.

There are three bones that need to be added to the imported CAD model in 3ds Max: (*i*) the boom bone; (*ii*) the crane body bone; and (*iii*) the tail-swing/superlift bone. The code for creating the boom bone in MAXScript is provided as below (the crane body and tail-swing/superlift bones can be added using similar code):

```
BoomObject = execute ("$" + BoomName + "")
BoomBoneCreation()
BoomBone = bonesys.createBone BoomObject.pivot
CranePickBoomTipPos ZAxis
BoomBone.name = "BoomBone"
```

```
mySkin = Skin()
addmodifier BoomObject mySkin
max modify mode
modpanel.setCurrentObject mySkin
SkinOps.addBone mySkin $BoomBone 1
```

Where: BoomBoneCreation() calculates the coordinates of the crane boom tip coordinates, shown in Figure 3-39, satisfying Eq. (35).

$$Boomtip = \left\{(x_t, y_t, z_t) \middle| x_t = x_{pick}, y_t = y_{pick}, z_t = \sqrt{L^2 - \left[(x_{pick} - x_{pivot})^2 + (y_{pick} - y_{pivot})^2\right]}\right. \tag{35}$$

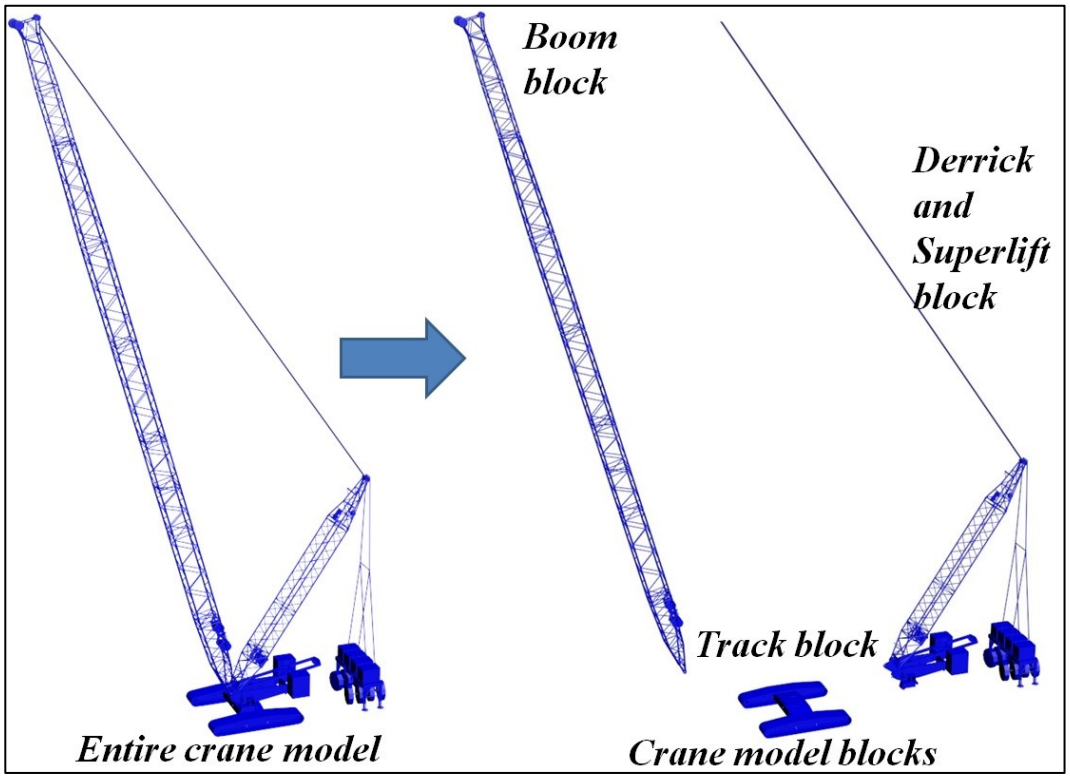

Figure 3-38 Crawler crane blocks

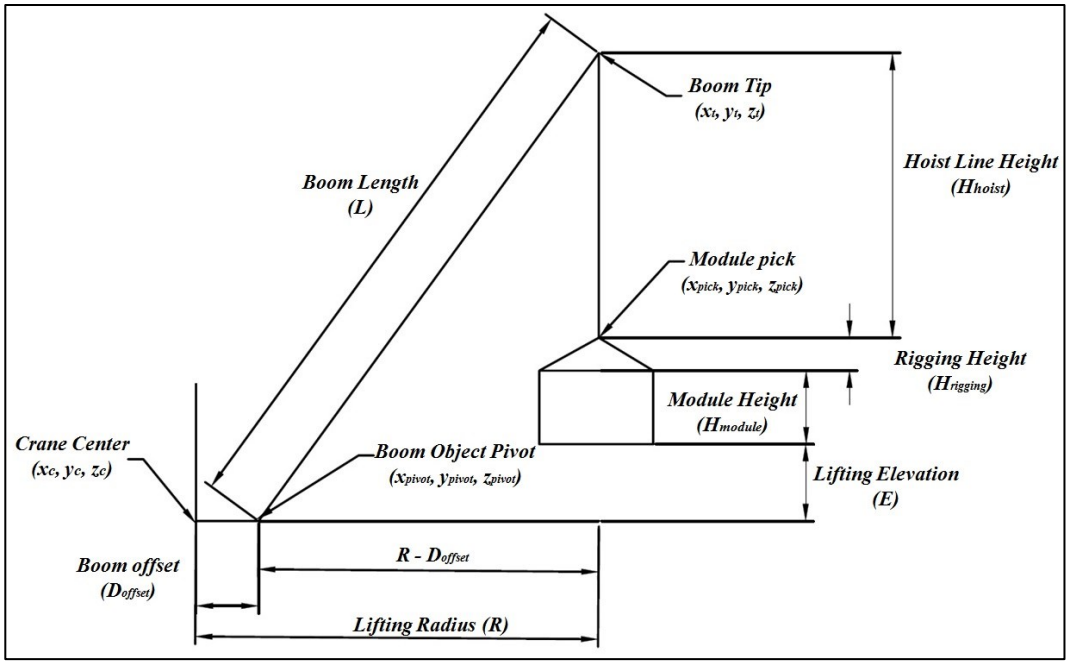

Figure 3-39 Boom tip coordinates calculation

Another component that needs to be added to the CAD model is a *dummy*, which is used for position tracking. Dummies can be added to the hook block, for example, in order to track the position of the lifted module during the crane movements. The boom tip dummy is used for positioning the boom at the appropriate angle. The hook block dummy and the boom tip dummy, in turn, can be used to locate the *hose* component. The hose component is used in 3ds Max to replace the crane's hoist line as adjustable slings. The added components need to be linked following a certain hierarchy in order to function simultaneously. A sample hierarchy is provided as Figure 3-40. The generic code for adding dummy and hose is provided as below:

```
-- Add dummy
LiftingObjectDummy = Dummy()
LiftingObjectDummy.boxsize = [10,10,10]
LiftingObjectDummy.pos = ModulePickPos
LiftingObjectDummy.pos.z = ModulePickPos.z + L3 +RiggingHeight
LiftingObjectDummy.name= "LiftingModuleDummy"
--Add hose
SlingHose = hose ()
SlingHose.End_Placement_Method =2
SlingHose.pos =$LiftingModuleDummy.pos
SlingHose.Hose_Height =$CranePickBoomTipDummy.pos.z-
$LiftingModuleDummy.pos.z
SlingHose.Round_Hose_Diameter=1
SlingHose.Top_Tension=0
SlingHose.Bottom_Tension =0
```

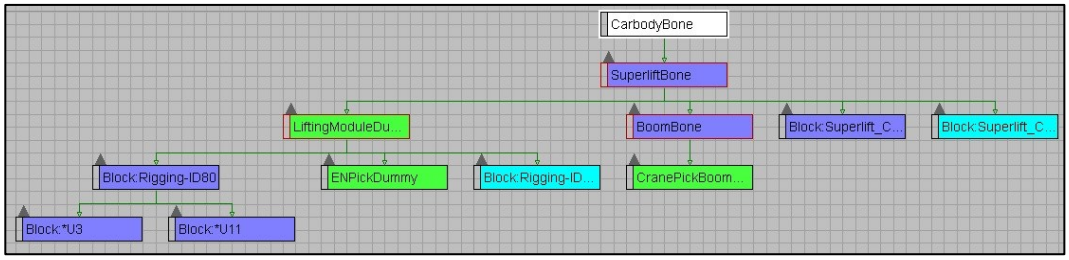

Figure 3-40 Crane component hierarchy

The animation process follows the procedures defined in Figure 3-34. It is assumed that by default each crane movement accounts for 20 frames on the timeline; however, the user can adjust the time consumed by different movements by assigning the corresponding speeds provided by the crane manufacturer. A sample code to animate crane walking is provided below:

```
animate on -- walk the crane
(
        at time 120 ($CarbodyBone.pos = $CarbodyBone.pos)
        at time 150 ($CarbodyBone.pos = CraneSetPos)
)
```

3.9 Summary

In this section, the proposed methodology has been presented. Previous developed systems, ACPO and ASICO, have been introduced: (*i*) ACPO deals with the crane location selection; and (*ii*) ASICO handles the lifting sequence. Both systems are linked to the database server, which stores the project and crane data. The CPCP system (the focus of this research), which is built based on the previously developed systems, involves analyzing two types of crane motions: (*i*) *pick-and-swing* analysis, where the mobile crane sits and performs the lift at one specific location; and (*ii*) *crane walking* analysis, where the mobile crane picks up and sets the module at different locations, between which a straight walking operation is required. Detailed algorithms have been presented for both crane motion analyses. In pick-and-swing analysis, the lifting path is checked at either an individual elevation or multiple elevations. The crane's feasible operational range is calculated based on the crane's lifting range and site constraints in order to describe the area in which the crane can operate. A pick area is used to understand the possible lifting points for the modules. Based on the crane feasible operation range and the pick area, the path is checked. For those paths that fail the path checks, crane walking analysis is performed. The core of crane walking planning

is to find an area that allows the crane to swing freely and pick the module, and then to connect this area to the crane's set location. An assumption is made that the mobile crane only walks following a straight-line direction. Considering the frequent boom clearance checking when planning the heavy lifts, a boom clearance checking algorithm is proposed for fast clearance checking. In the following chapter, the proposed methodology is tested and validated in different cases.

Chapter 4 Implementation and Case Studies

In this Chapter, implementation of the proposed methodology in Chapter 3 is presented. The idea here is to give an overall picture of how the proposed methodology is used to handle industrial projects in terms of individual lift and general site lift analyses. The system is first introduced with general remarks pertaining to how the server is set up to serve as the core for all the developed systems. Different cases illustrating the various features of the developed systems are then described.

4.1 System Development

All PCL's crane management systems are linked to a central database (see Figure 4-1 for the interface of the database). This database has various parameters, but can be categorized generally in terms of three types of data: (*i*) project data (e.g., module dimensions, site boundary); (*ii*) crane data (e.g., dimensions of different crane configurations that describe the geometry of the crane; lifting capacity chart for each type of crane obtained from the manufacturer); and (*iii*) rigging data (e.g., rigging height and block information). This database allows the engineers to retrieve needed project information and perform required analysis. Figure 4-2 shows the systems that have been developed and linked to this server.

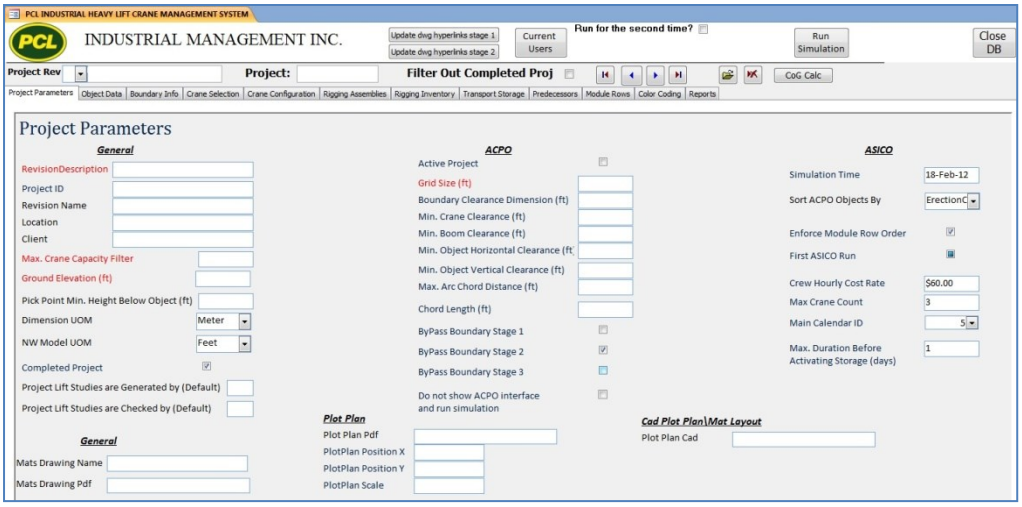

Figure 4-1 PCL crane management database interface sample

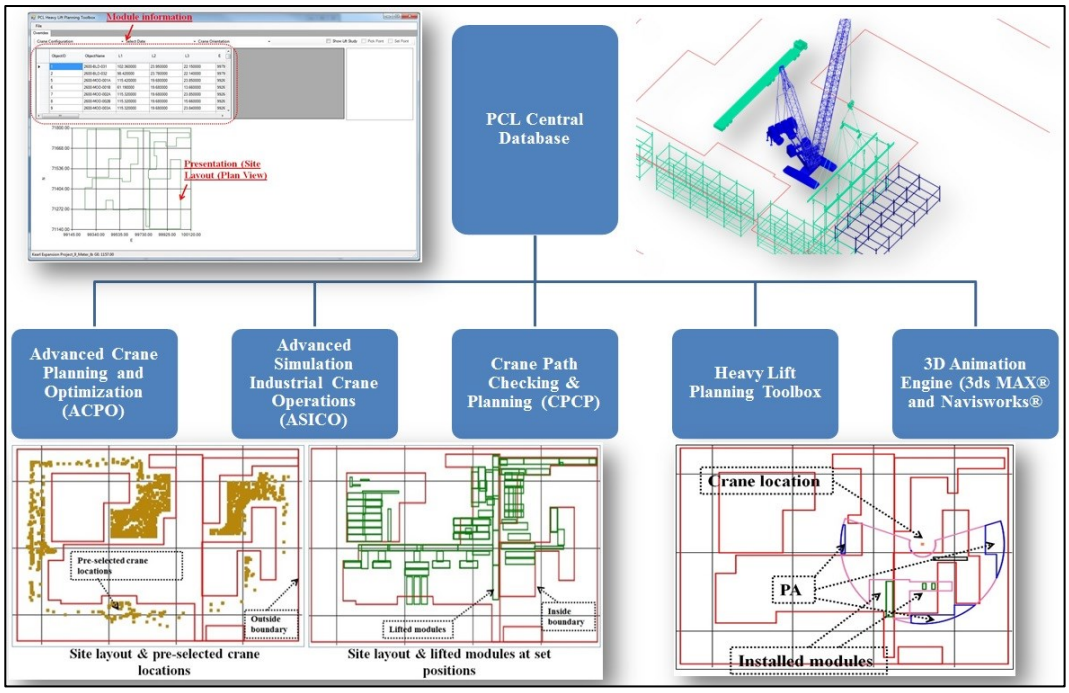

Figure 4-2 System structure

In general, the crane motion analysis takes all crane configurations and their corresponding crane locations into consideration; the crane locations for each crane configuration are generated using the Advanced Crane Planning and

Optimization (ACPO) system. The entire motion analysis process follows the Pseudo-code provided in Figure 4-3. Each crane location is looped through two functions, *Pick-and-swing-analysis()* and *Crane-walking-analysis()*, and the results are returned to the central database to generate lift study and animation. The system is programmed using Visual Studio (2010) VB.Net, and the main *classes* are defined as follows:

(i) *PathCheckingSingleElev.vb* (main loop for all crane configurations and crane locations—checks the lifting path on the highest project elevation and set elevation, called *PathChecking.vb*);

(ii) *PathCheckingOverlap.vb* (main loop for all crane configurations and crane locations—checks the lifting path on the highest project elevation and set elevation, called *Overlap.vb*);

(iii) *CraneWalkingPlanning.vb* (main loop for all crane configurations and crane locations that have failed in (*i*) and (*ii*)—finds the walking path);

(iv) *PathChecking.vb* (main algorithm for path checking on individual elevations);

(v) *Overlap.vb* (main algorithm for path checking on multiple elevations); and

(vi) *RminRmaxCalculation.vb* (main algorithm to calculate the R_{min} and R_{max} for selected crane elevations).

```
MOTION PLANNING AUTOMATION
1 forall crane ∈ C
2    CLs ← UCLs
3    forall CL ∈ CLs
4          Pick-and-swing-analysis ()
5          if Pick-and-swing-analysis.result = SUCCESS
6            CL→ lift possible AND record for lift study and animation
7          else Crane-walking-analysis ()
8               if Crane-walking-analysis.result = SUCCESS
9                  CL→ lift possible AND record for lift study and animation
10              else at CL → lift impossible
11              end if
12         end if
*Crane = one crane configuration;
  C = set of all crane configuration;
  CLs= crane locations for one Crane;
  UCLs =universal crane locations for C;
  CL = one crane location belonging to CLs.
```

Figure 4-3 Pseudo-code for crane motion analysis

4.2 Case One—Simple Path Checking Case

This case study selects a PCL project to validate the proposed method. The goal in implementing the proposed method here is to automate the lift path checking process for each lifted module. The site layout and boundaries onsite are retrieved in terms of coordinates and are automatically stored in the database. The proposed methodology is incorporated into a computer application to perform the path checking. The built application consists of a calculation module and a visualization interface; the calculation module carries out the path checking, and the results are presented in the designed interface. The targeted module, Module 159, is 6 m (19.68 ft) wide and 30 m (98.42 ft) long, and weighs 110,360 kg (243,300 lb). It is planned to be lifted to its set elevation from the ground. The selected crane for this job is the Liebherr LR 1400/2 with a superlift, and the length of the superlift counterweight is 15 m (49 ft).

4.2.1 R_{min} and R_{max} Calculation

The R_{min} and R_{max} for the lifted object are calculated according to the capacity chart, considering the module weight as well as the lift auxiliaries. The site layout and R_{min} and R_{max} for the lifted object are the designed interface (Figure 4-4). The built application reads data from the server database, and sorts them according to the modules' lifting dates. Only the modules with a lifting date prior to the date of the targeted module are shown. In Figure 4-4, the lifted module is shown at its set point (planned for lift on May 30, 2012). Modules with an earlier date are also shown (erected modules). The existing site structures (such as an oil tank and existing supporting structures) are denoted by the dashed line boundary in Figure 4-4.

4.2.2 Lifting Range Adjustment

The lifting range adjustments are subject to two constraints: (*i*) height of site obstructions, and (*ii*) tail-swing or superlift equipment. Figure 4-5 presents the impact of the height of the site obstruction constraint on R_{max}. Due to the height of site obstructions (Module 191 and Module 157 in Figure 4-4), the R_{max} is modified at "R_{max} modification 1" and "R_{max} modification 2" (see Figure 4-5). The green curves represent the modified R_{max} considering the height of site obstructions. The impact of the crane's superlift equipment is presented in Figure 4-6. A superlift circle (the brown circle in Figure 4-6(a)) with a radius equal to the superlift counterweight length is plotted which conflicts with existing site structures. A

sector is then erased from R_{min} and R_{max}, based on the opposite angle where the superlift conflicts with existing site structures in Figure 4-6(b).

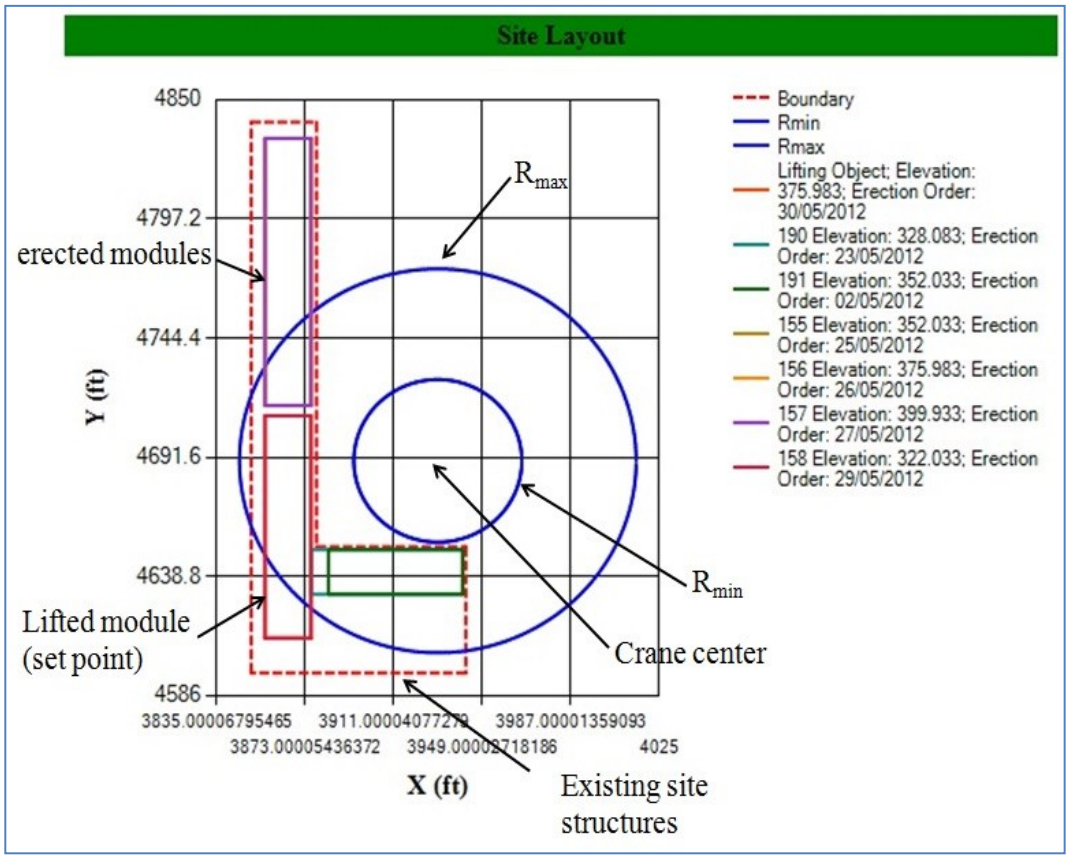

Figure 4-4 Case One—R_{min} and R_{max}

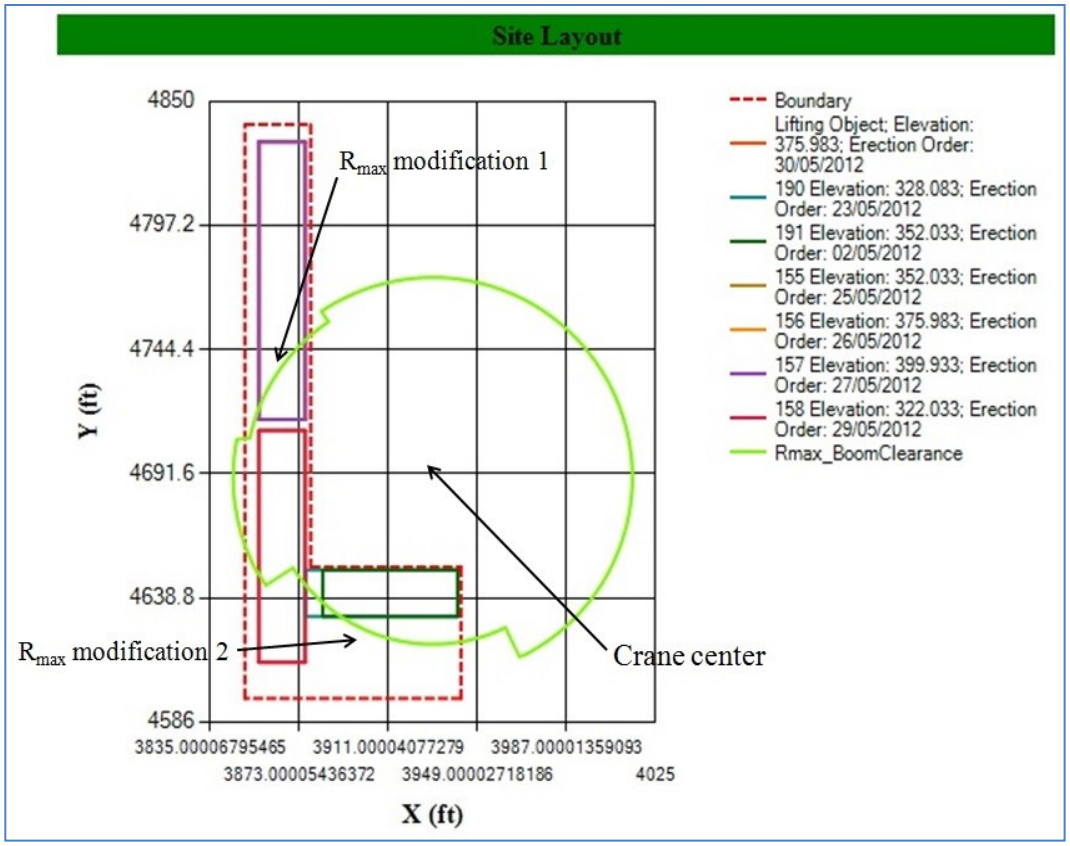

Figure 4-5 Case One—R_{max} modification based on boom clearance

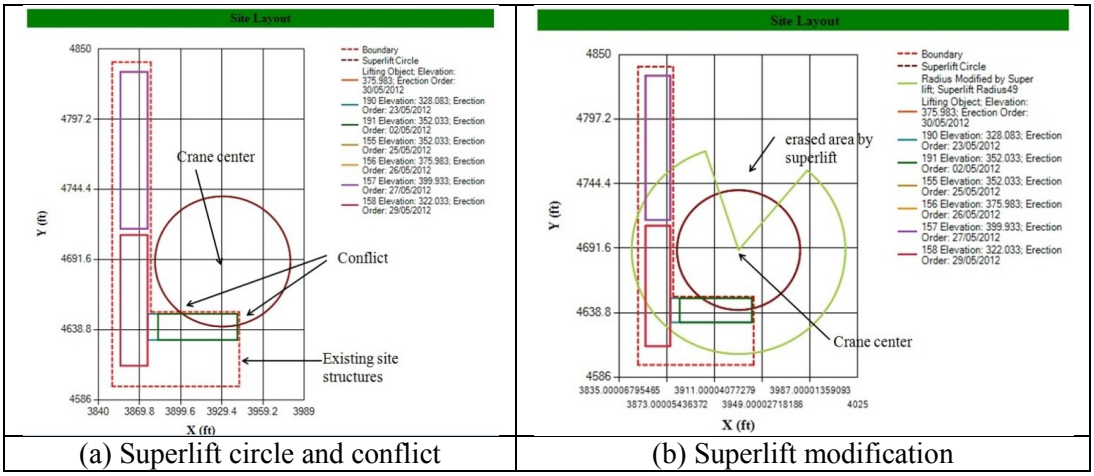

(a) Superlift circle and conflict

(b) Superlift modification

Figure 4-6 Case One—superlift modification

4.2.3 Constraint of C-Obstacle and Mapping Method

In Figure 4-7(a), the configuration space obstacle (C-Obstacle) is created for Module 157 since the elevation of Module 157 is higher than the lifted module's elevation. The C-Obstacle is created based on the lifted module's orientation at its set point, and the geometric center of the lifted module is selected as the representing point. Figure 4-7(b) presents the implementation of the mapping method with all site structures, and Figure 4-7(c) shows the results of the mapping method without any site structure. Compared with R_{min} and R_{max} in Figure 4-4, three parts are erased from R_{min} and R_{max} in Figure 4-7(c): the "*C-Obstacle* erased area," "R_{max} modification," and "Superlift erased area". The pink areas in Figure 4-7(c) illustrate the crane's feasible lifting area, in which the selected crane is capable of lifting the target module in consideration of constraints (crane capacity, boom clearance, superlift, and site obstructions). Path checking is performed as illustrated in Figure 4-7(d). The pick area (yellow dashed line in Figure 4-7(d)) overlaps with the crane's feasible lifting area, and the module's geometric center locates within the feasible lifting area; thus, the lifted module passes the path checking. The designed system then writes "yes" as a binary check result back to the database.

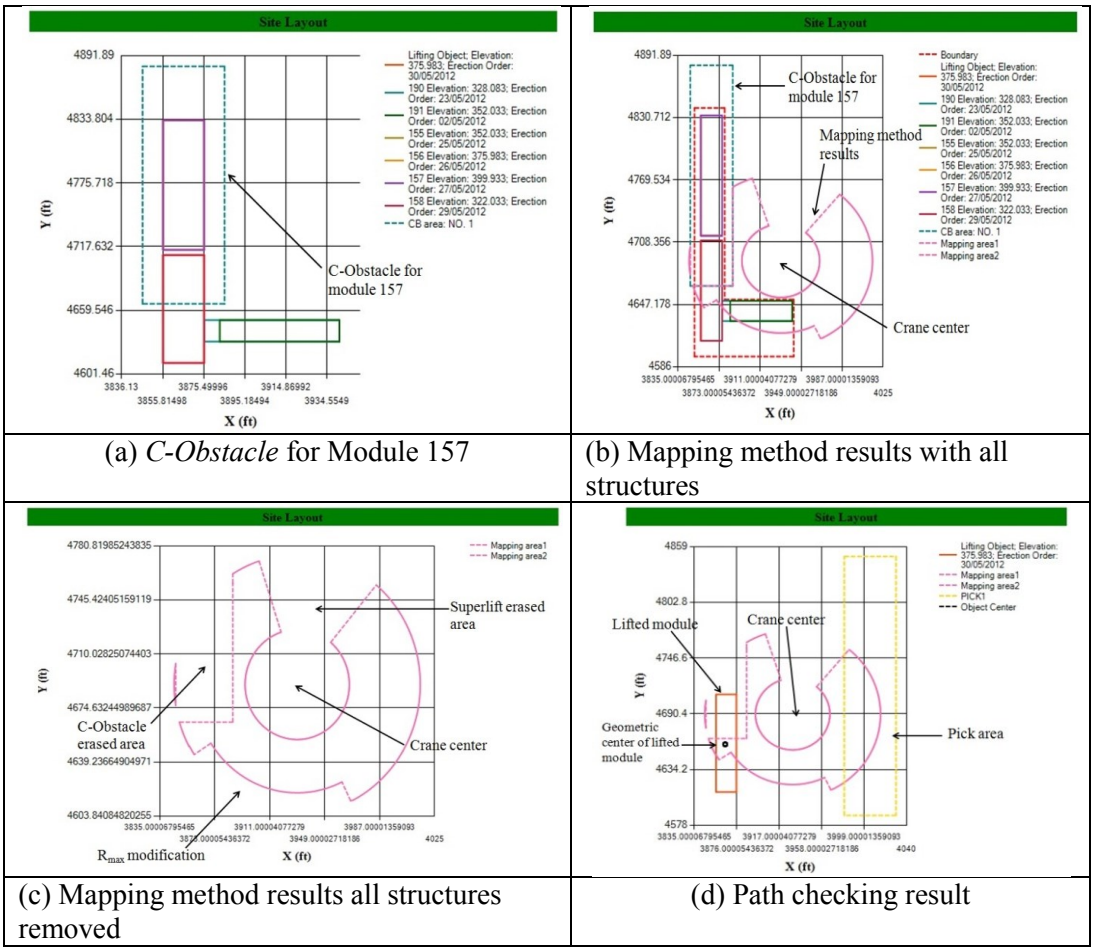

(a) *C-Obstacle* for Module 157

(b) Mapping method results with all structures

(c) Mapping method results all structures removed

(d) Path checking result

Figure 4-7 Case One—mapping method and path checking result

4.3 Case Two – Path Checking on Individual and Multiple Elevations

The case study is based on an industrial project in Alberta, Canada by PCL Industrial Management Inc. which involves lifting 200 modules and heavy vessels. The employed heavy mobile crane for this project is the Demag CC 2800, equipped with a 660-t capacity and a superlift tail-swing. The possible crane locations for each module are calculated using the ACPO system, and the lifting sequence is generated by the Advanced Simulation in Industrial Crane Operations (ASICO) system. ACPO divides the site layout using grids, based upon which each grid point is tested for the boom clearances, rigging height, and tail-swing

constraints for module lifting. The grid points that satisfy the engineering requirements are selected as potential crane locations. For this project, ACPO generates a total of 89,252 possible crane locations for all modules, and each module has multiple potential crane locations. ASICO, based on the selected crane locations, performs schedule planning, primarily considering lift logic issues. The logic issues are defined based on the precedential relationships among modules, which further generate a complete lift sequence.

Figure 4-8 presents all the calculated crane locations for the module and the site layout. The inside and outside boundaries define the inaccessible areas for crane settlement and the site boundary, respectively. The areas that are occupied by existing objects such as installed pipes are predefined as boundaries that prevent mobile crane entry. The objective of employing the proposed methodology in this project is to automatically check the lift path for every crane location, and filter out the locations which do not have feasible lift paths. The project elevations are determined based on the modules' installation elevations and elevation tolerance. The elevation tolerance is given as a user-defined parameter that defines the minimum height difference between two adjacent elevations. Since there is no industry standard for elevation tolerance, this value is determined by engineers based on their experience; in this project 1.5 m (5 ft) is used as the elevation tolerance. Based on the calculations of project elevations made using Eq. (1), a total of 11 project elevations are generated.

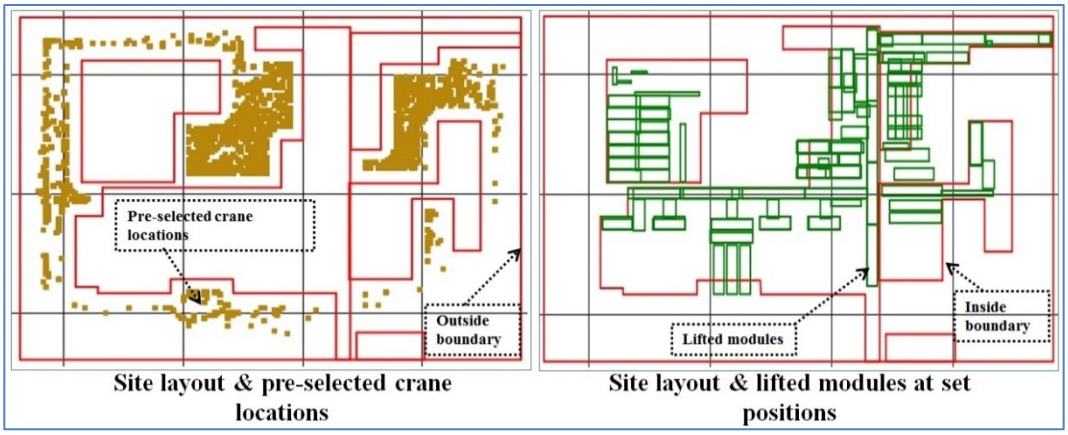

Figure 4-8 Case Two—site layout

4.3.1 Path Checking on Individual Elevations

In this section, module 2600-PR-075, with a gross weight of 30.53 t (67,305 lb), is selected for path-checking analysis. A total of 354 potential crane locations are selected for this module (Figure 4-9 shows the module at its set position with all the selected crane locations), among which one location is selected for path checking. The module's set elevation is used to demonstrate the calculation of the crane's feasible operational range and pick area. Figure 4-10 presents the calculated R_{min} and R_{max} at the selected crane location, based on which the crane's feasible operational range ($A_{feasible}$), shown in Figure 4-11, is calculated. At Area *A*, a sector is removed from R_{min} and R_{max} due to the superlift tail-swing constraint, and at Area *B* the R_{max} is modified due to the installed modules. The generated crane's feasible operational range ($A_{feasible}$) represents the area where the crane can perform the lift without any collision at the module's set elevation. Figure 4-12 presents the pick areas (A'_{pick}) (outlined in blue), which are the areas

within which the crane can pick the module. Since the crane's feasible operational range overlaps with the pick areas and the lifted module set position falls within the crane's feasible operational range ($A_{feasible}$), the path checking program determines that there is a lift path for the target module.

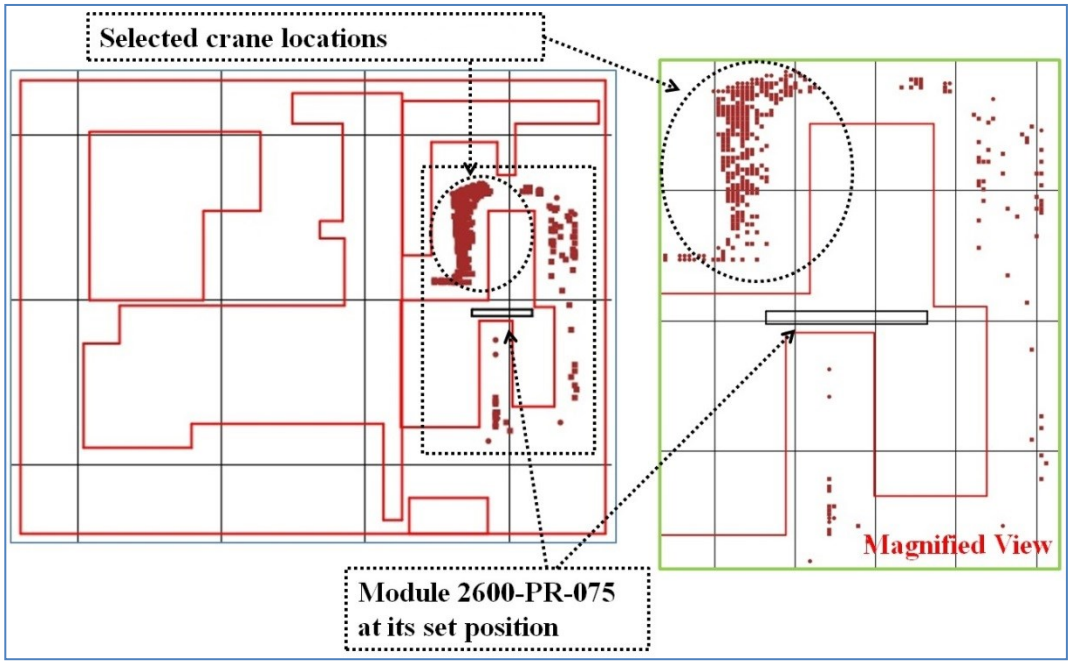

Figure 4-9 Case Two—module set position and crane locations

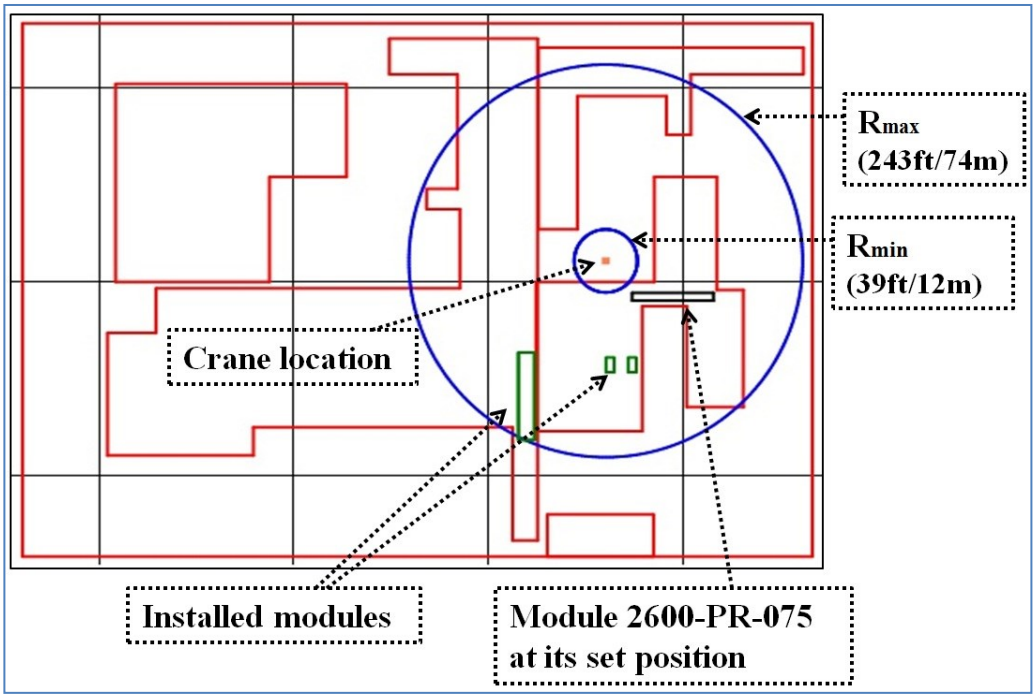

Figure 4-10 Case Two—R_{min} and R_{max}

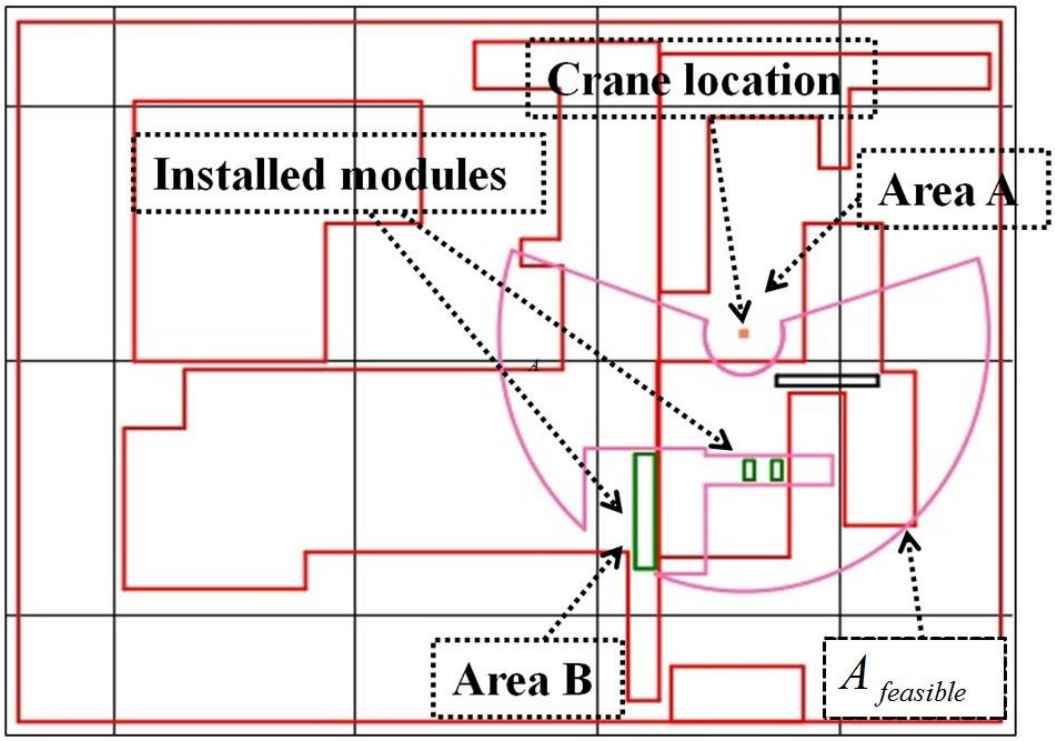

Figure 4-11 Case Two—crane feasible operational range ($A_{feasible}$)

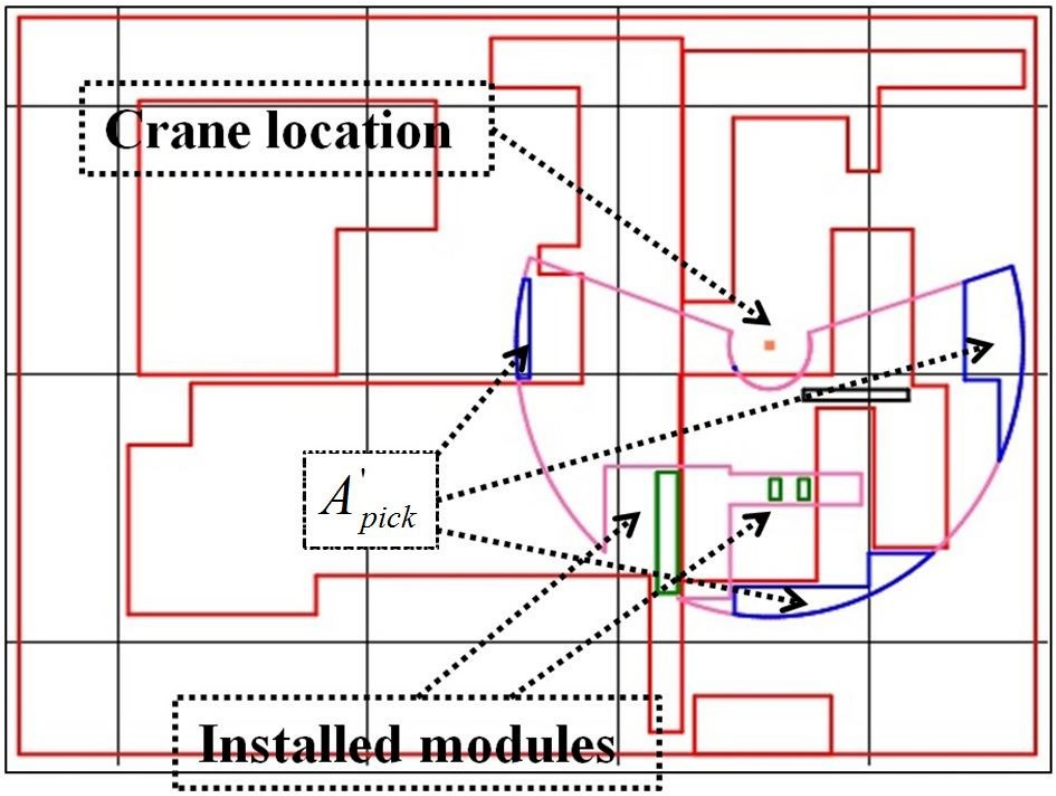

Figure 4-12 Case Two—pick area (A'_{pick})

To validate the results, a 3D lift study is conducted. The total module weight is calculated, including the module gross weight, load block weight, rigging weight, and additional weight. The calculated total module weight at the set position is 78.48 t (approximately 173,019 lb). By checking the capacity chart provided by the crane manufacturer, the maximum radii at the pick point and the set point for this weight are found to be 54.0 m (177.2 ft) and 26.0 m (85.3 ft), respectively, and the corresponding chart capacities are 100.92 t (approximately 222,500 lb) and 259 t (approximately 572,000 lb). The crane is proven to have enough capacity at its pick location and set location. At the pick location, the crane utilizes 77.8% of its full capacity, while at the set location, only 30.3% of its full

capacity is used. In addition, the boom clearance check is performed to guarantee sufficient clearance for the lift path (Figure 4-13). At the pick location, the crane has a boom clearance of 19.6 m (64.4 ft), while at the set location the clearance is 3.3 m (10.75 ft). The lift study also checks the lifting surroundings to ensure that the lift path is valid.

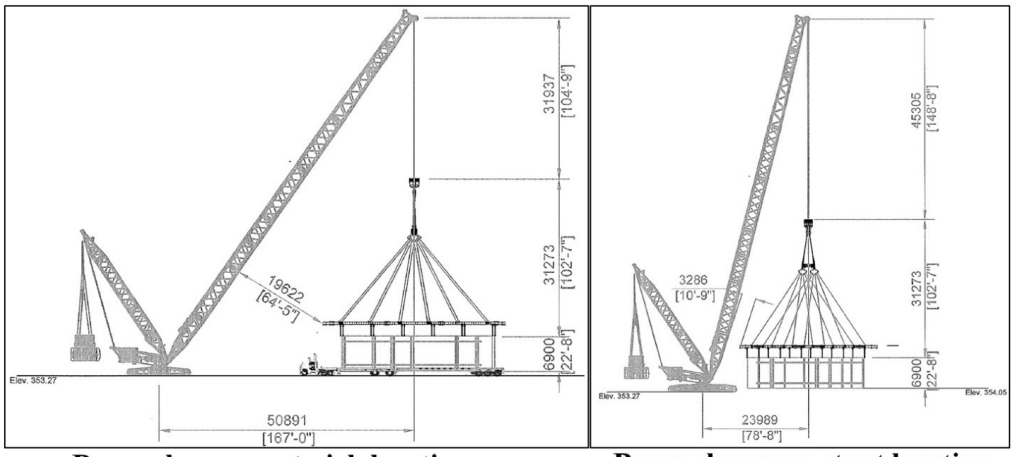

Figure 4-13 Case Two—boom clearance checking

4.3.2 Path Checking on Multiple Elevations

In this section, another module, 2600-PR-011A, with a gross weight of 111.92 t (approximately 246,741.41 lb), is selected to demonstrate how the overlaid elevation combination is used for path checking; (Figure 4-14 presents the module set position and selected crane location). For different project elevations, the crane's operation range varies due to the boom clearance, rigging height, and capacity requirements. The crane feasible operational ranges ($A_{feasible}$) and pick areas (A'_{pick}) are calculated for each project elevation (shown in Figure 4-15 and

4-16 with different colours). According to the results, the crane feasible operational ranges ($A_{feasible}$) on higher elevations represent more constrained operation ranges due to the boom clearance and rigging height requirements, but they also involve fewer obstructions than at the lower elevations. Similarly, the crane encounters more feasible operation ranges at lower elevations, but also more obstructions. By overlaying the crane feasible operational ranges ($A_{feasible}$) and pick areas (A'_{pick}) from different elevations (Figure 4-17), the overlaid crane feasible operational range ($A_{overlaid-feasible}$) and overlaid pick area ($A_{overlaid-pick}$) are obtained, which represent the feasibility of lifting and picking the module from different elevations. The obtained overlaid crane feasible operational range and overlaid pick area are used for path checking using Eq. (23), such that a feasible lift path is found to exist for the selected crane location. The corresponding lift study by professional engineers for this module shows that the crane uses 67% and 64% of its full capacity at its pick position and set position, respectively. The study also gives boom clearances of 3.2 m (10.4 ft) and 3.35 m (11.0 ft) at the pick position and set position, respectively. Automatic path checking is performed for the entire site using the built program. Selected for the modules are 155 crane positions, and the results show that there are 122 crane locations (78.71%) that have lift paths and 33 crane locations (21.29%) that do not have lift paths, considering fixed crane locations (Figure 4-18). For the failed crane locations, alternative solutions must be found, such as crane walking with load.

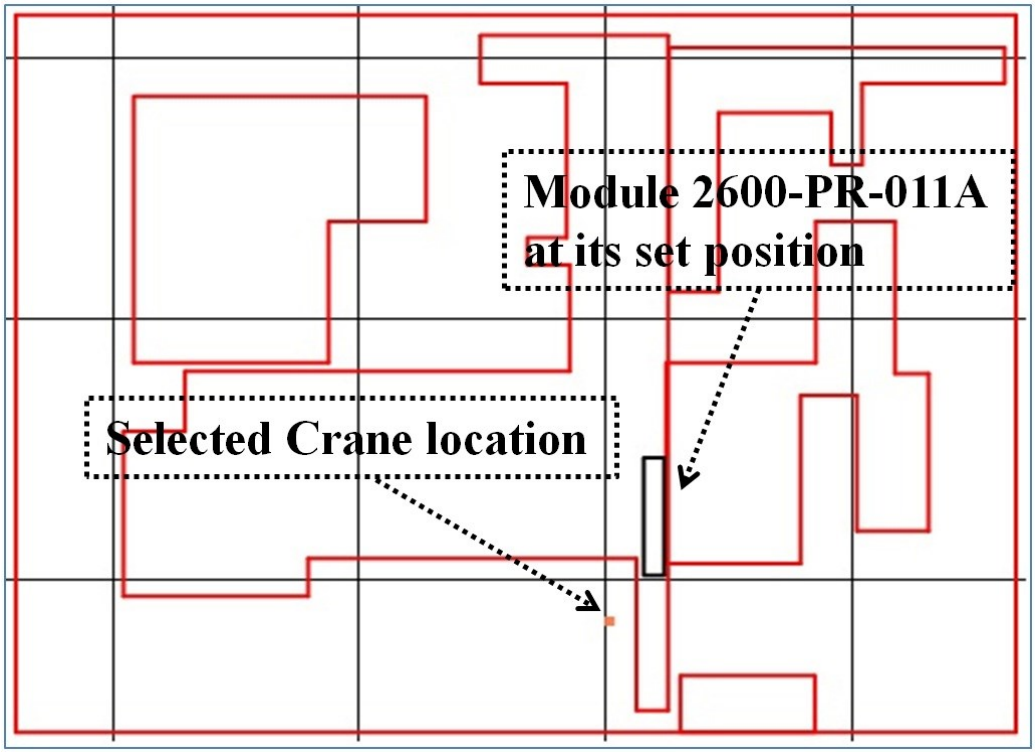

Figure 4-14 Case Two—scenario for multiple-elevation path checking

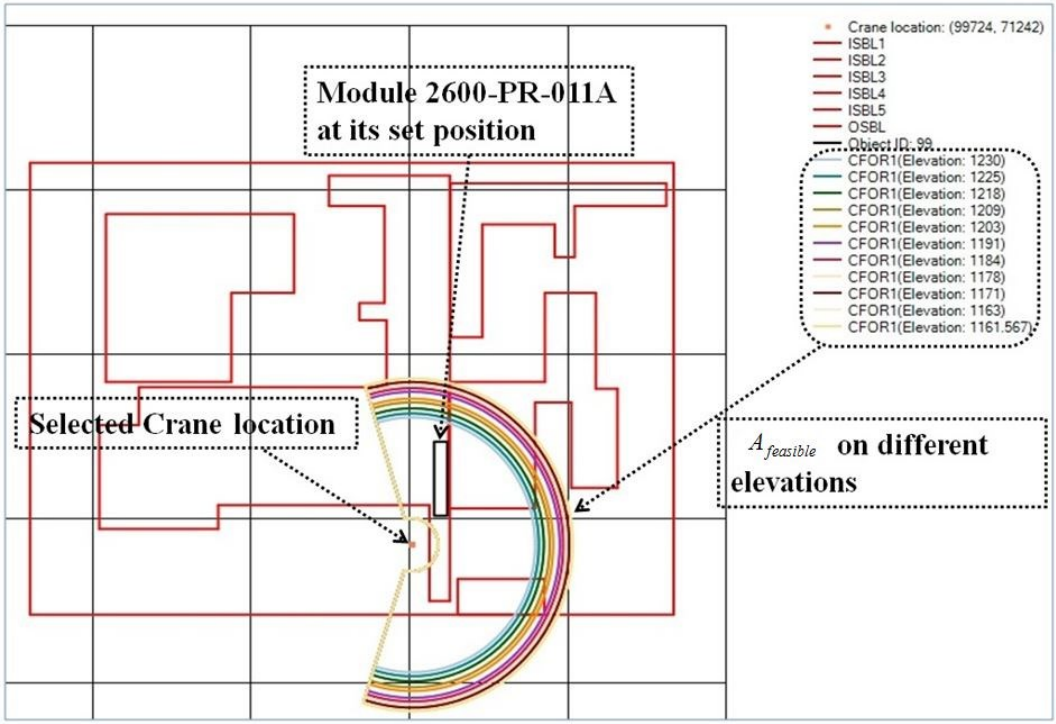

Figure 4-15 Case Two – $A_{feasible}$ on different elevations

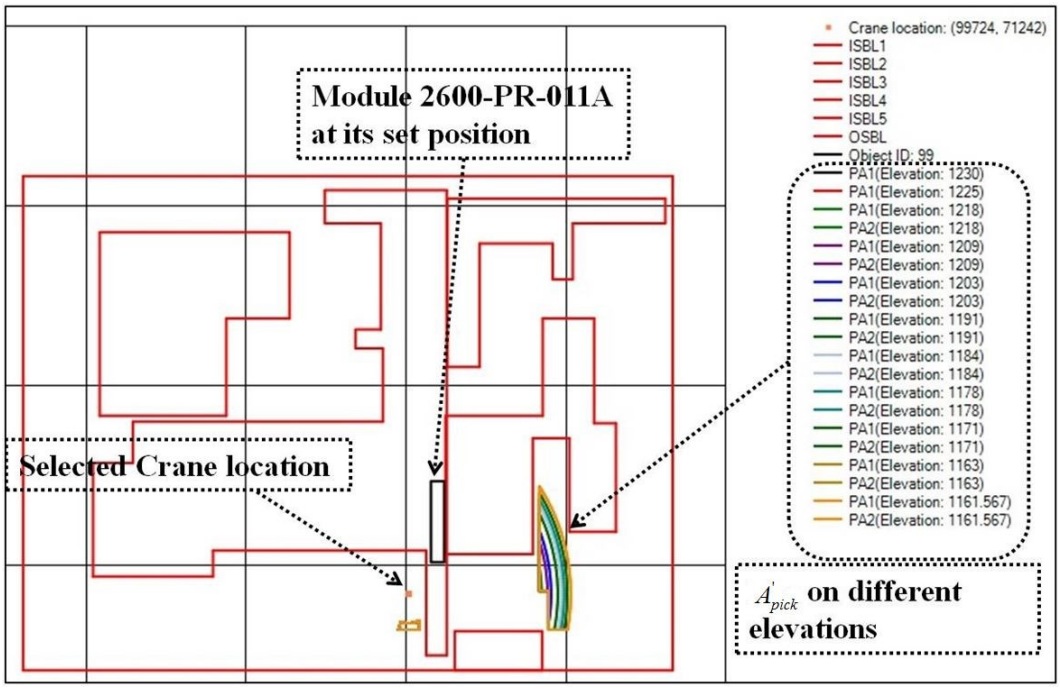

Figure 4-16 Case Two – A'_{pick} on different elevations

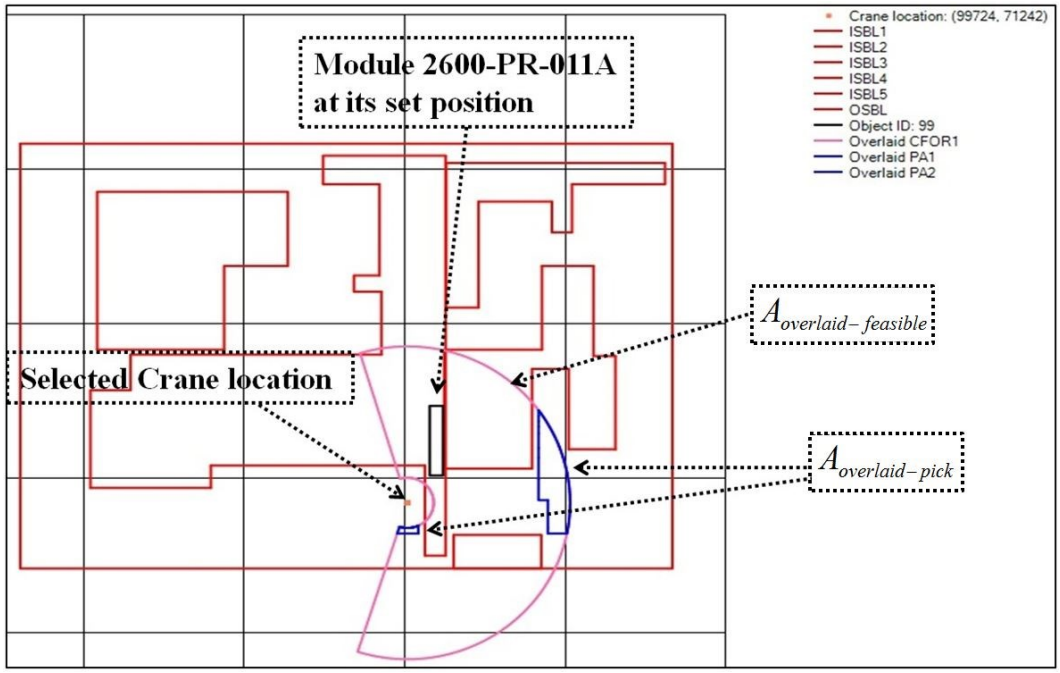

Figure 4-17 Case Two – $A_{overlaid-feasible}$ and $A_{overlaid-pick}$

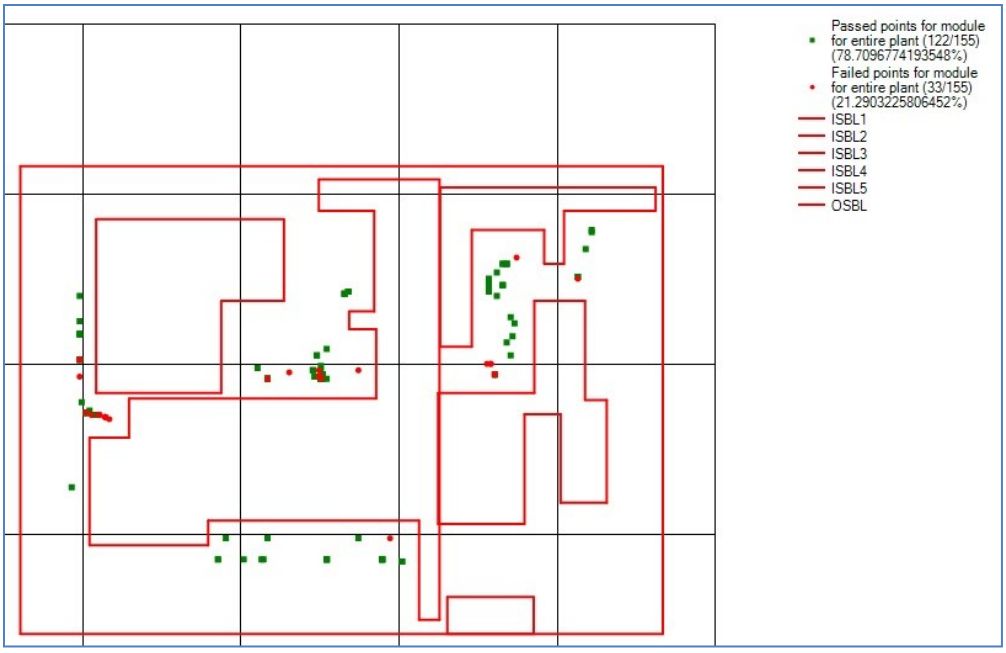

Figure 4-18 Case Two—entire site path checking results

4.4 Case Three – Crane Walking Analysis

This case study is based on a new steam-assisted gravity drainage (SAGD) project in Alberta, Canada. The proposed methodology is implemented in a Microsoft Visual Studio 2010 environment as a stand-alone computer application which uses the company's database as its main input stream. This database stores project-related information, including (*i*) site layout information; (*ii*) module information (set position coordinates, geometric size, weight, set elevation, and module weight); (*iii*) lifting schedule; and (*iv*) crane configurations. The computer application reads the required information from the database, performs the calculations, and writes the results back to the database. Also, a clipping algorithm developed at the University of Manchester, Vatti's polygon clipping method (Vatti 1992), is used in this research to intersect or unite the polygons.

The implementation of this research uses a non-commercial General Polygon Clipper (GPC) library based on Vatti's polygon clipping method.

Figure 4-19 presents the case study site layout, where there are a total of 107 modules to be lifted. The inside boundary limits define the area where the crane has no access, while the outside boundary limits are the outside boundaries of the site. Four different crane configurations are selected for analysis in this project: a Demag-CC2800 (660 imperial ton crane rating) crawler crane with a 72.0 m (236.2 ft) boom length; Demag-CC2500 (500 imperial ton crane rating) crawler cranes with and without superlift equipment with 72.0 m (236.2 ft) boom length; and a Manitowoc-M-18000 (825 imperial ton crane rating) with a boom length of approximately 73 m (240 ft). The superlift counterweight is 250 kg (551.2 lb).

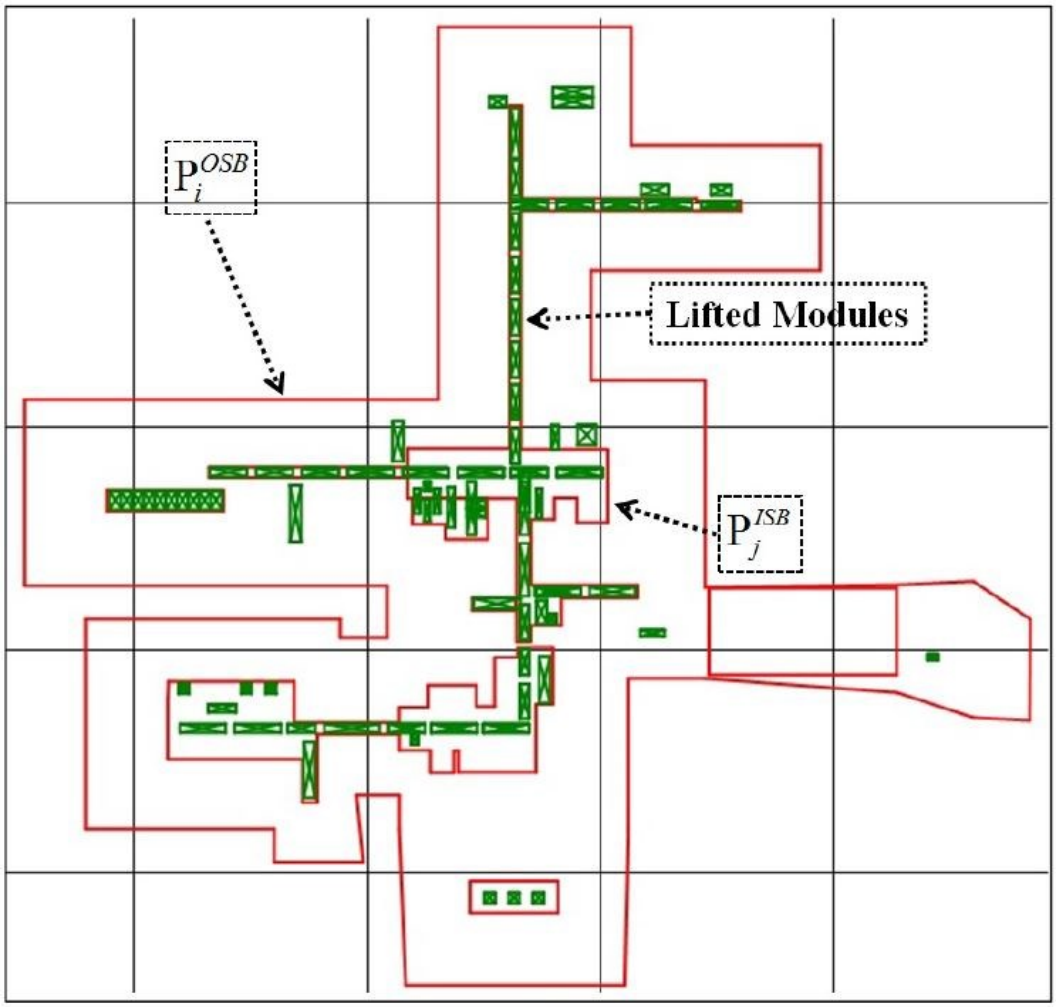

Figure 4-19 Case Three—site layout and lifted modules

Mobile crane operation planning for the entire site begins with using the ACPO system (developed by PCL Industrial Management Inc. and the University of Alberta) to select the crane positions for each module based on the crane configurations; (for details regarding crane location selection, see Hermann et al. 2010 and Safouhi et al. 2011). There are a total of 9,770 possible crane locations selected for this project: 673 for the Demag-CC2800; 320 for the Demag-CC2500 without superlift; 6,651 for the Demag-CC2500 with superlift; and 2,126 for the

Manitowoc-M-18000. All these locations must be checked to determine the capable/suitable mobile crane type(s) for the project, and two types of analyses need to be conducted in this regard: pick-and-swing analysis and crane walking analysis. The pick-and-swing analysis aims to determine whether or not the crane can perform the lift from a given selected crane location without needing to walk; (for details regarding the pick-and-swing analysis, see Lei et al. 2013a, 2013b). Next, the crane locations that have failed in the pick-and-swing analysis are further checked for possible crane walking paths. Both analyses require repeatable calculations and the manual planning process is tedious. Considering the large amount of selected crane locations, the analysis process can be time-consuming, to say nothing of the potential for error. Therefore, an automatic system is needed that can remove the human component involved in the analysis process. Indeed, without automation, exploration of all possible crane locations practically becomes impossible.

Figure 4-20 presents a crane walking case in a congested area for Module 13 (weight: 121,893 kg; height: 6.023 m). There are 14 crane locations selected which satisfy the lifting capacity and boom clearance at the crane's set location for the Demag-CC2500 with superlift equipment, as shown in Figure 4-20. One crane location is selected for crane walking planning, as shown in Figure 4-21. A total of 30 walking start points are generated, among which the one with the shortest distance (30.39 m) is selected as the crane walking path.

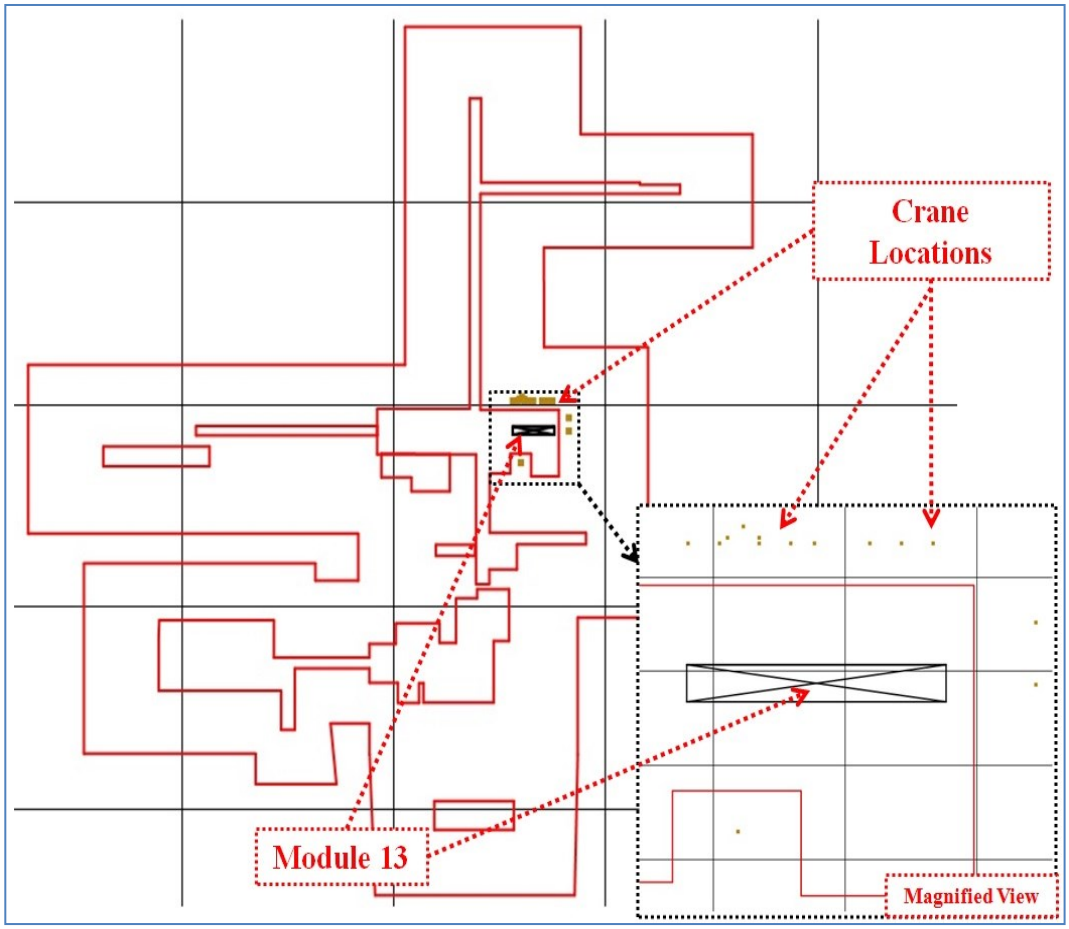

Figure 4-20 Case Three—module 13 and the selected crane locations

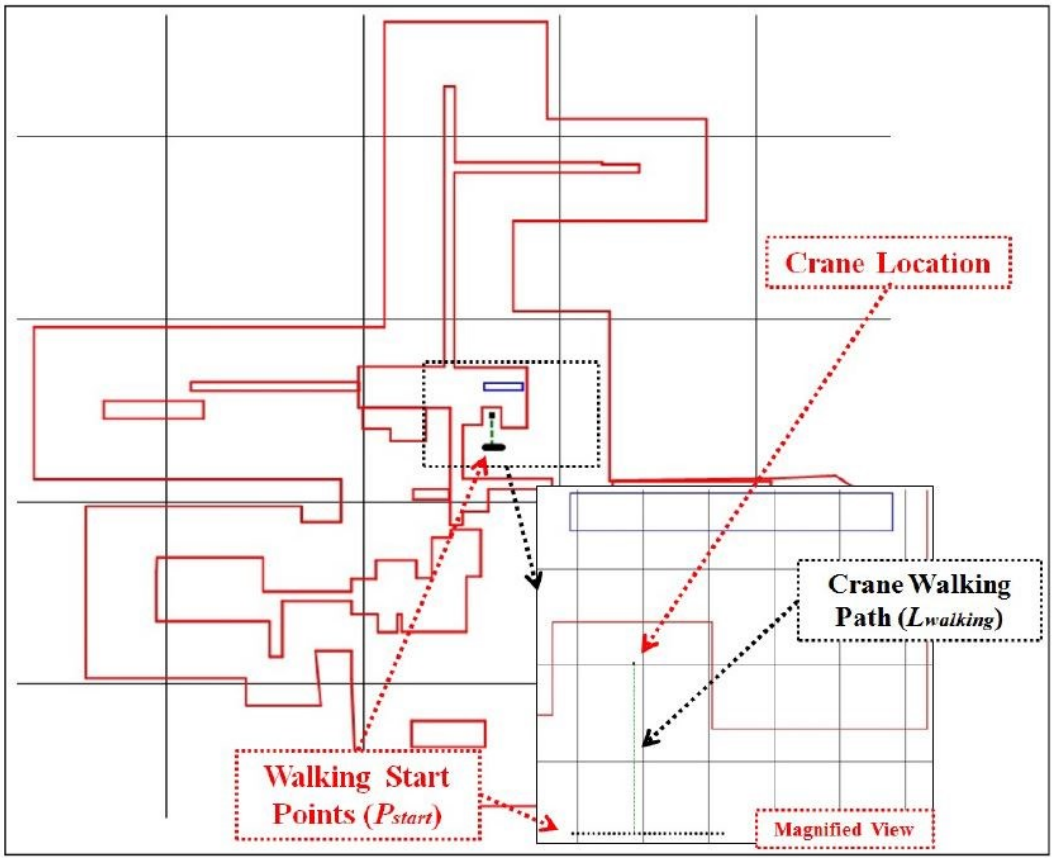

Figure 4-21 Case Three—crane walking path case

In order to validate the planned walking path, a heavy lift study is prepared by professional engineers using AutoCAD (plan view shown in Figure 4-22). As illustrated in Figure 4-22, the crane is located at its pick location with northeast coordinates (5195, 17420), and then walks with the load to its set location with the northeast coordinates of (5195, 17475); the total walking length is 16.75 m (54.95 ft). The crane has a lifting capacity of 83.93% at the module's pick position, and uses 84% capacity at its set position. The lift study also shows a similar crane walking path to the one generated by the newly built program, which serves to validate the methodology. In addition, this program analyzes the

entire site, including the pick-and-swing and crane walking analyses. In general, it is found that two crane configurations can be used for this project (Demag-CC 2500 and Manitowoc-M-18000). Although the Demag-CC 2500 with superlift equipment has a greater capacity, due to the congestion of the site many of the crane walking paths fail. Figure 4-23 shows the results for the Demag-CC 2500 with superlift equipment, where the red points represent the failed crane locations and the green points are the feasible crane locations with lifting paths/walking paths. In total the analysis takes 7 hours to complete for all 9,770 crane locations.

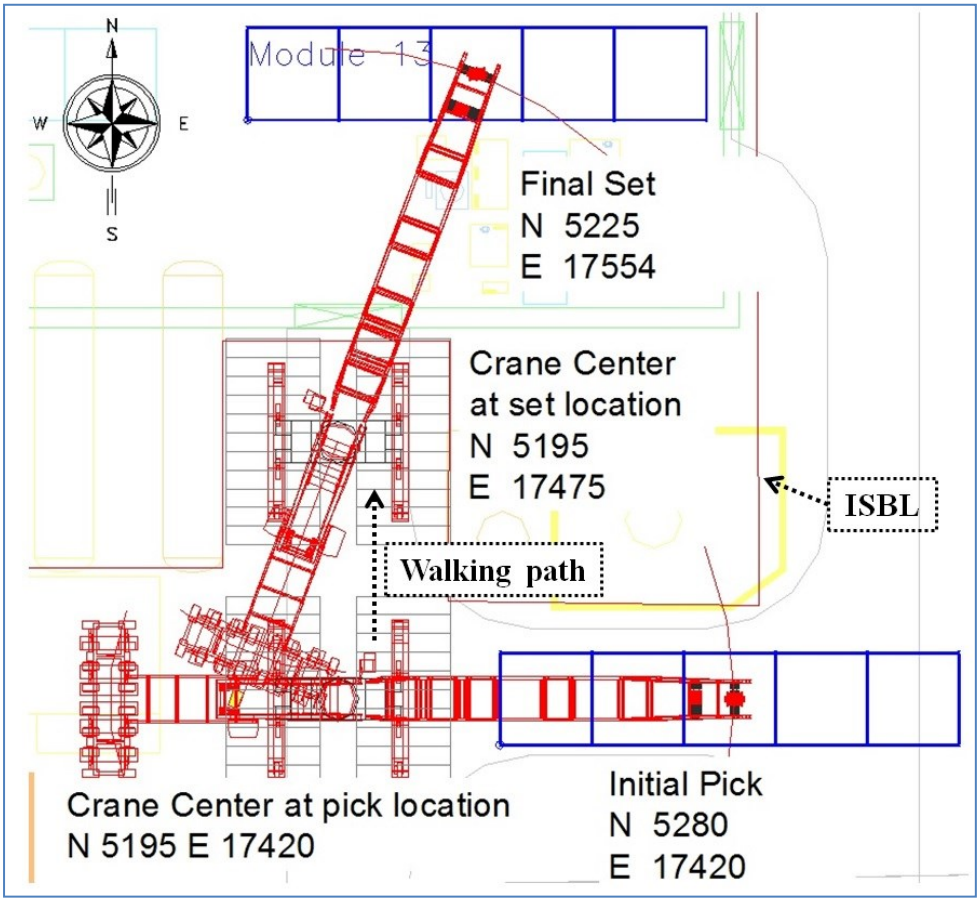

Figure 4-22 Case Three—crane walking path validation

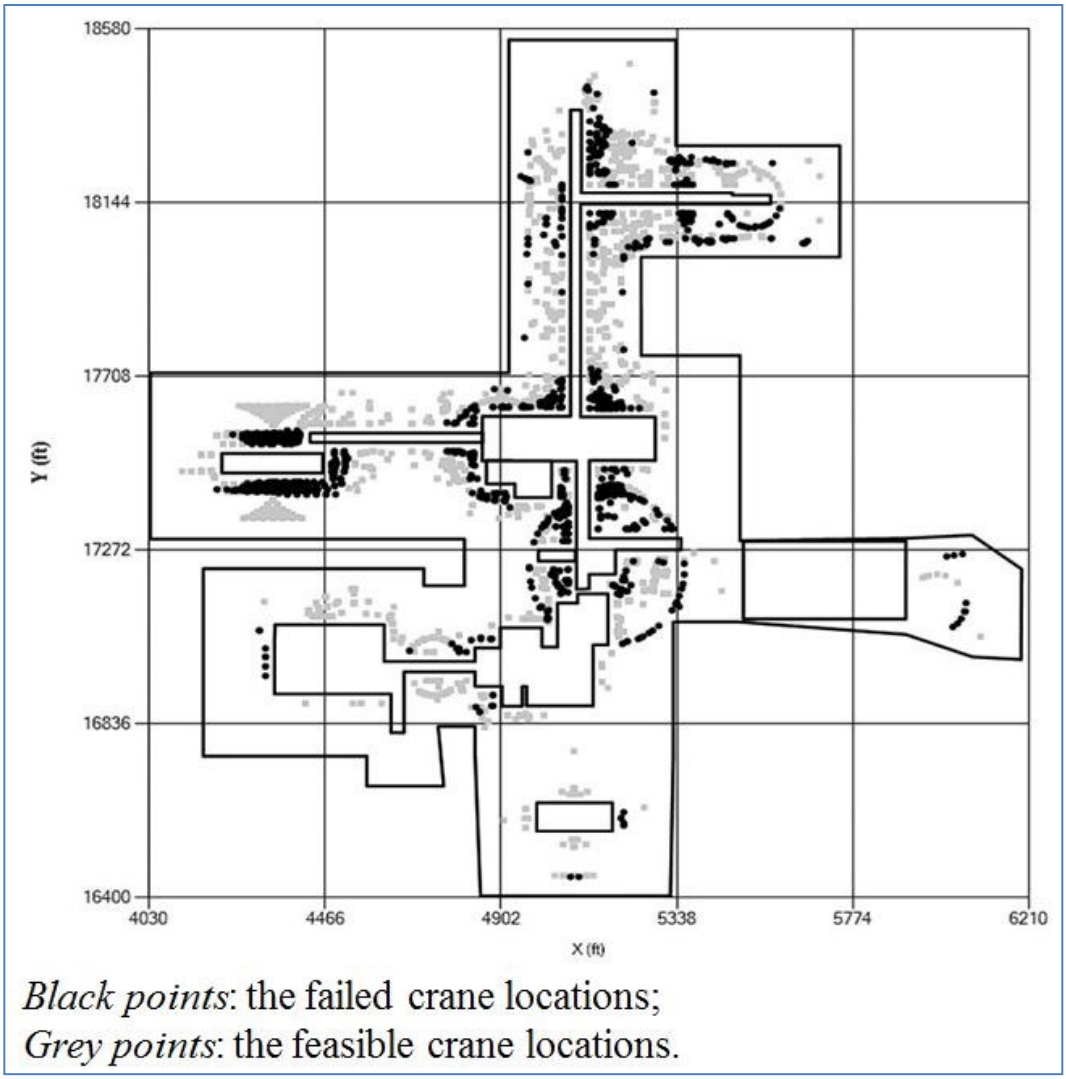

Figure 4-23 Sample results for Demag-CC 2500

4.5 Case Four – Clearance Checking

Boom clearance checking is critical in motion planning and analysis, and needs to be conducted often due to frequent design changes. In this case, a computer system is developed to automate the boom clearance process based on the approach described in section 3.7 ("Clearance Checking at Selected Crane Locations").

4.5.1 Site Layout and Crane Presentation

A PCL *Heavy Lift Planning Toolbox (HLPT)* has been developed for fast clearance checking (see Figure 4-24 for the designed interface). *HLPT* is connected to the server database, where project and crane data are stored. The project information can be downloaded from the server and displayed in the interface. Module information is stored temporarily in a *datagridview* in the interface (Figure 4-24), and a *MSChart* is used to show the site layout from a plan view. In Figure 4-25, examples of modules (plan view) are presented time-dependently. The lift for the module on the left is carried out on April 27, 2013 when the site is relatively spacious; on July 13, 2013, the site is quite congested due to project progress. Mobile cranes at both pick and set locations can be plotted according to the crane configuration assigned to each module.

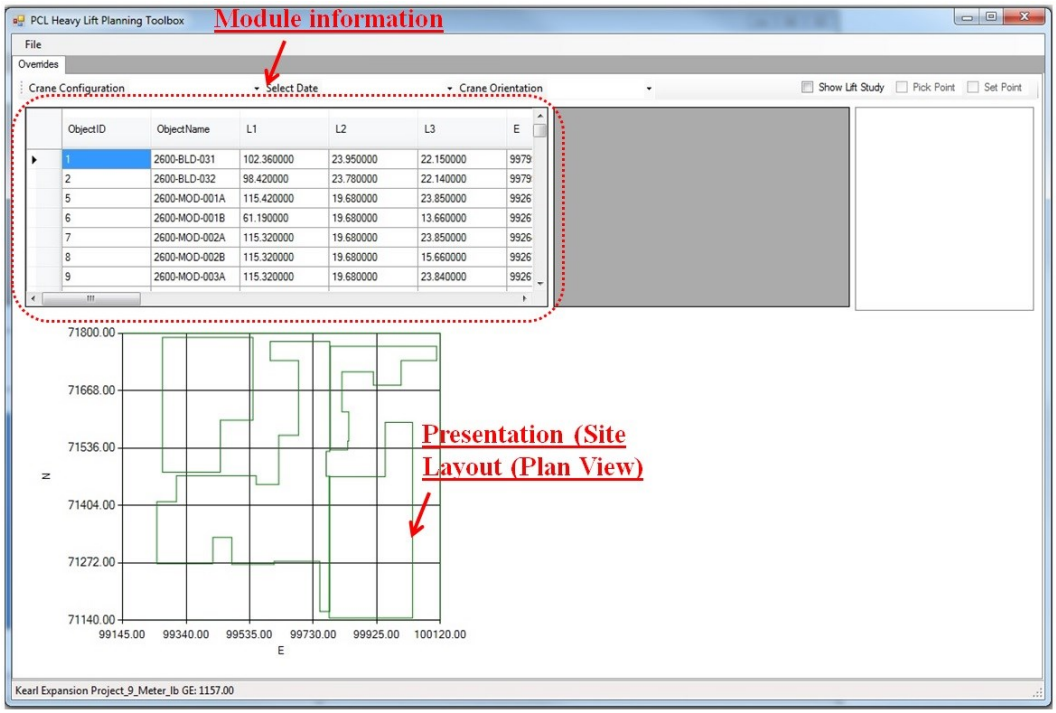

Figure 4-24 Case Four—designed interface

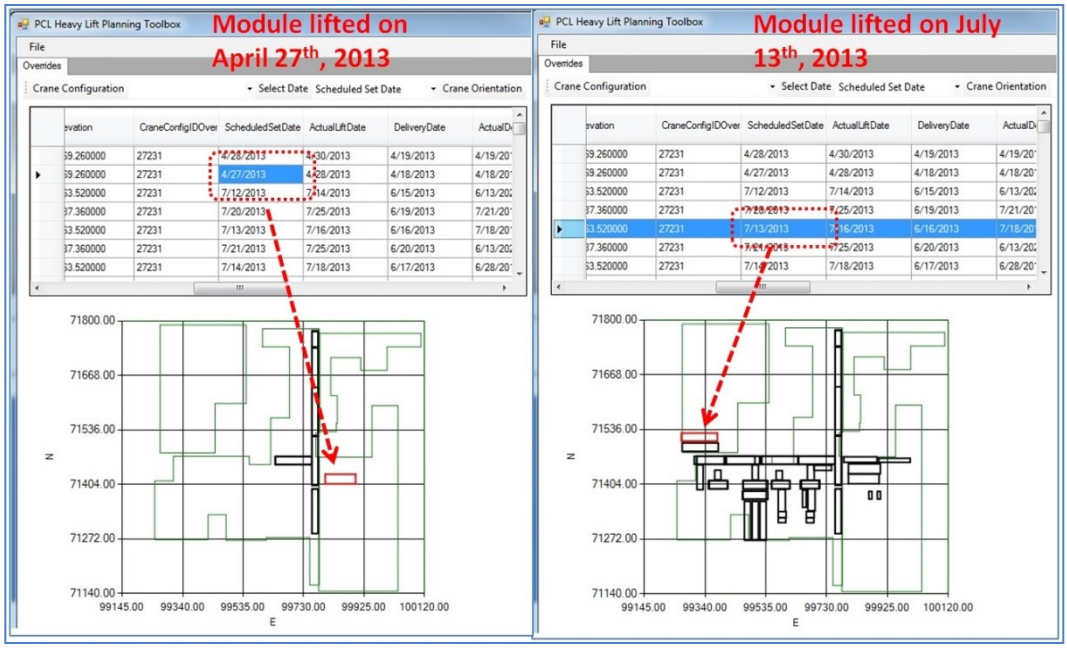

Figure 4-25 Case Four—time-dependent module on site

One boom clearance checking example is given in Figure 4-26, in which the weight of the lifted module is 277,832 lb. The Demag CC-2800 with Superlift attachment is used to lift the module, and the lift date is July 13, 2013. The site is plotted time-dependently; (the mobile crane is shown at its set location). An AutoCAD model is used for comparison with the plotted symbolic model. In addition, the designed interface has a magnifying feature that allows the user to zoom in to view the details. It is calculated that the mobile crane takes 70.8% of its lifting capacity at the pick position and 65.5% at its set position. Using the *Clipping Algorithm*, the clearance checking results are generated as shown in Figure 4-27. The shortest distance from the boom to the obstructions is 25.16 ft, which means this partiuclar lift can be performed.

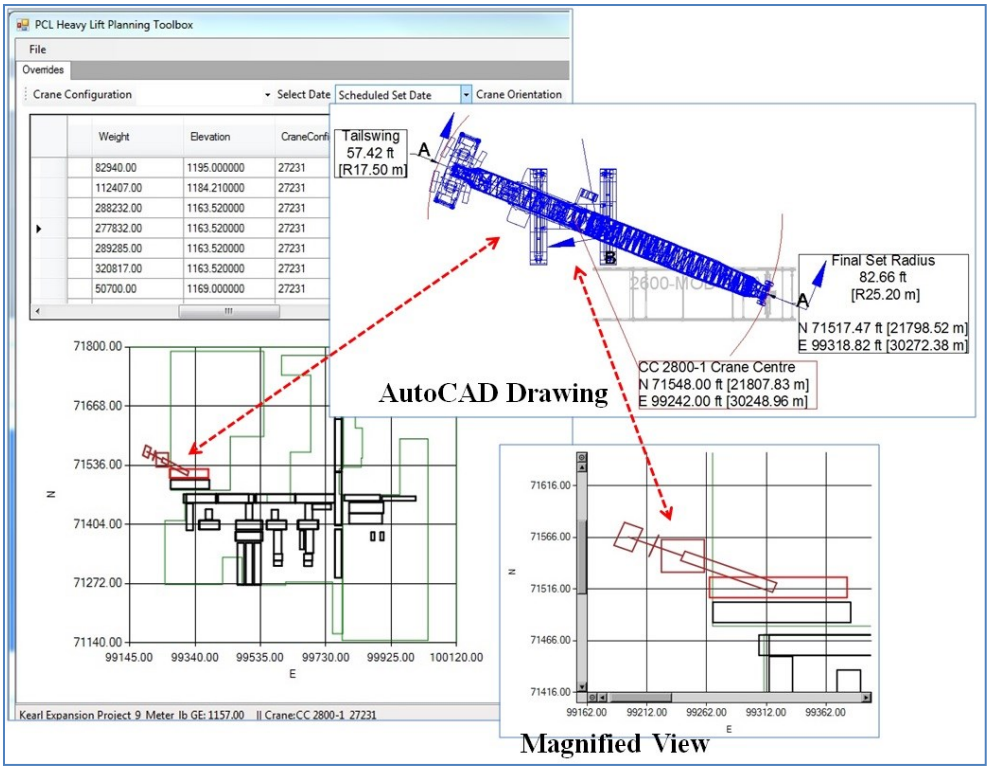

Figure 4-26 Case Four—symbolic crane model for Demag CC-2800

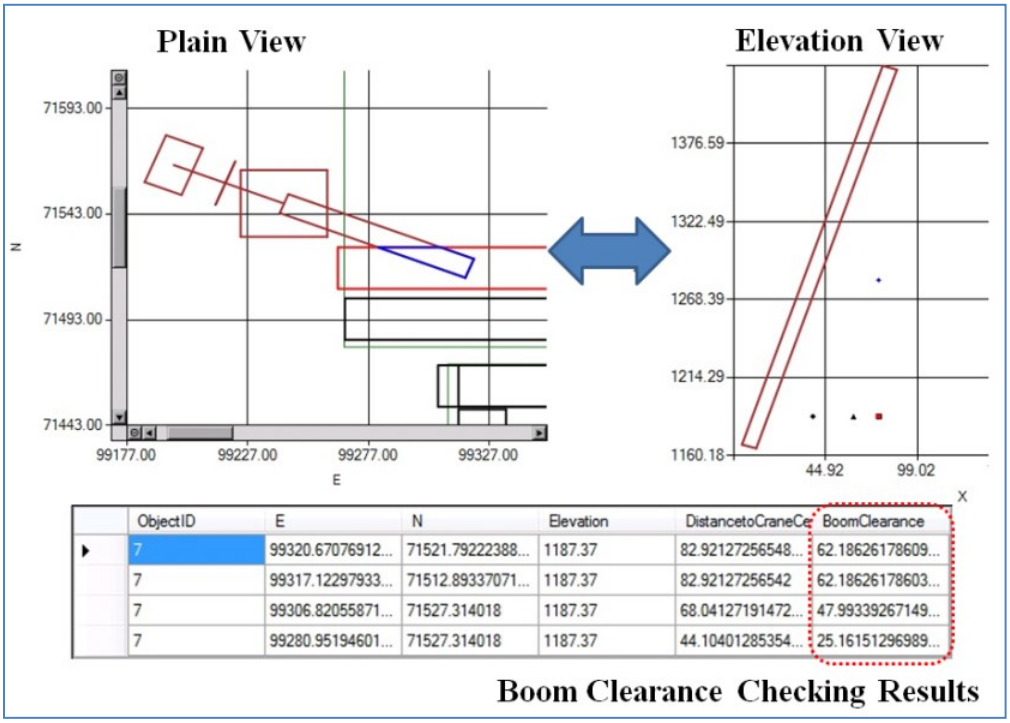

Figure 4-27 Boom clearance checking results

4.6 Visualization of Crane Motions

The designed visualization system is applied to an industrial project in FortMcMurray, Alberta, Canada. This project consists of a total of 210 prefabricated modules, and the mobile crane primarily used in this project is the Demag CC2800 (crane capacity rating 660 t) with superlift equipment (Superlift radius = 15 m, weight = 300,000 kg). The designed system is capable of animating time-dependent lift studies generated in AutoCAD by professional engineers. In this section, three cases from the project are elaborated on, with one focusing on pick-and-swing lifting and the other analyzing the crane walking scenario. The last case provides a rare scenario in which typical *crane walking* is not allowed.

4.6.1 Pick-and-swing Lifting Visualization

Case One shows a module lift using the pick-and-swing lifting process. The piperack module weighs 129,747.4 kg (286,044 lb), with a length of 36.1 m (118.4 ft), width of 6.0 m (19.7 ft), and a height of 9.3 m (30.51 ft). The lift study shows that the mobile crane uses 69.4% of its lifting capacity at both the pick location and set location. Figure 4-28 shows the lifting process animation automatically generated in 3ds Max. During the animation, the mobile crane stays at one specific location to perform the lift without walking.

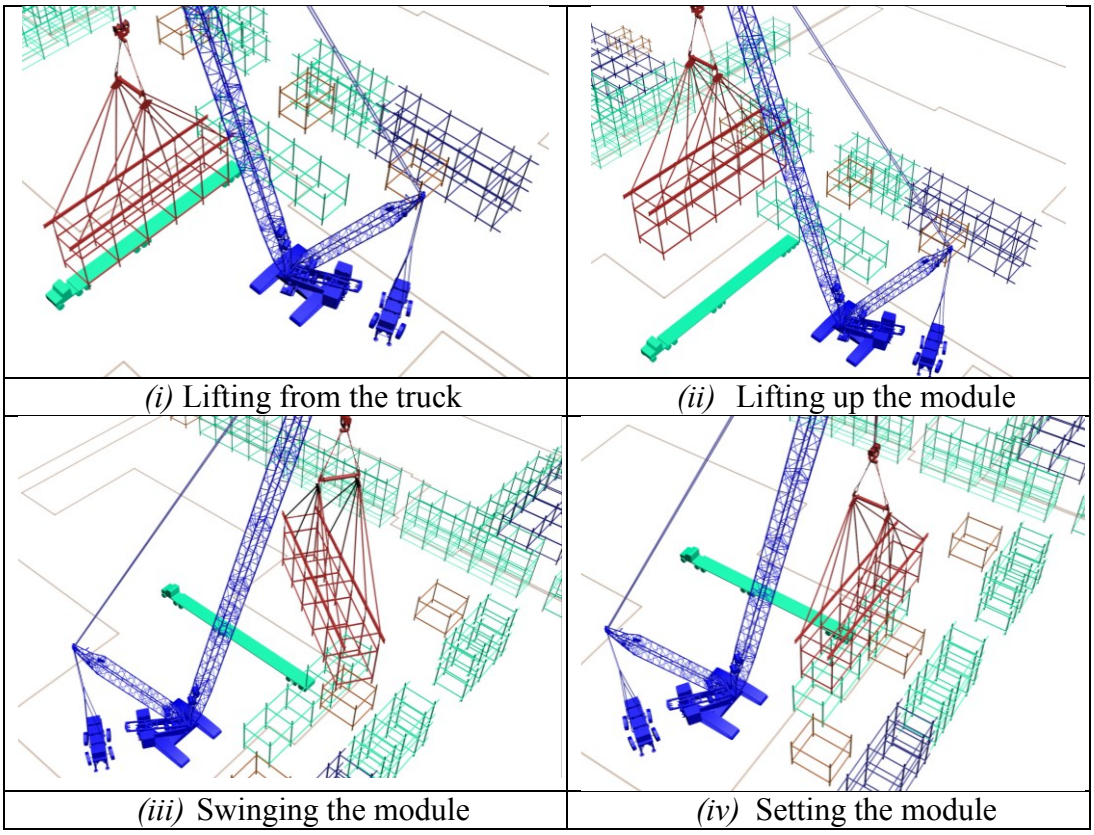

(i) Lifting from the truck | *(ii)* Lifting up the module

(iii) Swinging the module | *(iv)* Setting the module

Figure 4-28 Pick-and-swing lifting animation

4.6.2 Crane Walking Lifting Visualization

Case Two presents a case walking lifting scenario, where the module weighs 158,606 kg (349,667 lb), with a length of 30.0 m (98.4 ft), a width of 7.25 m (23.78 ft), and a height of 6.75 m (22.15 ft). Due to the congestion of the site layout, the crane must pick the module (using 73.6% of its full lifting capacity), swing the module to the carbody's front, and walk with the module to its set location, where the mobile crane uses 80.7% of its full lifting capacity to set the module. Figure 4-29 shows the details of each step in the *crane walking lifting* process.

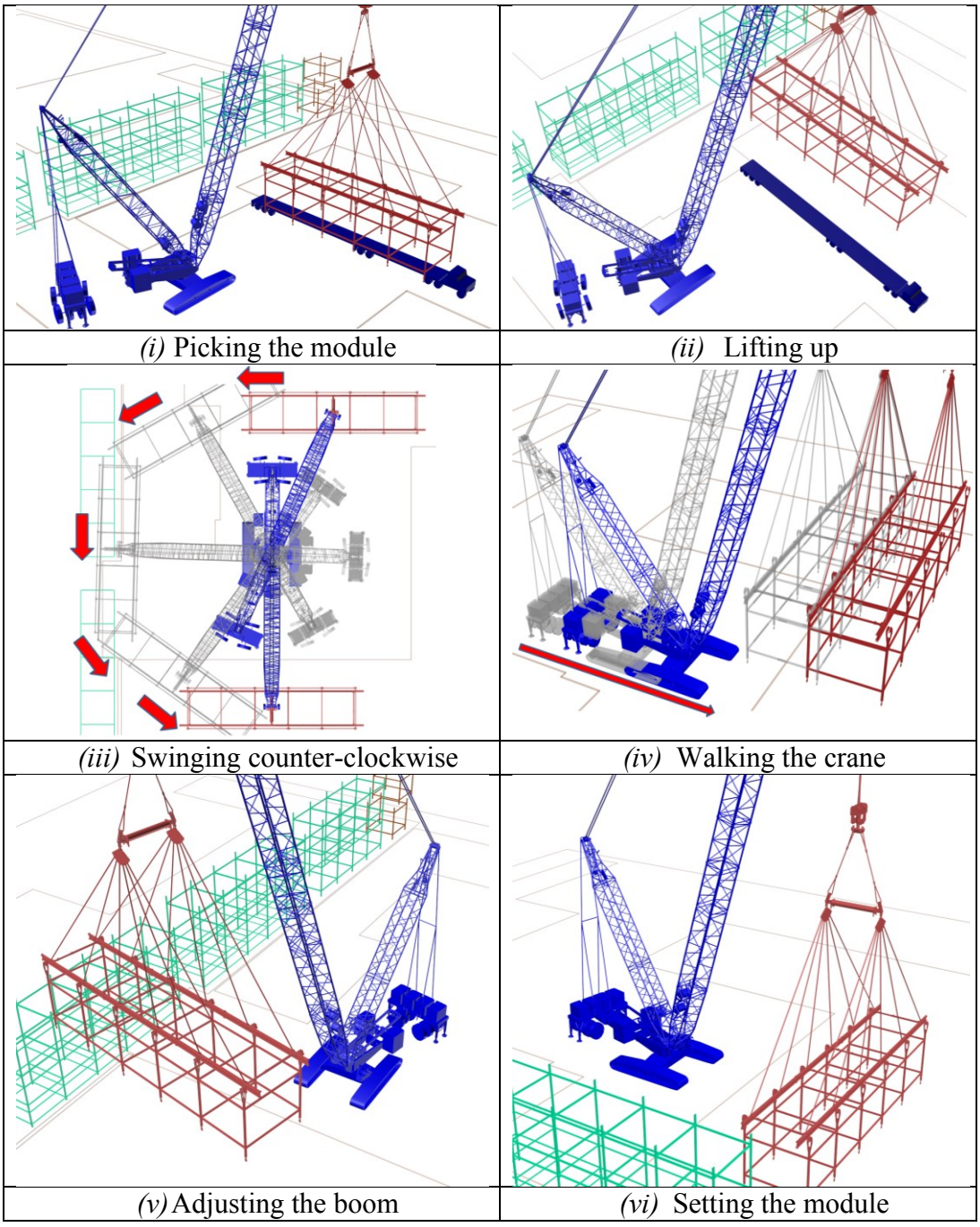

Figure 4-29 Crane walking lifting animation

4.6.3 Crane Crab Walking

In most cases, the module hangs in front of the mobile crane as the crane walks, as shown in Figure 4-29. However, in some exceptional cases, due to the presence

of an obstacle in the direction of crane walking, the mobile crane must hang the lifted module at an offset angle to its walking direction. Figure 4-30 illustrates the case of crab walking. In (*iv*) and (*v*), the mobile crane walks with load hanging at an angle to the walking direction (module not aligned perpendicular to the front of the mobile crane during its walk). This crab walking is necessitated by the presence of existing modules that constrain the crane's walking path (i.e., the stacked piperack modules in front of the mobile crane in (*v*)).

4.7 Summary

In this chapter, four cases have been presented to demonstrate crane motion planning (pick-and-swing and crane walking) and clearance checking. Case One focuses on a single lift, in which the path checking is conducted on the module's lifting elevation. This is extended in Case Two, where the module lifting is checked on multiple elevations. Case Two also demonstrates the efficiency of the system in terms of entire site lifting planning: all crane locations are checked for the feasibility of lifting, based on which the crane configuration is selected. For those paths which fail the path checking, crane walking paths are planned as shown in Case Three. In Case Four, the features of the developed system, PCL's *Heavy Lift Planning Toolbox (HLPT)*, are demonstrated. The *HLPT* plots the module according to the assigned schedule and creates a crane symbolic model for clearance checking. The boom clearance of each crane location is also checked and presented in an elevation view. All the boom clearance distances from the potential collision points to the boom perpendicularly are calculated to validate the clearance checking. In the end, a visualization model is developed in 3ds Max

using MAXScript to automate the crane motion visualization process. The cases shown in this chapter serve to validate the proposed methodology and the designed system.

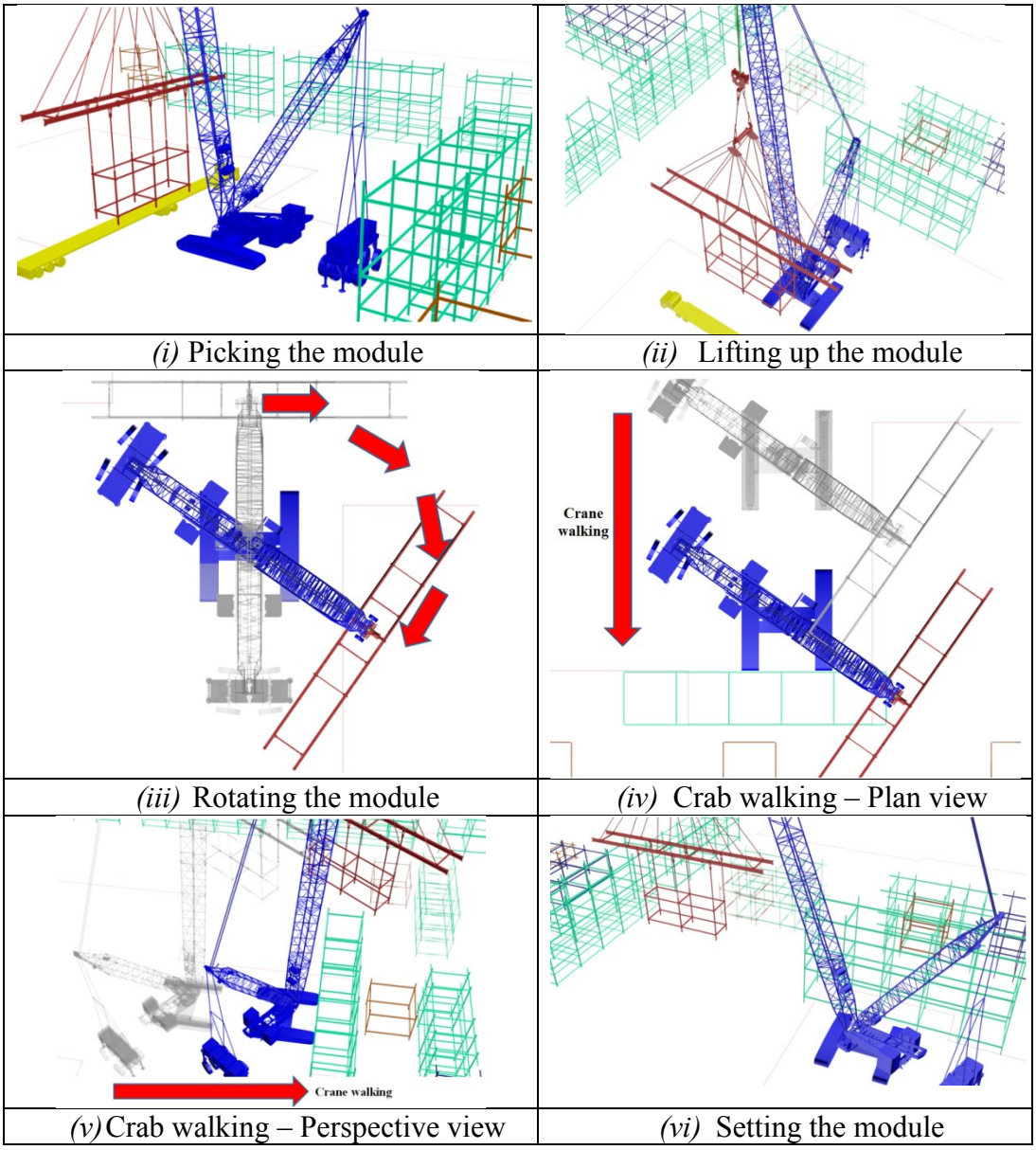

(i) Picking the module | *(ii)* Lifting up the module

(iii) Rotating the module | *(iv)* Crab walking – Plan view

(v) Crab walking – Perspective view | *(vi)* Setting the module

Figure 4-30 Crane crab walking scenario

Chapter 5 Conclusions & Future Work

5.1 Research Summary

The onsite installation of industrial modules involves frequent use of mobile cranes. Appropriate planning of these heavy lifts can lead to cost savings and reduced construction cycle time, but many subjects need to be analyzed for these heavy lifts, such as: (*i*) crane type selection; (*ii*) crane potential locations; (*iii*) lifting sequence; and (*iv*) feasibility of lifts. The feasibility of lifts can be checked in terms of many factors (e.g., lifting capacity, crane clearance). However, the current manual-based process of checking the lifting feasibility is tedious and error-prone. In order to achieve higher efficiency in the planning process and avoid errors, a generic method is proposed in this research that can automate the crane motion planning process and check the feasibility of lifts. In general, there are two types of mobile crane operations: *pick-and-swing*, where the mobile crane sits at one particular location to perform the lift, and *crane walking*, where the mobile crane must pick up the module from an open area and walk to its set location to place the module. In this research, both operations are taken into consideration and two assumptions are made: the module is treated as a cubic shape and the project site is simplified as multiple elevations. The rationales for these two assumptions are that: (*i*) in modular construction, module shape is standard in most cases; and (*ii*) site construction structures are often in regular shapes.

In pick-and-swing analysis, the mobile crane's lifting radii are determined based on its lifting capacity, boom clearance, and rigging height requirements. In this

study, a robotic motion planning method, the configuration space (C-Space) method, is implemented to simplify the site layout. Based on the generated feasible crane operation area, the lifting path is checked by investigating the relationship between the crane feasible operation area and the pick area. For the case in which the pick-and-swing analysis fails, *crane walking* analysis needs to be carried out to explore the opportunity of walking the crane. Following these analyses, the crane lifting process is then checked with respect to the crane's pick and set locations using the PCL Heavy Lifting Planning Toolbox. This toolbox checks the boom clearance of the mobile crane at the pick and set locations considering the surrounding environment. The crane lifting operation is eventually automatically animated in 3ds Max using MAXScript. The limitations of the research are: (*i*) the developed algorithms consider two common crane movements, namely the "pick-and-swing" and "crane walking" movements, while some rare lifting cases are ignored, such as long vessels that require two-crane lifts; (*ii*) the current visualization does not consider the speeds for the crane movements; and (*iii*) the errors found in the lifting paths are still corrected adjusted manually; an automatic mechanism should be developed to fix the failed crane lifts.

5.2 Research Contributions and Future Works

This research makes the following contributions:

(i) Applies a robotic motion planning method (C-Space) to check the mobile crane lift path on different project elevations.

(ii) Develops and implements an algorithm for checking the feasibility of mobile crane walking.

(iii) Develops a fast, accurate, and time-dependent clearance checking mechanism for checking different crane locations.

(iv) Develops an automated visualization tool in 3ds Max to visualize the planned crane motions.

(v) Achieves automation for the crane motion planning, which eliminates a large proportion of the human components and error.

Based on this research, the following future research topics are proposed:

(i) Use game engines to develop software that allows engineers to operate the mobile crane in a 3D environment in order to support better understanding of the lifting process and avoidance of potential safety issues.

(ii) Integrate simulation tools with the current developed system to simulate the lifting process and improve productivity. Simulation can also be used to analyze the entire site mobile crane operations, such as construction cycle and optimal lifting sequence.

(iii) Include other engineering design aspects, such as mat design for mobile cranes. These aspects can be taken into account in order to determine the optimal crane operations and locations.

(iv) Add a collision detection feature into the 3D visualization so that practitioners can detect the blocking obstacles for lifting and adjust the

lifting schedule accordingly; also, install sensors on site for real-time lifting analysis, and capture potential collisions.

(v) Integrate the current lifting analysis with the crane location optimization. The objective function can be expressed as follows:

$$F = Min\{t_{lifting}, t_{travel}\}$$

Where $t_{lifting}$ = the crane's total lifting time for all the modules; and t_{travel} = the crane's travel time spent between different crane locations, which includes the assembly and disassembly time. The objective function is subject to the following constraints: the number of crews; the number of cranes; the site traveling paths; and the lifting sequence. Also, certain penalties can be considered in the optimization models. For example, the crane should keep the module as close as possible to the ground elevation while lifting, so lifting up would cause a penalty.

Publications

Publications of particular relevance to this research:

Lei, Z., Han, S., Bouferguene, A., Al-Hussein, M., and Hermann, U. (2014). "Automation for mobile crane motion planning in industrial projects." *Proceedings, International Symposium on Automation and Robotics in Construction (ISARC)*, Sydney, Australia, 410-417.

Han, S., Lei, Z., Bouferguene, A., Al-Hussein, M., and Hermann, U. (2014). "Integrated visualization and simulation for lifting operations of modules under congested environment." *Proceedings, International Symposium on Automation and Robotics in Construction (ISARC)*, Sydney, Australia, 262-269.

Lei, Z., Han, S., Bouferguene, A., Taghaddos, H., Hermann, U., and Al-Hussein, M. (2014. "Algorithm for mobile crane walking path planning in congested industrial plants." *Journal of Construction Engineering and Management*, ASCE, 10.1061/(ASCE)CO.1943-7862.0000929

Lei, Z., Taghaddos, H., Olearczyk, J., Al-Hussein, M., and Hermann, U. (2013). "Automated crane path checking for heavy lifts in industrial projects." *Journal of Construction Engineering and Management*, 139(10).

Lei, Z., Taghaddos, H., Hermann, U., and Al-Hussein, M. (2013). "A methodology for mobile crane lift path checking in heavy industrial projects." *Automation in Construction*, 31, 41-53.

Lei, Z., Taghaddos, H., Hermann, U., and Al-Hussein, M. (2013). "Integrating mobile crane lift path checks into an industrial crane management system." *Proceedings, International Symposium on Automation and Robotics in Construction (ISARC)*, Montréal, QC, Canada, 1-8.

Lei, Z., Behzadipour, S., Al-Hussein, M., and Hermann, U. (2011). "Application of robotic obstacle avoidance in crane lift path planning." *Proceedings, International Symposium on Automation and Robotics in Construction (ISARC)*, Seoul, Korea, 292-297.

Other publications:

Liu, H., Lei, Z., Li, H. X., and Al-Hussein, M. (2014). "An automatic scheduling approach: Building information modeling-based on-site scheduling for panelized construction." *Proceedings, Construction Research Congress*, Atlanta, GA, USA, May 19-21, 1666-1675.

Han, S., Hasan, S., Lei, Z., Altaf, M. S., and Al-Hussein, M. (2013). "A framework for crane selection in large-scale industrial construction projects." *Proceedings, International Symposium on Automation and Robotics in Construction (ISARC)*, Montréal, QC, Canada, 387-394.

Li, H. X., Al-Hussein, M., Lei, Z., and Ajweh, Z. (2013). "Risk identification and assessment of modular construction utilizing fuzzy analytic hierarchy process (AHP) and simulation." *Canadian Journal of Civil Engineering*, 40(12), 1184-1195 (***Received Honourable Mention in Stephen G. Revay Award 2014 Competition, Canadian Society of Civil Engineering***).

Li, H. X., Al-Hussein, M., and Lei, Z. (2011). "Incentive genetic algorithm based time-cost trade-off analysis across a build-operate-transfer project concession period." *Canadian Journal of Civil Engineering*, 38(2), 166-174.

Bibliography

AbouRizk, S. and Hajjar, D. (1998). "A framework for applying simulation in construction industry." *Canadian Journal of Civil Engineering*, 25(3), 604-617.

AbouRizk, S. (2010). "Role of simulation in construction engineering and management." *Journal of Construction Engineering and Management*, 136(10), 1140-1153.

AbouRizk, S., Halpin, D., Mohamed, Y., and Hermann, U. (2011). "Research in modeling and simulation for improving construction engineering operations." *Journal of Construction Engineering and Management*, 137(10), 843-852.

Akinci, B., Fischer, M., and Kunz, J. (2002). "Automated generation of work spaces required by construction activities." *Journal of Construction Engineering and Management*, 128(4), 306-315.

AlBahnassi, H. and Hammad, A. (2012). "Near real-time motion planning and simulation of cranes in construction: Framework and system architecture." *Journal of Computing in Civil Engineering*, 26(1), 54-63.

Alberta Government (2013). "Annual Report of Energy 2012-2013." http://www.energy.alberta.ca/Org/Publications/AR2013.pdf (Accessed Mar. 29, 2014).

Alberta Government (2014). http://oilsands.alberta.ca/economicinvestment.html; and http://www.energy.alberta.ca/oilsands/791.asp (Accessed Mar. 29, 2014).

Al-Hussein, M., Alkass, S., and Moselhi, O. (2000). "D-CRANE: A database system for utilization of cranes." *Canadian Journal of Civil Engineering*, 27, 1130-1138.

Al-Hussein, M., Alkass, S., and Moselhi, O. (2005). "Optimization algorithm for selection and on site location of mobile cranes." *Journal of Construction Engineering and Management*, 131(5), 579-590.

Al-Hussein, M., Niaz, M. A., Yu, H., and Kim, H. (2006). "Integrating 3D visualization and simulation for tower crane operations on construction sites." *Automation in Construction*, 15(5), 554-562.

Ali, A. D. M. S., Babu, N. R., and Varghese, K. (2002). "Offline path planning of cooperative manipulators using coevolutionary genetic algorithm." *Proceedings, International Symposium on Automation and Robotics in Construction (ISARC)*, Netherlands, 415-424.

Ali, M. S., Babu, N. R., and Varghese, K. (2005). "Collision free path planning of cooperative crane manipulators using genetic algorithm." *Journal of Computing in Civil Engineering*, 19(2), 182-193.

Alwisy, A., Al-Hussein, M., and Al-Jibouri, S. H. (2012). "BIM approach for automated drafting and design for modular construction manufacturing."

Proceedings, International Conference on Computing in Civil Engineering, Clearwater Beach, FL, USA, 221-228.

Araya, H., Kakuzen, M., Kinugawa, H., and Arai, T. (2004). "Level luffing control system for crawler cranes." *Automation in Construction*, 13(5), 689-697.

Asano, T., Guibas, L., Hershberger, J., and Imai, H. (1985). "Visibility-polygon search and Euclidean shortest path." *Proceedings, Symposium on Foundations of Computer Science*, Portland, OR, USA, 155-164.

Aurenhammer, F. (1991). "Voronoi diagrams: A survey of fundamental geometric data structure." *ACM Computer Survey*, 23(3), 345-405.

Bryson, L. S., Maynard, C., Castro-Lacouture, D., and William, R. L. (2005). "Fully autonomous robot for paving operations." *Proceedings, Construction Research Congress*, San Diego, CA, USA.

Canada Weather Stats (2014). http://fortmcmurray.weatherstats.ca/ (Accessed Aug. 11, 2014).

Chang, Y. C., Hung, W. H., and Kang, S. C. (2012). "A fast path planning method for single and dual crane erections." *Automation in Construction*, 22, 468-480.

Cheng, Z. and Hammad, A. (2012). "Improving lifting motion planning and re-planning of cranes with consideration for safety and efficiency." *Advanced Engineering Informatics*, 26(2), 396-410.

Cheng, T. and Teizer, J. (2014). "Modeling tower crane operator visibility to minimize the risk of limited situational awareness." *Journal of Computing in Civil Engineering*, 28(3).

Chi, H. L., and Kang, S. C. (2010). "A physics-based simulation approach for cooperative erection activities." *Automation in Construction*, 19(6), 750-761.

Cho, Y. K., Alaskar, S., and Bode, T. A. (2010). "BIM-integrated sustainable material and renewable energy simulation." *Proceedings, Construction Research Congress*, Banff, AB, Canada, 288-297.

Chong, H. Y. and Phuah, T., H. (2013). "Incorporation of database approach into contractual issues: Methodology and practical guide for organizations." *Automation in Construction*, 31, 149-157.

Construction Industry Institute (CII) (2002). "Prefabrication, preassembly, modularization, and offsite fabrication in industrial construction: A framework for decision-making." University of Texas, Austin, TX, USA.

Duong, S. C., Uezato, E., Kinjo, H., and Yamamoto, T. (2012). "A hybrid evolutionary algorithm for recurrent neural network control of a three-dimensional tower crane." *Automation in Construction*, 23, 55-63.

Eastman, C. M. and Sacks, R. (2008). "Relative productivity in the AEC industries in the United States for on-site and off-site activities." *Journal of Construction Engineering and Management*, 134(7), 517-526.

Ge, S. S. and Cui, Y. J. (2002). "Dynamic motion planning for mobile robots using potential field method." *Autonomous Robots*, 13(3), 207-222.

GPC library, http://www.cs.man.ac.uk/~toby/alan/software/gpc.html (Accessed Jun. 8, 2014).

Haas, C. T., O'Connor, J. T., Tucker, R. L., Eickmann, J. A., and Fagerlund, W. R. (2000). "Prefabrication and preassembly trends and effects on the construction workforce." *Center for Construction Industry Studies*, University of Texas, Austin, TX, USA.

Halpin, D. W. (1977). "CYCLONE: Method for modeling of job site processes." *Journal of the Construction Division*, 103(3), 489-499.

Hanna, A. S. and Lotfallah, W. B. (1999). "A fuzzy logic approach to the selection of cranes." *Automation in Construction*, 8(5), 597-608.

Hasan, S., Al-Hussein, M., Hermann, U., and Safouhi, H. (2010). "Interactive and dynamic integrated module for mobile cranes supporting system design." *Journal of Construction Engineering and Management*, 136(2), 179-186.

Hasan, S., Zaman, H., Han, S., Al-Hussein, M., and Su, Y. (2012). "Integrated building information model to identify possible crane instability caused by strong winds." *Proceedings, Construction Research Congress*, West Lafayette, IN, USA, 1281-1290.

Hermann, U., Hendi, A., Olearczyk, J., and Al-Hussein, M. (2010). "An integrated system to select, position, and simulate mobile cranes for

complex industrial projects." *Proceedings, Construction Research Congress*, Banff, AB, Canada, 267-276.

Hermann, U. H., Hasan, S., Al-Hussein, M., and Bouferguene, A. (2011). "Innovative system for off-the-ground rotation of long objects using mobile cranes." *Journal of Construction Engineering and Management*, 137(7), 478-485.

Huang, C., Wong, C. K., and Tam, C. M. (2011). "Optimization of tower crane and material supply locations in a high-rise building site by mixer-integer linear programming." *Automation in Construction*, 20(5), 571-580.

Hornaday, W. C., Haas, C. T., O'Connor, J. T., and Wen, J. (1993). "Computer-aided planning for heavy lifts." *Journal of Construction Engineering and Management*, 119(3), 498-515.

Jung, J., Hong, S., Jeong, S., Kim, S., and Cho, H. (2014). "Productive modeling for development of as-built BIM of existing indoor structures." *Automation in Construction*, 42, 68-77.

Kamat, V. R. and Martinez, J. C. (2003). "Validating complex construction simulation models using 3D visualization." *Systems Analysis Modelling Simulation*, 43(4), 455-456.

Kang, S. C. and Miranda, E. (2006). "Planning and visualization for automated robotic crane erection processes in construction." *Automation in Construction*, 15(4), 398-414.

Kang, S. C., Chi, H. L., and Miranda, E. (2009). "Three-dimensional simulation and visualization of crane assisted construction erection processes." *Journal of Computing in Civil Engineering*, 23(6), 363-371.

Kato, H., Tsuruta, T., Ishihara, Y., Shimizu, M., and Hashimoto, M. (2012). "Development of robot motion performance platform for auto generation of robot motion planning." *Proceedings, SICE Annual Conference,* Akita, Japan, 1685-1690.

Kuo, T. Y. T. and Kang, S. C. J. (2014). "Control of fast crane operation." *Automation in Construction*, 42, 25-35.

Latombe, J. C. (1991). *Robot Motion Planning*. Kluwer Academic Publishers, Norwell, MA, USA.

Lee, J. K., Lee, J., Jeong, Y., Sheward, H., Sanguinetti, P., Abdelmohsen, S., and Eastman, C. M. (2012a). "Development of space database for automated building design review systems." *Automation in Construction*, 24, 203-212.

Lee, G., Cho, J., Ham, S., Lee, T., Lee, G., Yun, S. H., and Yang, H. J. (2012b). "A BIM- and sensor-based tower crane navigation system for blind lifts." *Automation in Construction*, 26, 1-10.

Lei, Z., Behzadipour, S., Al-Hussein, M., and Hermann, U. (2011). "Application of robotic obstacle avoidance in crane lift path planning." *Proceedings, International Symposium on Automation and Robotics in Construction (ISARC)*, Seoul, Korea, 292-297.

Lei, Z., Taghaddos, H., Hermann, U., and Al-Hussein, M. (2013a). "A methodology of mobile crane lift path checking in heavy industrial projects." *Automation in Construction*, 31, 41-53.

Lei, Z., Taghaddos, H., Olearczyk, J., Al-Hussein, M, and Hermann, U. (2013b). "Automated method for checking crane paths for heavy lifts in industrial projects." *Journal of Construction Engineering and Management*, 139(10).

Lei, Z., Taghaddos, T., Hermann, U., and Al-Hussein, M. (2013c). "Integrating mobile crane lift path checks into an industrial crane management system." *Proceedings, International Symposium on Automation and Robotics in Construction (ISARC)*, Montréal, Canada, 1-8.

Li, H., Chan, G., and Skitmore, M. (2012). "Multiuser virtual safety training system for tower crane dismantlement." *Journal of Computing in Civil Engineering*, 26(5), 638-647.

Li, Y. and Liu, C. (2012). "Integrating field data and 3D simulation for tower crane activity monitoring and alarming." *Automation in Construction*, 27, 111-119.

Liang, K. and Lian-Cheng, M. (2011). "Mobile robot motion planning based on heat conduction equation." *Proceedings, Consumer Electronics, Communications and Networks (CECNet) 2011*, XianNing, China, 2326-2329.

Lin, Y., Wu, D., Wang, X., Wang, X., and Gao, S. (2012). "Statics-based simulation approach for two-crane lift." *Journal of Construction Engineering and Management*, 138(10), 1139-1149.

Lin, Y. H., Liu, Y. S., Gao, G., Han, X. G., Lai, C. Y., and Gu, M. (2013). "The IFC-based path planning for 3D indoor spaces." *Advanced Engineering Informatics*, 27(2), 189-205.

Lin, S. H. E. and Gerber, D. J. (2014). "Designing-in performance: A framework for evolutionary energy performance feedback in early stage design." *Automation in Construction*, 38, 59-73.

Lingelbach, F. (2004). "Path planning using probabilistic cell decomposition." *Proceedings, IEEE International Conference on Robotics and Automation*, 467-472.

Lozano-Pèrez, T. (1983). "Spatial planning: A configuration space approach." *IEEE Transactions on Computers*, 32(2), 108-119.

Mahalingam, A., Nair, H. S., and Varghese, K. (2000). "A computer-aided heavy lift planning model." *Proceedings, International Conference on Computing in Civil and Building Engineering (ICCCBE-VII)*, Standford, CA, USA, 996-1003.

Manrique, J. D., Al-Hussein, M., Telyas, A., and Funston, G. (2007). "Constructing a complex precast tilt-up-panel structure utilizing an

optimization model, 3D CAD, and animation." *Journal of Construction Engineering and Management*, 133(3), 199-207.

Mara, T. G. (2010). "Effects of a construction tower crane on the wind loading of a high-rise building." *Journal of Structural Engineering*, 136(1), 1453-1460.

Moghadam, M., Alwisy, A., and Al-Hussein, M. (2012). "Integrated BIM/lean base production line schedule model for modular construction manufacturing." *Proceedings, Construction Research Congress*, West Lafayette, IN, USA, 1271-1280.

Moselhi, O., Alkass, S., and Al-Hussein, M. (2004). "Innovative 3D-modelling for selecting and locating mobile cranes." *Engineering, Construction and Architectural Management*, 11(5), 373-380.

National Research Council (NRC) (2009). "Advancing the competitiveness and efficiency of the U.S. construction industry." NRC Committee on Advancing the Competitiveness and Productivity of the U.S. Construction Industry, National Academies, National Academies Press, Washington, DC, USA, 122.

O'Connor, J. T., O'Brien, W. J., and Choi, J. O. (2014). "Critical success factors and enablers for optimum and maximum industrial modularization." *Journal of Construction Engineering and Management*, 140(6).

Ota, J. (2006). “Multi-agent robot systems as distributed autonomous systems.” *Advanced Engineering Informatics*, 20(1), 59-70.

Paulson, B. C., Jr., Chan, W. T., and Koo, C. C. (1987). “Construction operation simulation by microcomputer.” *Journal of Construction Engineering and Management*, 113(2), 302-314.

Ray, S. J. and Teizer, J. (2012). “Coarse head pose estimation of construction equipment operators to formulate dynamic blind spots.” *Advanced Engineering Informatics*, 26(1), 117-130.

Rodriguez-Ramos, W. E. and Francis, R. L. (1983). “Single crane location optimization.” *Journal of Construction Engineering and Management*, 109(4), 387-397.

Reddy, H. R. and Varghese, K. (2002). “Automated path planning for mobile crane lifts.” *Computer-Aided Civil and Infrastructure Engineering*, 17(6), 43-448.

Safouhi, H., Mouattamid, M., Hermann, U., and Hendi, A. (2011). “An algorithm for the calculation of feasible mobile crane position areas.” *Automation in Construction*, 20(4), 360-367.

Sawhney, A. and Mund, A. (2002). “Adaptive probabilistic neural network-based crane type selection system.” *Journal of Construction Engineering and Management*, 128(3), 265-273.

Shapiro, A. and Glascock, J. D. (1996). "Culture of using mobile cranes for building construction." *Journal of Construction Engineering and Management*, 122(4), 298-307.

Shapira, A., Lucko, G., and Schexanyder, C. J. (2007). "Cranes for building construction projects." *Journal of Construction Engineering and Management*, 133(9), 690-700.

Shapira, A. and Lyachin, B. (2009a). "Identification and analysis of factors affecting safety on construction sites with tower cranes." *Journal of Construction Engineering and Management*, 135(1), 24-33.

Shapira, A. and Simcha, M. (2009b). "AHP-based weighting of factors affecting safety on construction sites with tower cranes." *Journal of construction Engineering and Management*, 135(4), 307-318.

Sivakumar, P. L., Varghese, K., and Babu, N. R. (2000). "Path planning of cooperative construction manipulators using genetic algorithms." *Proceedings, International Symposium on Automation and Robotics in Construction (ISARC)*, Taipei, Taiwan, 18-20.

Sivakumar, P. L., Varghese, K., and Babu, N. R. (2003). "Automated path planning of cooperative crane lifts using heuristic search." *Journal of Computing in Civil Engineering*, 17(3), 197-207.

Soltani, A. R., Tawfik, H., Goulermas, J. Y., and Fernando, T. (2002). "Path planning in construction sites: Performance evaluation of the Dijkstra, A*,

and GA search algorithms." *Advanced Engineering Informatics*, 16(4), 291-303.

Statistics Canada (2014). "Private and public investment in Canada, intentions." http://www.statcan.gc.ca/ (Accessed Mar. 31, 2014).

Taghaddos, T., AbouRizk, S., Mohamed, Y., and Hermann, U. (2009). "Integrated simulation-based scheduling for module assembly yard." *Proceedings, Construction Research Congress*, Seattle, WA, USA, 1270-1279.

Taghaddos, T., AbouRizk, S., Mohamed, Y., and Hermann, U. (2010). "Simulation-based multiple heavy lift planning in industrial construction." *Proceedings, Construction Research Congress*, Banff, AB, Canada, 349-358.

Taghaddos, T., AbouRizk, S., Mohamed, Y., and Hermann, U. (2012). "Simulation-based auction protocol for resource scheduling problems." *Journal of Construction Engineering and Management*, 138(1), 31-42.

Taghddos, H., Hermann, U., AbouRizk, S., and Mohamed, Y. (2014). "Simulation-based multiagent approach for scheduling modular construction." *Journal of Computing in Civil Engineering*, 28(2), 263-274.

Tam, C. M., Tong, T. K. L., and Chan, W. K. W. (2001). "Genetic algorithm for optimizing supply locations around tower crane." *Journal of Construction Engineering and Management*, 127(4), 315-321.

Tantisevi, K. and Akinci, B. (2008). "Simulation-based identification of possible locations of mobile cranes on construction sites." *Journal of Computing in Civil Engineering*, 22(1), 21-30.

Tatum, C. B., Vanegas, J. A., and Williams, J. M. (1987). "Constructability improvement using prefabrication, preassembly, and modularization." University of Texas, Construction Industry Institute, Austin, TX, USA.

Vatti B. R. (1992). "A generic solution to polygon clipping." *Communications of the ACM*, 35(7), 57-63.

Wang, X., Love, P. E., and Davis, P. R. (2012). "BIM + AR: A framework of bringing BIM to construction site." *Proceedings, Construction Research Congress*, West Lafayette, IN, USA, 1175-1181.

Warszawski, A. and Navon, R. (1991). "Robot for interior-finishing works." *Journal of Construction Engineering and Management*, 117(3), 402-422.

Williams, C., Cho, Y. K., and Youn, J. H. (2007). "Wireless sensor-driven intelligent navigation method for mobile robot applications in construction." *Proceedings, International Workshop on Computing in Civil Engineering*, Pittsburgh, PA, USA, 640-647.

Wu, D., Lin, Y., Wang, X., Wang, X., and Gao, S. (2012). "Algorithm of crane selection for heavy lifts." *Journal of Computing in Civil Engineering*, 25(1), 57-65.

Xu, J. and AbouRizk, S. M. (1999). "Product-based model representation for integrating 3-D CAD with computer simulation." *Proceedings, Winter Simulation Conference*, New York, NY, USA, 917-977.

Xu, J., AbouRizk, S. M., and Fraser, C. (2003). "Integrated three-dimensional computer-aided design and discrete-event simulation models." *Canadian Journal of Civil Engineering*, 30(2), 449-459.

Zhang, P., Harris, F. C., Olomolaiye, P. O., and Holt, G. D. (1999). "Location optimization for a group of tower cranes." *Journal of Construction Engineering and Management*, 125(2), 115-122.

Zhang, Y., AbouRizk, S. M., Xie, H., and Moghani, E. (2012). "Design and implementation of loose-coupling visualization components in distributed construction simulation environment with HLA." *Journal of Computing in Civil Engineering*, 26(2), 248-258.